US008941084B2

(12) **United States Patent**
Balakin

(10) **Patent No.: US 8,941,084 B2**
(45) **Date of Patent: Jan. 27, 2015**

(54) **CHARGED PARTICLE CANCER THERAPY DOSE DISTRIBUTION METHOD AND APPARATUS**

(71) Applicant: **Vladimir Balakin**, Protvino (RU)

(72) Inventor: **Vladimir Balakin**, Protvino (RU)

(*) Notice: Subject to any disclaimer, the term of this patent is extended or adjusted under 35 U.S.C. 154(b) by 0 days.

(21) Appl. No.: **13/887,339**

(22) Filed: **May 5, 2013**

(65) **Prior Publication Data**

US 2014/0330063 A1 Nov. 6, 2014

Related U.S. Application Data

(60) Division of application No. 12/687,387, filed on Jan. 14, 2010, now Pat. No. 8,642,978, which is a continuation-in-part of application No. 12/425,683, filed on Apr. 17, 2009, now Pat. No. 7,939,809.

(Continued)

(51) **Int. Cl.**
G21K 5/04 (2006.01)
A61N 5/10 (2006.01)

(52) **U.S. Cl.**
CPC ***A61N 5/107*** (2013.01); ***A61N 5/1081*** (2013.01); ***A61N 5/1067*** (2013.01)
USPC **250/492.3**; 250/492.1; 600/1; 315/500

(58) **Field of Classification Search**
CPC G21K 5/00; G21K 5/04; G21K 5/05; A61N 5/00; A61N 5/01; A61N 5/1077; A61N 5/10
USPC 250/492.1, 492.3; 600/1; 315/500, 501, 315/502, 503, 504, 505, 506, 507
See application file for complete search history.

(56) **References Cited**

U.S. PATENT DOCUMENTS

2,306,875 A 12/1942 Fremlin
2,533,688 A 12/1950 Quam

(Continued)

FOREIGN PATENT DOCUMENTS

CN 1178667 A 4/1998
CN 1242594 A 1/2000

(Continued)

OTHER PUBLICATIONS

Biophysics Group et al. "Design, Construction and First Experiment of a Magnetic Scanning System for Therapy, Radiobiological Experiment on the Radiobiological Action of Carbon, Oxygen and Neon" GSI Report, Gessellschaft fur Schwerionenforschung MBH. vol. GSI-91-18, Jun. 1, 1991, pp. 1-31.

(Continued)

Primary Examiner — Nicole Ippolito
(74) *Attorney, Agent, or Firm* — Kevin Hazen

(57) **ABSTRACT**

The invention relates generally to treatment of solid cancers. More particularly, a method and apparatus for efficient radiation dose delivery to a tumor is described. Preferably, radiation is delivered through an entry point into the tumor and Bragg peak energy is targeted to a distal or far side of the tumor from an ingress point. Delivering Bragg peak energy to the distal side of the tumor from the ingress point is repeated from multiple rotational directions. Beam intensity is proportional to radiation dose delivery efficiency. The multi-field irradiation process with energy levels targeting the far side of the tumor from each irradiation direction provides even and efficient charged particle radiation dose delivery to the tumor. Preferably, the charged particle therapy is timed to patient respiration via control of charged particle beam injection, acceleration, extraction, and/or targeting methods and apparatus.

17 Claims, 35 Drawing Sheets

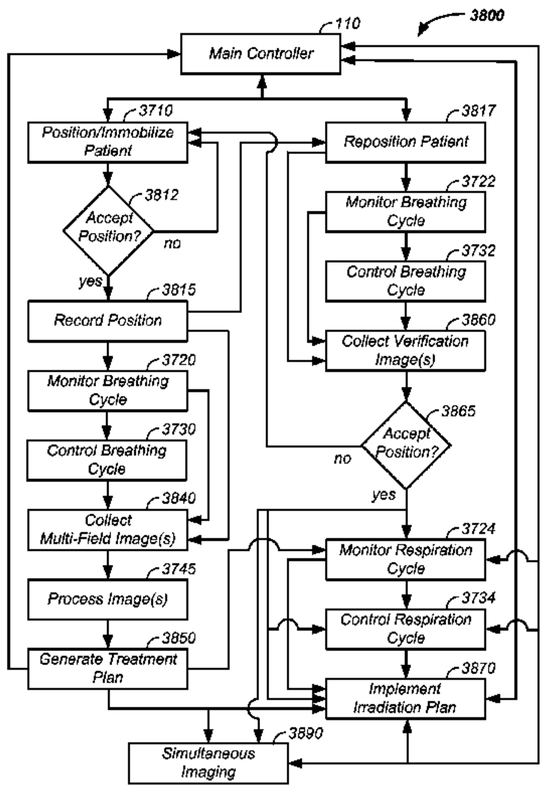

Related U.S. Application Data

(60) Provisional application No. 61/055,395, filed on May 22, 2008, provisional application No. 61/137,574, filed on Aug. 1, 2008, provisional application No. 61/192,245, filed on Sep. 17, 2008, provisional application No. 61/055,409, filed on May 22, 2008, provisional application No. 61/203,308, filed on Dec. 22, 2008, provisional application No. 61/188,407, filed on Aug. 11, 2008, provisional application No. 61/188,406, filed on Aug. 11, 2008, provisional application No. 61/189,815, filed on Aug. 25, 2008, provisional application No. 61/201,731, filed on Dec. 15, 2008, provisional application No. 61/205,362, filed on Jan. 21, 2009, provisional application No. 61/134,717, filed on Jul. 14, 2008, provisional application No. 61/134,707, filed on Jul. 14, 2008, provisional application No. 61/201,732, filed on Dec. 15, 2008, provisional application No. 61/198,509, filed on Nov. 7, 2008, provisional application No. 61/134,718, filed on Jul. 14, 2008, provisional application No. 61/190,613, filed on Sep. 2, 2008, provisional application No. 61/191,043, filed on Sep. 8, 2008, provisional application No. 61/192,237, filed on Sep. 17, 2008, provisional application No. 61/201,728, filed on Dec. 15, 2008, provisional application No. 61/190,546, filed on Sep. 2, 2008, provisional application No. 61/189,017, filed on Aug. 15, 2008, provisional application No. 61/198,248, filed on Nov. 5, 2008, provisional application No. 61/198,508, filed on Nov. 7, 2008, provisional application No. 61/197,971, filed on Nov. 3, 2008, provisional application No. 61/199,405, filed on Nov. 17, 2008, provisional application No. 61/199,403, filed on Nov. 17, 2008, provisional application No. 61/199,404, filed on Nov. 17, 2008.

(56) **References Cited**

U.S. PATENT DOCUMENTS

2,613,726	A	10/1952	Paatero
2,790,902	A	4/1957	Wright
3,128,405	A	4/1964	Lambertson
3,328,708	A	6/1967	Smith et al.
3,412,337	A	11/1968	Lothrop
3,582,650	A	6/1971	Avery
3,585,386	A	6/1971	Horton
3,655,968	A	4/1972	Moore
3,867,705	A	2/1975	Hudson
3,882,339	A	5/1975	Rate
3,906,280	A	9/1975	Andelfinger
3,911,280	A	10/1975	Hyman et al.
4,002,912	A	1/1977	Johnson
4,344,011	A	8/1982	Hayashi
4,472,822	A	9/1984	Swift
4,607,380	A	8/1986	Oliver
4,612,660	A	9/1986	Huang
4,622,687	A	11/1986	Whitaker
4,705,955	A	11/1987	Mileikowsky
4,726,046	A	2/1988	Nunan
4,730,353	A	3/1988	Ono
4,740,758	A	4/1988	Ries
4,843,333	A	6/1989	Marsing
4,868,844	A	9/1989	Nunan
4,870,287	A	9/1989	Cole
4,908,580	A	3/1990	Yamada et al.
4,989,225	A	1/1991	Gupta et al.
4,992,746	A	2/1991	Martin
4,996,496	A	2/1991	Kitamura et al.
4,998,258	A	3/1991	Ikeda
5,010,562	A	4/1991	Hernandez et al.
5,017,789	A	5/1991	Young
5,017,882	A	5/1991	Finlan
5,039,867	A	8/1991	Nishihara
5,046,078	A	9/1991	Hernandez et al.
5,073,913	A	12/1991	Martin
5,098,158	A	3/1992	Palarski
5,101,169	A	3/1992	Gomei
5,117,194	A	5/1992	Nakanishi
5,168,241	A	12/1992	Hirota
5,168,514	A	12/1992	Horton
5,177,448	A	1/1993	Ikeguchi
5,216,377	A	6/1993	Nakata
5,260,581	A	11/1993	Lesyna
5,285,166	A	2/1994	Hiramoto
5,349,198	A	9/1994	Takanaka
5,363,008	A	11/1994	Hiramoto
5,388,580	A	2/1995	Sullivan
5,402,462	A	3/1995	Nobuta
5,423,328	A	6/1995	Gavish
5,440,133	A	8/1995	Moyers
5,483,129	A	1/1996	Yamamoto
5,511,549	A	4/1996	Legg
5,538,494	A	7/1996	Matsuda
5,568,109	A	10/1996	Takayama
5,576,549	A	11/1996	Hell
5,576,602	A	11/1996	Hiramoto
5,585,642	A	12/1996	Britton
5,595,191	A	1/1997	Kirk
5,600,213	A	2/1997	Hiramoto
5,626,682	A	5/1997	Kobari
5,633,907	A	5/1997	Gravelle
5,642,302	A	6/1997	Dumont
5,659,223	A	8/1997	Goodman
5,661,366	A	8/1997	Hirota
5,668,371	A	9/1997	Deasy
5,698,954	A	12/1997	Hirota
5,760,395	A	6/1998	Johnstone
5,789,875	A	8/1998	Hiramoto
5,790,997	A	8/1998	Ruehl
5,818,058	A	10/1998	Nakanishi
5,820,320	A	10/1998	Kobari
5,825,845	A	10/1998	Blair
5,825,847	A	10/1998	Ruth
5,854,531	A	12/1998	Young et al.
5,866,912	A	2/1999	Slater
5,895,926	A	4/1999	Britton
5,907,595	A	5/1999	Sommerer
5,917,293	A	6/1999	Saito
5,949,080	A	9/1999	Ueda et al.
5,969,367	A	10/1999	Hiramoto
5,986,274	A	11/1999	Akiyama
5,993,373	A	11/1999	Nonaka
6,008,499	A	12/1999	Hiramoto
6,034,377	A	3/2000	Pu
6,057,655	A	5/2000	Jongen
6,087,670	A	7/2000	Hiramoto
6,087,672	A	7/2000	Matsuda
6,148,058	A	11/2000	Dobbs
6,201,851	B1	3/2001	Piestrup et al.
6,207,952	B1	3/2001	Kan
6,218,675	B1	4/2001	Akiyama
6,236,043	B1	5/2001	Tadokoro
6,265,837	B1	7/2001	Akiyama
6,282,263	B1	8/2001	Arndt
6,298,260	B1	10/2001	Sontag
6,316,776	B1	11/2001	Hiramoto
6,322,249	B1	11/2001	Wofford
6,335,535	B1	1/2002	Miyake
6,339,635	B1	1/2002	Schardt
6,356,617	B1	3/2002	Besch
6,365,894	B2	4/2002	Tadokoro
6,421,416	B1	7/2002	Sliski
6,433,336	B1	8/2002	Jongen
6,433,349	B2	8/2002	Akiyama
6,433,494	B1	8/2002	Kulish
6,437,513	B1	8/2002	Stelzer
6,444,990	B1	9/2002	Morgan
6,462,490	B1	10/2002	Matsuda
6,470,068	B2	10/2002	Cheng
6,472,834	B2	10/2002	Hiramoto

(56) **References Cited**

U.S. PATENT DOCUMENTS

6,476,403	B1	11/2002	Dolinskii
6,545,436	B1	4/2003	Gary
6,560,354	B1	5/2003	Maurer, Jr.
6,580,084	B1	6/2003	Hiramoto
6,597,005	B1	7/2003	Badura
6,600,164	B1	7/2003	Badura
6,614,038	B1	9/2003	Brand
6,617,598	B1	9/2003	Matsuda
6,626,842	B2	9/2003	Oka
6,635,882	B1	10/2003	Pavlovic
6,639,234	B1	10/2003	Badura
6,670,618	B1	12/2003	Hartmann
6,683,318	B1	1/2004	Haberer
6,683,426	B1	1/2004	Kleeven
6,710,362	B2	3/2004	Kraft
6,717,162	B1	4/2004	Jongen
6,725,078	B2	4/2004	Bucholz
6,730,921	B2	5/2004	Kraft
6,736,831	B1	5/2004	Hartmann
6,745,072	B1	6/2004	Badura
6,774,383	B2	8/2004	Norimine
6,777,700	B2	8/2004	Yanagisawa
6,785,359	B2	8/2004	Lemaitre
6,787,771	B2	9/2004	Bashkirov
6,792,078	B2	9/2004	Kato
6,799,068	B1	9/2004	Hartmann
6,800,866	B2	10/2004	Amemiya
6,803,591	B2	10/2004	Muramatsu
6,809,325	B2	10/2004	Dahl
6,819,743	B2	11/2004	Kato
6,822,244	B2	11/2004	Beloussov
6,823,045	B2	11/2004	Kato
6,838,676	B1	1/2005	Jackson
6,842,502	B2	1/2005	Jaffray
6,859,741	B2	2/2005	Haberer
6,862,469	B2	3/2005	Bucholz
6,873,123	B2	3/2005	Marchand
6,881,970	B2	4/2005	Akiyama
6,891,177	B1	5/2005	Kraft
6,897,451	B2	5/2005	Kaercher
6,900,446	B2	5/2005	Akiyama
6,903,351	B1	6/2005	Akiyama
6,903,356	B2	6/2005	Muramatsu
6,931,100	B2	8/2005	Kato
6,936,832	B2	8/2005	Norimine
6,937,696	B1	8/2005	Mostafavi
6,953,943	B2	10/2005	Yanagisawa
6,979,832	B2	12/2005	Yanagisawa
6,984,835	B2	1/2006	Harada
6,992,312	B2	1/2006	Yanagisawa
6,998,258	B1	2/2006	Kesseler
7,012,267	B2	3/2006	Moriyama
7,026,636	B2	4/2006	Yanagisawa
7,030,396	B2	4/2006	Muramatsu
7,045,781	B2	5/2006	Adamec
7,049,613	B2	5/2006	Yanagisawa
7,053,389	B2	5/2006	Yanagisawa
7,054,801	B2	5/2006	Sakamoto
7,058,158	B2	6/2006	Sako
7,060,997	B2	6/2006	Norimine
7,071,479	B2	7/2006	Yanagisawa
7,081,619	B2	7/2006	Bashkirov
7,084,410	B2	8/2006	Beloussov
7,091,478	B2	8/2006	Haberer
7,102,144	B2	9/2006	Matsuda
7,109,505	B1	9/2006	Sliski
7,122,811	B2	10/2006	Matsuda
7,141,810	B2	11/2006	Kakiuchi
7,154,107	B2	12/2006	Yanagisawa
7,154,108	B2	12/2006	Tadokoro
7,173,264	B2	2/2007	Moriyama
7,173,265	B2	2/2007	Miller
7,193,227	B2	3/2007	Hiramoto
7,199,382	B2	4/2007	Rigney
7,208,748	B2	4/2007	Sliski
7,212,608	B2	5/2007	Nagamine
7,212,609	B2	5/2007	Nagamine
7,227,161	B2	6/2007	Matsuda
7,247,869	B2	7/2007	Tadokoro
7,252,745	B2	8/2007	Gorokhovsky
7,259,529	B2	8/2007	Tanaka
7,262,424	B2	8/2007	Moriyama
7,274,018	B2	9/2007	Adamec
7,274,025	B2	9/2007	Berdermann
7,280,633	B2	10/2007	Cheng
7,297,967	B2	11/2007	Yanagisawa
7,301,162	B2	11/2007	Matsuda
7,307,264	B2	12/2007	Brusasco
7,310,404	B2	12/2007	Tashiro
7,315,606	B2	1/2008	Tsujii
7,319,231	B2	1/2008	Moriyama
7,342,516	B2	3/2008	Kato et al.
7,345,291	B2	3/2008	Kats
7,345,292	B2	3/2008	Moriyama
7,349,522	B2	3/2008	Yan
7,351,988	B2	4/2008	Naumann
7,355,189	B2	4/2008	Yanagisawa
7,356,112	B2	4/2008	Brown
7,368,740	B2	5/2008	Beloussov
7,372,053	B2	5/2008	Yamashita
7,378,672	B2	5/2008	Harada
7,381,979	B2	6/2008	Yamashita
7,385,203	B2	6/2008	Nakayama
7,394,082	B2	7/2008	Fujimaki
7,397,054	B2	7/2008	Natori
7,397,901	B1	7/2008	Johnsen
7,402,822	B2	7/2008	Guertin
7,402,823	B2	7/2008	Guertin
7,402,824	B2	7/2008	Guertin
7,402,963	B2	7/2008	Sliski
7,425,717	B2	9/2008	Matsuda
7,432,516	B2	10/2008	Peggs
7,439,528	B2	10/2008	Nishiuchi
7,446,490	B2	11/2008	Jongen
7,449,701	B2	11/2008	Fujimaki
7,453,076	B2	11/2008	Welch et al.
7,456,415	B2	11/2008	Yanagisawa
7,456,591	B2	11/2008	Jongen
7,465,944	B2	12/2008	Ueno
7,471,765	B2	12/2008	Jaffray
7,476,883	B2	1/2009	Nutt
7,492,858	B2	2/2009	Partain
7,531,818	B2	5/2009	Brahme
7,555,103	B2	6/2009	Johnsen
7,560,717	B2	7/2009	Matsuda
7,576,342	B2	8/2009	Hiramoto
7,586,112	B2	9/2009	Chiba
7,589,334	B2	9/2009	Hiramoto
7,626,347	B2	12/2009	Sliski
7,634,057	B2	12/2009	Ein-Gal
7,659,521	B2	2/2010	Pedroni
7,668,585	B2	2/2010	Green
7,692,168	B2	4/2010	Moriyama
7,701,677	B2	4/2010	Schultz
7,709,818	B2	5/2010	Matsuda
7,718,982	B2	5/2010	Sliski
7,728,311	B2	6/2010	Gall
7,729,469	B2	6/2010	Kobayashi
7,737,422	B2	6/2010	Platzgummer et al.
7,741,623	B2	6/2010	Sommer
7,755,305	B2	7/2010	Umezawa
7,772,577	B2	8/2010	Saito
7,796,730	B2	9/2010	Marash
7,801,277	B2	9/2010	Zou
7,807,982	B2	10/2010	Nishiuchi
7,817,774	B2	10/2010	Partain
7,817,778	B2	10/2010	Nord
7,825,388	B2	11/2010	Nihongi
7,826,592	B2	11/2010	Jaffray
7,826,593	B2	11/2010	Svensson
7,834,336	B2	11/2010	Boeh
7,838,855	B2	11/2010	Fujii
7,848,488	B2	12/2010	Mansfield
7,860,216	B2	12/2010	Jongen

(56) **References Cited**

U.S. PATENT DOCUMENTS

7,875,868	B2	1/2011	Moriyama	
7,894,574	B1	2/2011	Nord	
7,906,769	B2	3/2011	Blasche	
7,919,765	B2	4/2011	Timmer	
7,939,809	B2	5/2011	Balakin	
7,940,891	B2	5/2011	Star-Lack	
7,940,894	B2	5/2011	Balakin	
7,943,913	B2	5/2011	Balakin	
7,953,205	B2	5/2011	Balakin	
7,961,844	B2	6/2011	Takeda	
7,977,656	B2	7/2011	Fujimaki	
7,982,198	B2	7/2011	Nishiuchi	
7,987,053	B2	7/2011	Schaffner	
7,995,813	B2	8/2011	Foshee	
8,002,465	B2	8/2011	Ahn	
8,003,964	B2	8/2011	Stark	
8,009,804	B2	8/2011	Siljamaki	
8,045,679	B2	10/2011	Balakin	
8,067,748	B2	11/2011	Balakin	
8,089,054	B2	1/2012	Balakin	
8,093,564	B2	1/2012	Balakin	
8,139,712	B2	3/2012	Kojima	
8,309,941	B2	11/2012	Balakin	
8,374,314	B2	2/2013	Balakin	
2001/0009267	A1	7/2001	Tadokoro	
2003/0048080	A1	3/2003	Amemiya et al.	
2003/0104207	A1	6/2003	Arakida	
2003/0141460	A1	7/2003	Kraft	
2003/0163015	A1	8/2003	Yanagisawa	
2003/0164459	A1	9/2003	Schardt	
2004/0002641	A1	1/2004	Sjogren et al.	
2004/0022361	A1	2/2004	Lemaitre	
2004/0062354	A1	4/2004	Kato	
2004/0155206	A1	8/2004	Marchand	
2004/0162457	A1	8/2004	Maggiore et al.	
2004/0184583	A1	9/2004	Nagamine et al.	
2004/0218725	A1	11/2004	Radley	
2004/0227074	A1	11/2004	Benveniste et al.	
2004/0254492	A1	12/2004	Zhang	
2005/0017193	A1	1/2005	Jackson	
2005/0063516	A1*	3/2005	Kato et al.	378/152
2005/0099145	A1	5/2005	Nishiuchi et al.	
2005/0148808	A1	7/2005	Cameron	
2005/0161618	A1	7/2005	Pedroni	
2005/0167610	A1	8/2005	Tajima	
2005/0211905	A1	9/2005	Stark	
2005/0226378	A1	10/2005	Cocks et al.	
2005/0238134	A1	10/2005	Brusasco	
2005/0269497	A1	12/2005	Jongen	
2005/0284233	A1	12/2005	Teraura et al.	
2006/0050848	A1	3/2006	Vilsmeier	
2006/0106301	A1	5/2006	Kats	
2006/0163495	A1	7/2006	Hiramoto	
2006/0171508	A1	8/2006	Noda	
2006/0180158	A1	8/2006	McKnight et al.	
2006/0226372	A1	10/2006	Yanagisawa	
2006/0255285	A1	11/2006	Jongen	
2006/0262898	A1	11/2006	Partain	
2007/0018121	A1	1/2007	Leyman	
2007/0027389	A1	2/2007	Wesse	
2007/0040115	A1	2/2007	Publicover	
2007/0051905	A1	3/2007	Fujimaki et al.	
2007/0093723	A1	4/2007	Keall	
2007/0121788	A1	5/2007	Mildner	
2007/0170994	A1	7/2007	Peggs	
2007/0181815	A1	8/2007	Ebstein	
2007/0189461	A1	8/2007	Sommer	
2007/0211854	A1	9/2007	Koshnitsky et al.	
2007/0215819	A1	9/2007	Hiramoto	
2007/0228291	A1	10/2007	Hiramoto	
2007/0228304	A1	10/2007	Nishiuchi	
2007/0269000	A1	11/2007	Partain et al.	
2008/0023644	A1	1/2008	Pedroni	
2008/0067405	A1	3/2008	Nihongi et al.	
2008/0093567	A1	4/2008	Gall	
2008/0139955	A1	6/2008	Hansmann	
2008/0191142	A1	8/2008	Pedroni	
2008/0267352	A1	10/2008	Aoi	
2008/0290297	A1	11/2008	Blasche et al.	
2008/0317202	A1	12/2008	Partain et al.	
2009/0096179	A1	4/2009	Stark	
2009/0140672	A1	6/2009	Gall	
2009/0168960	A1	7/2009	Jongen	
2009/0184263	A1	7/2009	Moriyama	
2009/0189095	A1	7/2009	Flynn	
2009/0200483	A1	8/2009	Gall	
2009/0236545	A1	9/2009	Timmer	
2009/0249863	A1	10/2009	Kim et al.	
2009/0261248	A1	10/2009	Glavish et al.	
2009/0283704	A1	11/2009	Nishiuchi	
2009/0289194	A1	11/2009	Saito	
2009/0304153	A1	12/2009	Amelia	
2009/0314960	A1	12/2009	Balakin	
2009/0314961	A1	12/2009	Balakin	
2010/0001212	A1	1/2010	Nishiuchi	
2010/0006106	A1	1/2010	Balakin	
2010/0008468	A1	1/2010	Balakin	
2010/0008469	A1	1/2010	Balakin	
2010/0027745	A1	2/2010	Balakin	
2010/0033115	A1	2/2010	Cleland	
2010/0045213	A1	2/2010	Sliski	
2010/0059688	A1	3/2010	Claereboudt	
2010/0060209	A1	3/2010	Balakin	
2010/0090122	A1	4/2010	Balakin	
2010/0091948	A1*	4/2010	Balakin	378/65
2010/0128846	A1	5/2010	Balakin	
2010/0230617	A1	9/2010	Gall	
2010/0272241	A1	10/2010	Amelia	
2010/0308235	A1	12/2010	Sliski	
2011/0073778	A1	3/2011	Natori	
2011/0080172	A1	4/2011	Banning-Geertsma	
2011/0089329	A1	4/2011	Jongen	
2011/0127443	A1	6/2011	Comer	
2011/0137159	A1	6/2011	Jongen	
2011/0147608	A1	6/2011	Balakin	
2011/0174984	A1	7/2011	Balakin	
2011/0178359	A1	7/2011	Hirschman et al.	
2011/0186720	A1	8/2011	Jongen	
2011/0233423	A1	9/2011	Balakin	
2011/0278477	A1	11/2011	Balakin	
2011/0284760	A1	11/2011	Balakin	
2011/0284762	A1	11/2011	Balakin	
2011/0313232	A1	12/2011	Balakin	
2012/0043472	A1	2/2012	Balakin	
2012/0205551	A1	8/2012	Balakin	
2012/0209109	A1	8/2012	Balakin	

FOREIGN PATENT DOCUMENTS

EP	1683545	A2	7/2006
GB	1270619	A	4/1972
WO	WO 99/53998	A1	10/1999
WO	WO 01/89625	A2	11/2001
WO	WO2007014026	A2	1/2007
WO	WO 2008/044194	A2	4/2008
WO	WO 2008/024463	A3	1/2009
WO	WO 2009/142546	A2	11/2009
WO	WO 2009/142550	A2	11/2009
WO	WO2010/101489	A2	9/2010

OTHER PUBLICATIONS

Adams, "Electrostatic cylinder lenses II: Three Element Einzel Lenses", Journal, Feb. 1, 1972, pp. 150-155, XP002554355, vol. 5 No. 2, Journal of Physics E.

Amaldi, "A Hospital-Based Hadrontherapy Complex", Journal, Jun. 27, 1994, pp. 49-51, XP002552288, Proceedings of Epac 94, London, England.

Arimoto, "A Study of the PRISM-FFAG Magnet", Journal, Oct. 18, 2004,Oct. 22, 2004, pp. 243-245, XP002551810, Proceedings of Cyclotron 2004 Conference, Tokyo, Japan.

Biophysics Group, "Design Construction and First Experiments of a Magnetic Scanning System for Therapy. Radiobiological Experi-

(56) **References Cited**

OTHER PUBLICATIONS

ment on the Radiobiological Action of Carbon, Oxygen and Neon", Book, Jun. 1, 1991, pp. 1-31, XP009121701, vol. GSI-91-18, GSI Report, Darmstadt ,DE.
Blackmore, "Operation of the TRIUMF Proton Therapy Facility", Book, May 12, 1997, pp. 3831-3833, XP010322373, vol. 3, Proceedings of the 1997 Particle Accelerator Conference, NJ, USA.
Bryant, "Proton-Ion Medical Machine Study (PIMMS) Part II", Book, Jul. 27, 2000, p.23,p. 228,pp. 289-290, XP002551811, European Organisation for Nuclear Research Cern-Ps Division, Geneva, Switzerland.
Craddock, "New Concepts in FFAG Design for Secondary Beam Facilities and other Applications", Journal, May 16, 2005,May 20, 2005, pp. 261-265, XP002551806, Proceedings of 2005 Particle Accelerator Conference, Knoxville, Tennessee, USA.
Dzhelepov, "Use of USSR Proton Accelerators for Medical Purposes", Journal,Jun. 1973, pp.268-270, vol. ns-2-No. 3, XP002553045, IEEE Transactions on Nuclear Science USA, USA.
Endo, "Medical Synchrotron for Proton Therapy" Journal, Jun. 7, 1988,Jun. 11, 1988, pp. 1459-1461, XP002551808, Proceedings of Epac 88, Rome, Italy.
European Organization for Nuclear Research Cern, Jul. 27, 2000, pp. 1-352.
Johnstone, Koscielniak, "Tune-Stabilized Linear-Field FFAG for Carbon Therapy", Journal, Jun. 26, 2006,Jun. 30, 2006, XP002551807, Proceedings of Epac 2006, Edinburgh, Scotland, UK.
Kalnins, "The use of electric multiple lenses for bending and focusing polar molecules, with application to the design of a rotational-state separator", Journal, May 17, 2003,May 21, 2003, pp. 2951-2953, XP002554356, Proceeding of Pac 2003, Portland, Oregon, USA.
Kim, "50 MeV Proton Beam Test Facility for Low Flux Beam Utilization Studies of PEFP", Journal, Oct. 31, 2005, pp. 441-443, XP002568008, Proceedings of Apac 2004, Pohang, Korea.
Lapostolle, "Introduction a la theorie des accelerateurs lineaires", Book, Jul. 10, 1987, pp. 4-5, XP002554354, Cern Yellow Book Cern, Geneva, Switzerland.
Li, "A thin Beryllium Injection Window for CESR-C", Book, May 12, 2003, pp. 2264-2266, XP002568010, vol. 4, PAC03, Portland, Oregon, USA.
Noda, "Slow beam extraction by a transverse RF field with AM and FM", Journal, May 21, 1996, pp. 269-277, vol. A374, XP002552289, Nuclear Instruments and Methods in Physics Research A, Eslevier, Amsterdam, NL.
Noda, "Performance of a respiration-gated beam control system for patient treatment", Journal, Jun. 10, 1996,Jun. 14, 1996, pp. 2656-2658, XP002552290, Proceedings Epac 96, Barcelona, Spain..
Peters, "Negative ion sources for high energy accelerators", Journal, Feb. 1, 2000, pp. 1069-1074, XP012037926, vol. 71-No. 2,Review of Scientific Instruments, Melville, NY, USA.
Pohlit, "Optimization of Cancer Treatment with Accelerator Produced Radiations", Journal, Jun. 22, 1998, pp. 192-194, XP002552855, Proceedings EPAC 98, Stockholm, Sweden.
Proceeding of 2004 Cyclotron Conference, Oct. 18, 2004, pp. 246-428.
Proceedings of Cyclotron 2004 Conference, Oct. 18, 2004, pp. 243-245 (Presentation Material pp. 1-30).
Proceedings of EPAC 2006, Jun. 30, 2006, pp. 2290-2292.
Proceeding of 2005 Particle Accelerator Conference, May 16, 2005, pp. 261-265.
Saito, "RF Accelerating System for Compact Ion Synchrotron", Journal, Jun. 18, 2001, pp. 966-968, XP002568009, Proceeding of 2001 Pac, Chicago, USA.
Suda, "Medical Application of the Positron Emitter Beam at HIMAC", Journal, Jun. 26, 2000, Jun. 30, 2000, pp. 2554-2556, XP002553046, Proceedings of EPAC 2000, Vienna, Austria.
Tanigaki, "Construction of FFAG Accelerators in Kurri for ADS Study", May 16, 2005,May 20, 2005, pp. 350-352, XP002551809, Proceedings of 2005 Particle Accelerator Conference, Knoxville, Tennessee, USA.
Trbojevic, "Design of a Non-Scaling FFAG Accelerator for Proton Therapy", Journal, Oct. 18,2004,Oct. 22, 2004, pp. 246-248, XP002551805, Proceedings of 2004 Cyclotron Conference, Tokyo, Japan.
Winkler, "Charge Exchange Extraction at the Experimental Storage Ring ESR at GSI", Journal, Jun. 22, 1998, p. 559-561, XP002552287, Proceedings of Epac 98, Stockholm, Sweden.

* cited by examiner

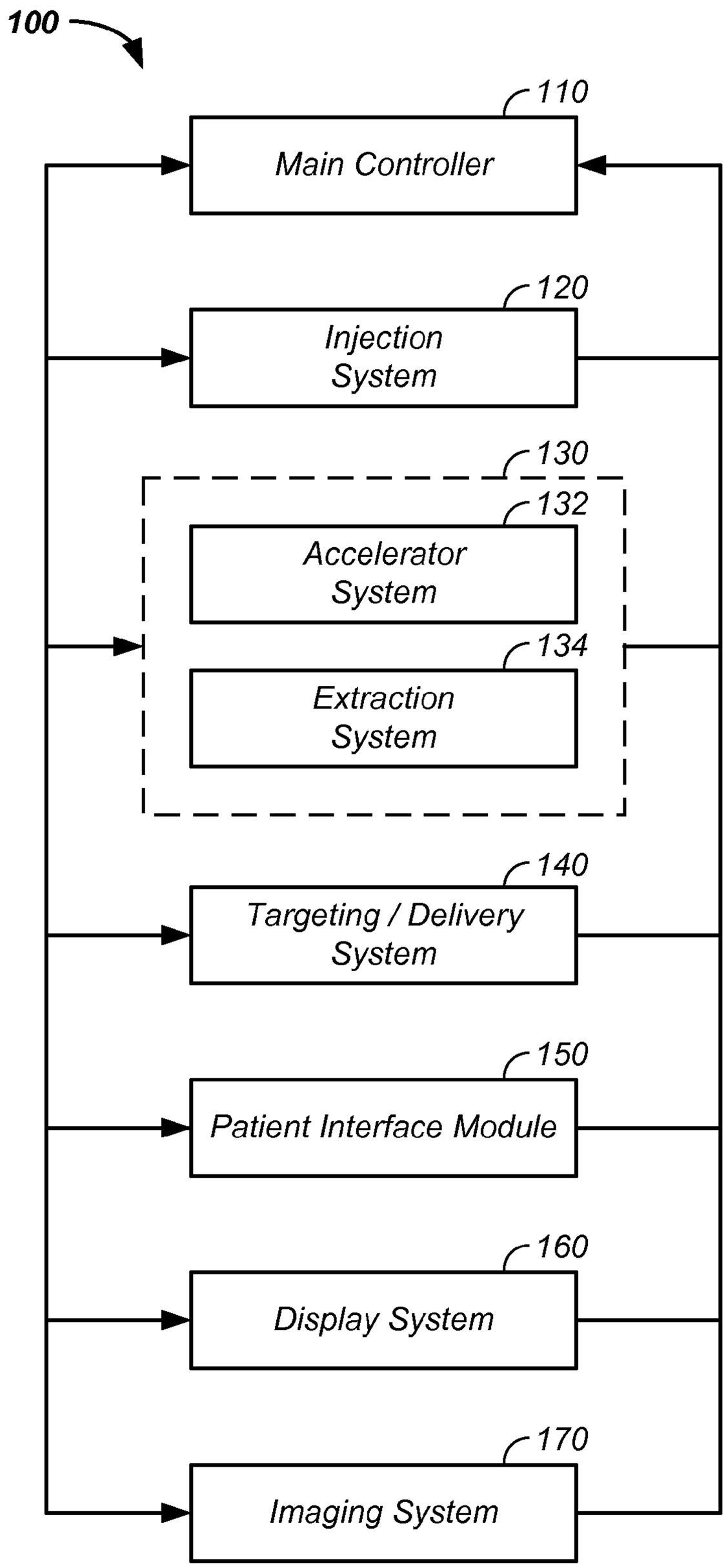
100
110
Main Controller
120
Injection System
130
132
Accelerator System
134
Extraction System
140
Targeting / Delivery System
150
Patient Interface Module
160
Display System
170
Imaging System

FIG. 1

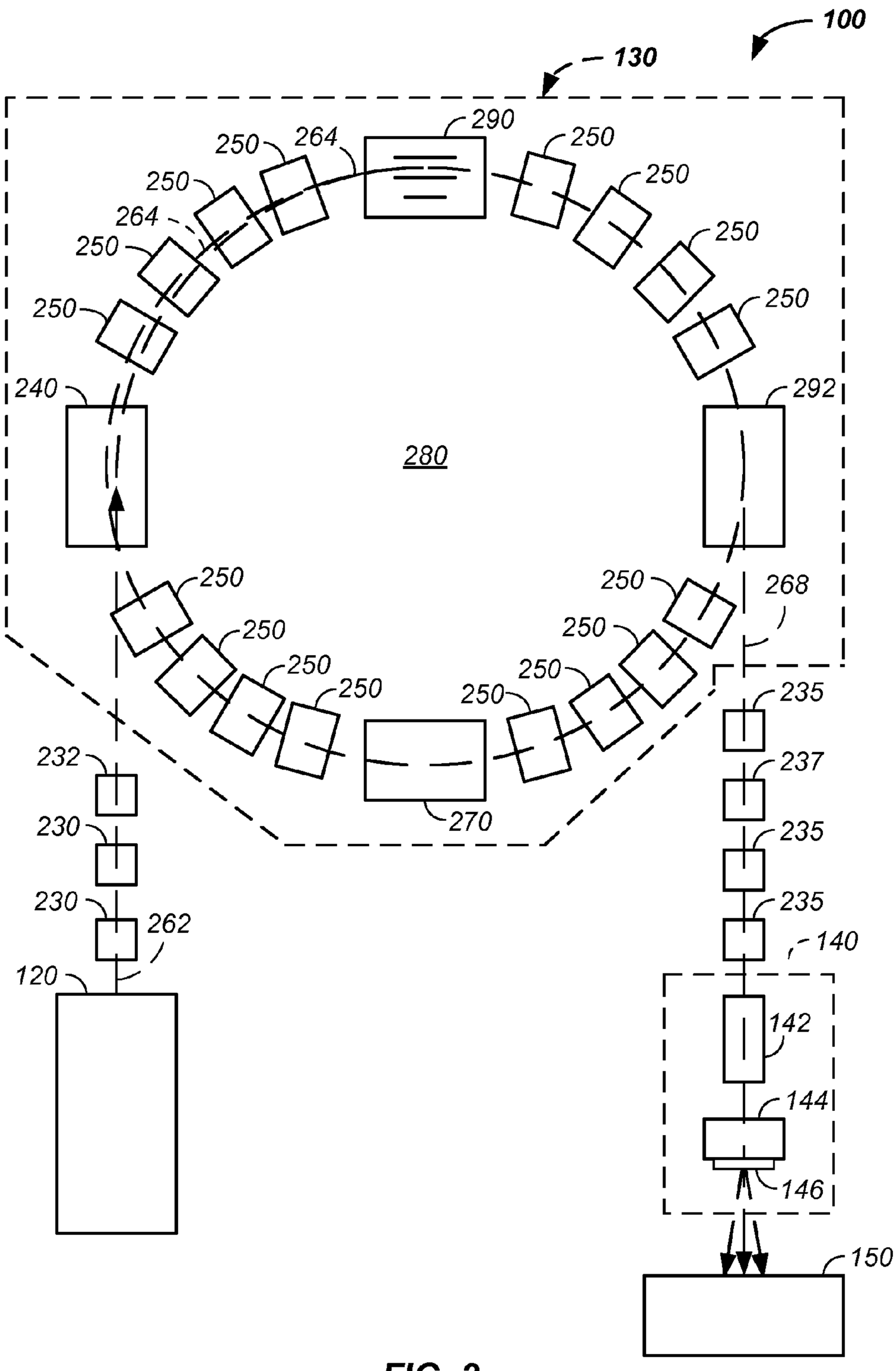
100
130
290
250
264
240
280
292
268
235
237
232
230
262
120
270
140
142
144
146
150

FIG. 2

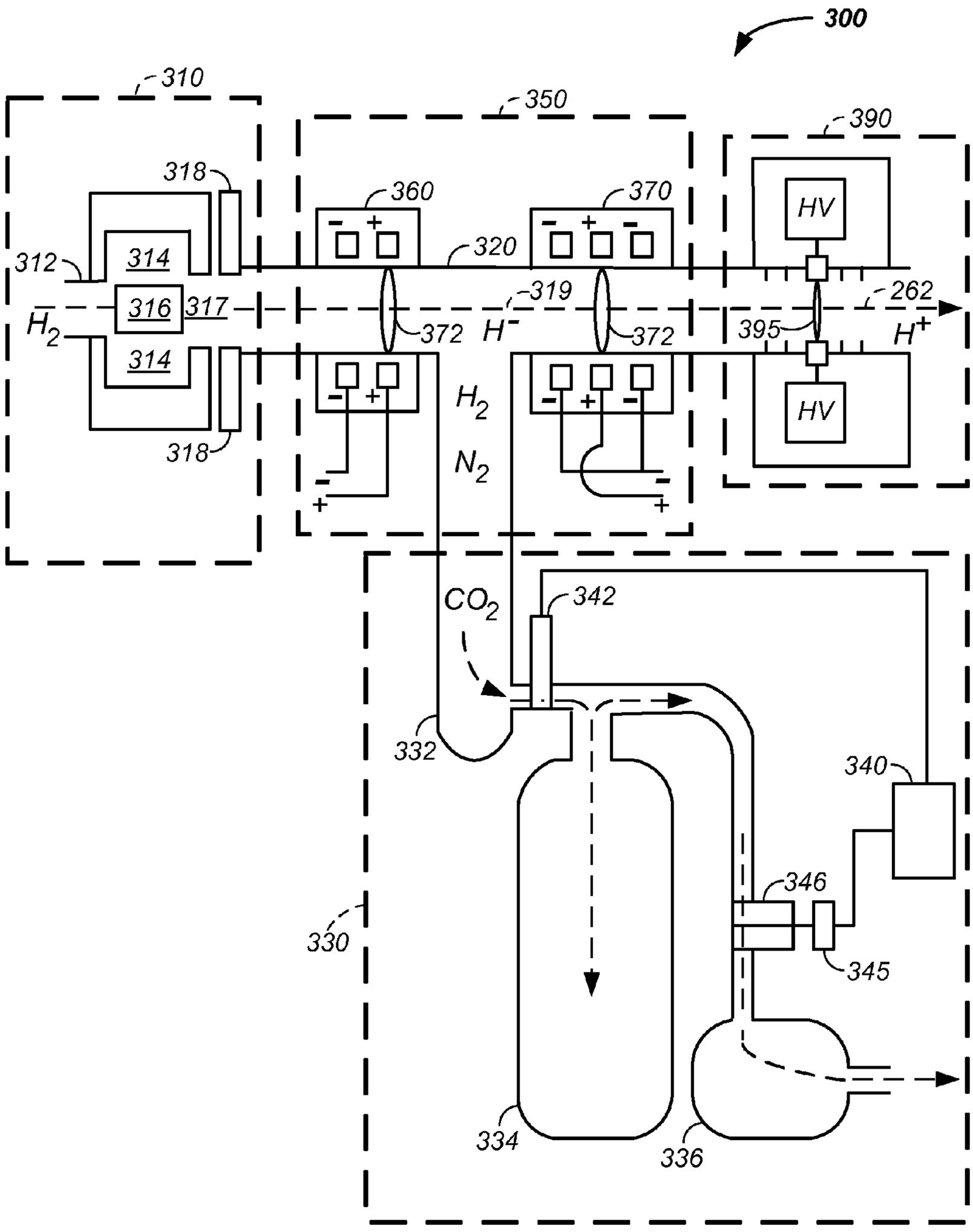
300
310
350
390
318
360
370
HV
320
312
314
316
317
319
262
H_2
372
H^-
372
395
H^+
314
HV
318
H_2
N_2
CO_2
342
332
340
346
330
345
334
336

FIG. 3

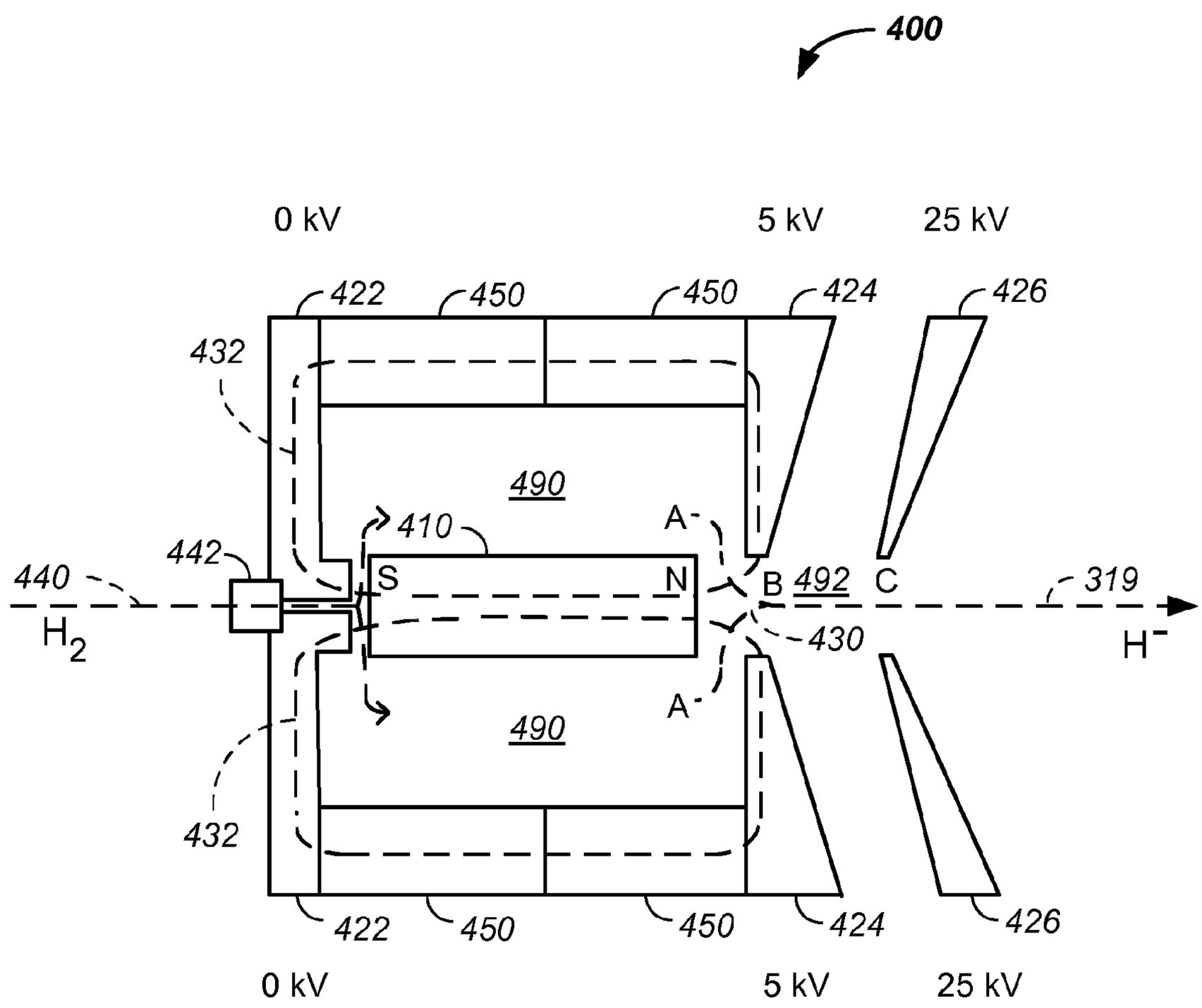
400
0 kV
5 kV
25 kV
422
450
450
424
426
432
490
410
A-
442
440
S
N
B
492
C
319
H2
H-
430
A-
490
432
422
450
450
424
426
0 kV
5 kV
25 kV

FIG. 4

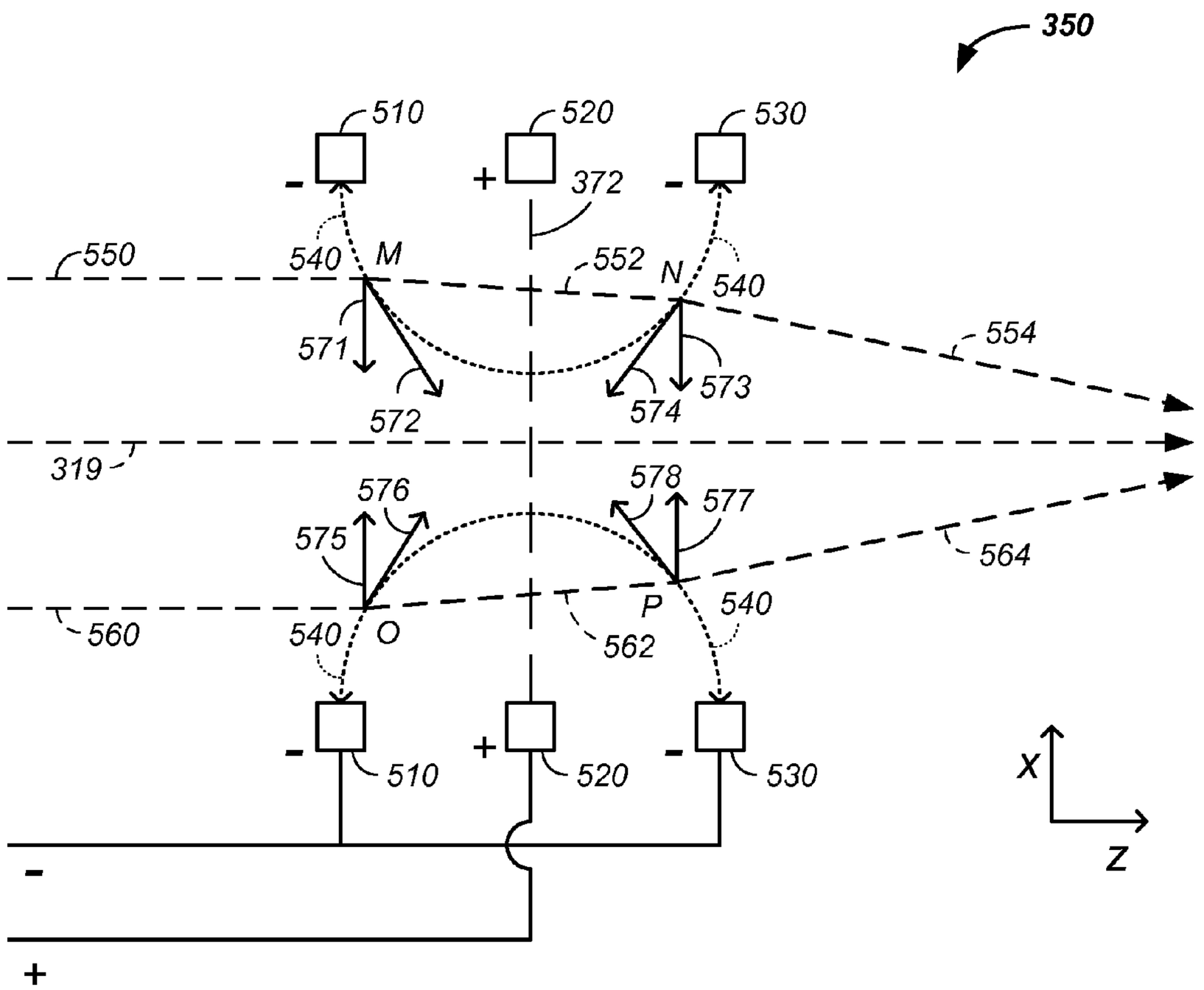
350
510
520
530
372
550
540
M
552
N
540
554
571
572
573
574
319
576
575
578
577
564
560
540
O
P
540
562
510
520
530
X
Z
-
+

FIG. 5

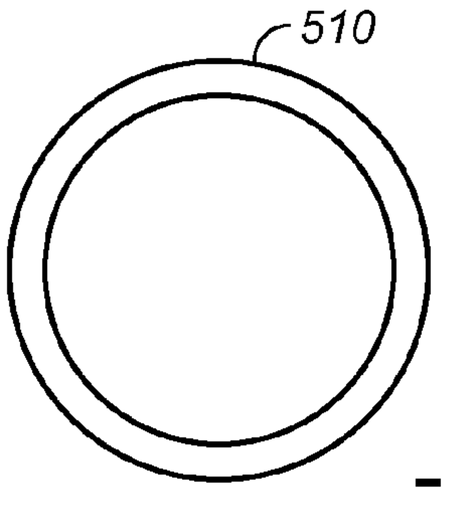

FIG. 6A

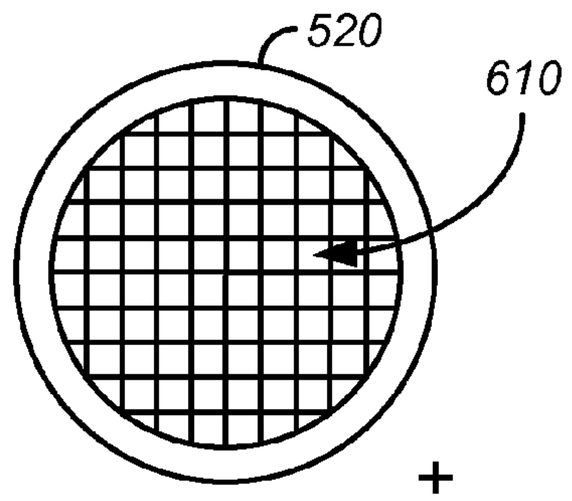

FIG. 6B

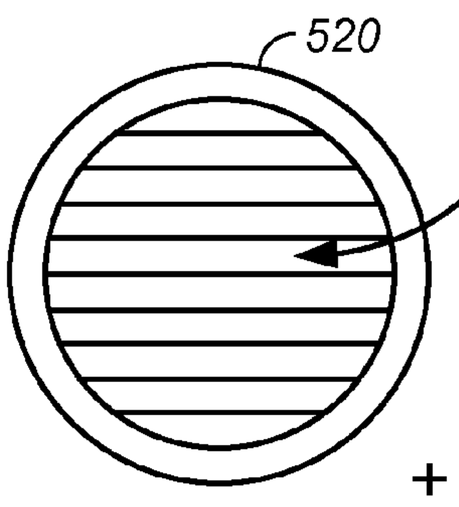

FIG. 6C

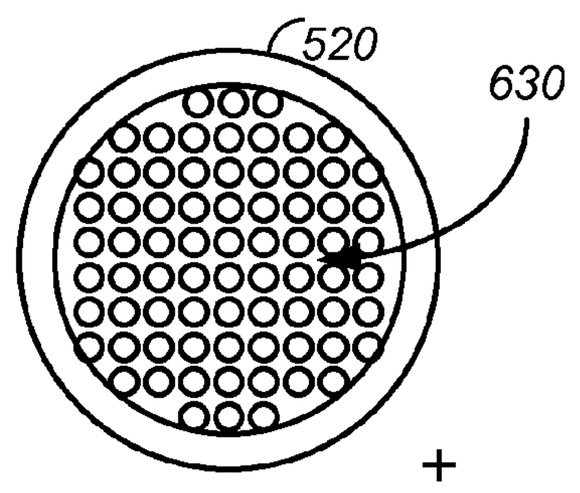

FIG. 6D

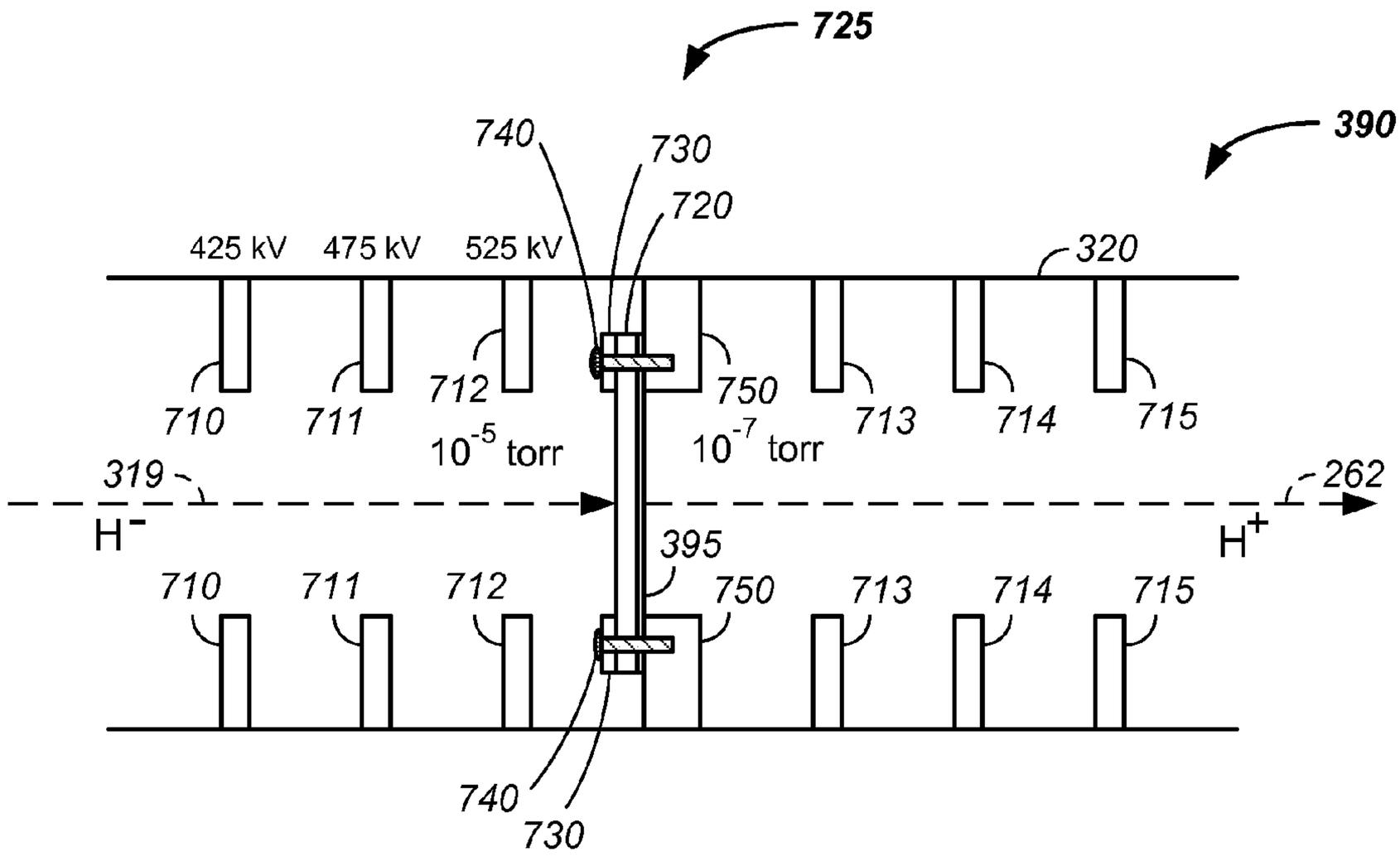

FIG. 7A

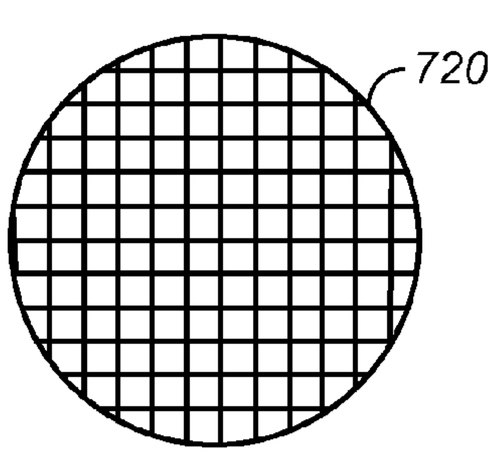

FIG. 7B

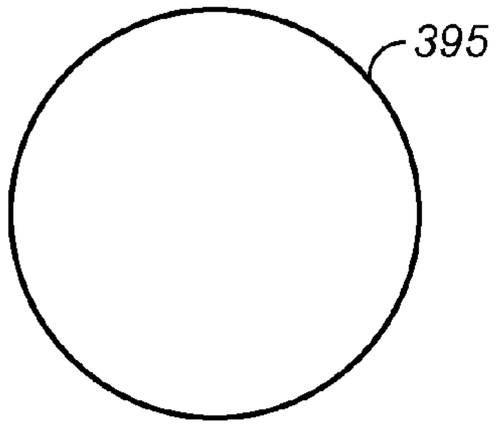

FIG. 7C

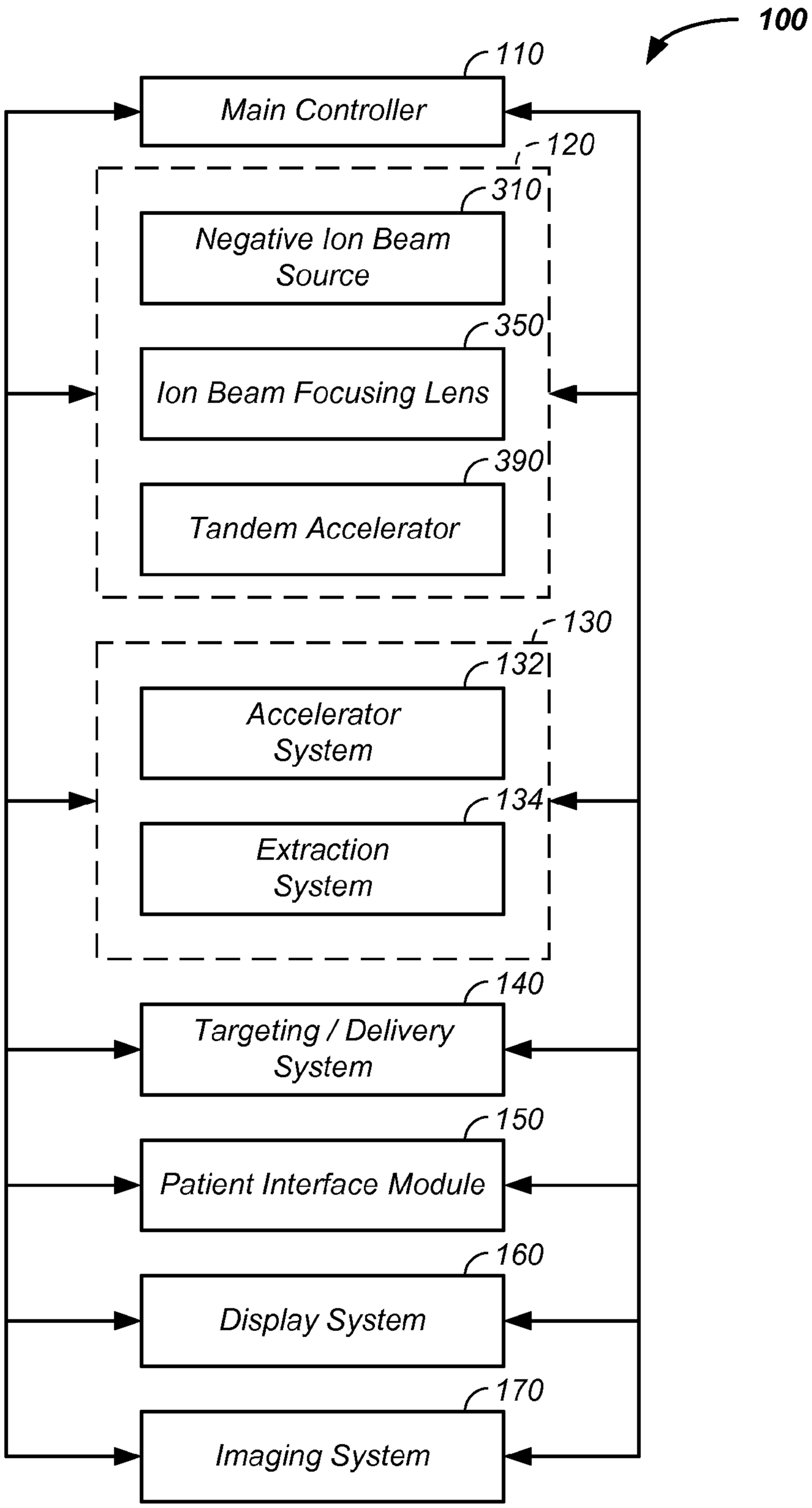
100
110
Main Controller
120
310
Negative Ion Beam Source
350
Ion Beam Focusing Lens
390
Tandem Accelerator
130
132
Accelerator System
134
Extraction System
140
Targeting / Delivery System
150
Patient Interface Module
160
Display System
170
Imaging System

FIG. 8

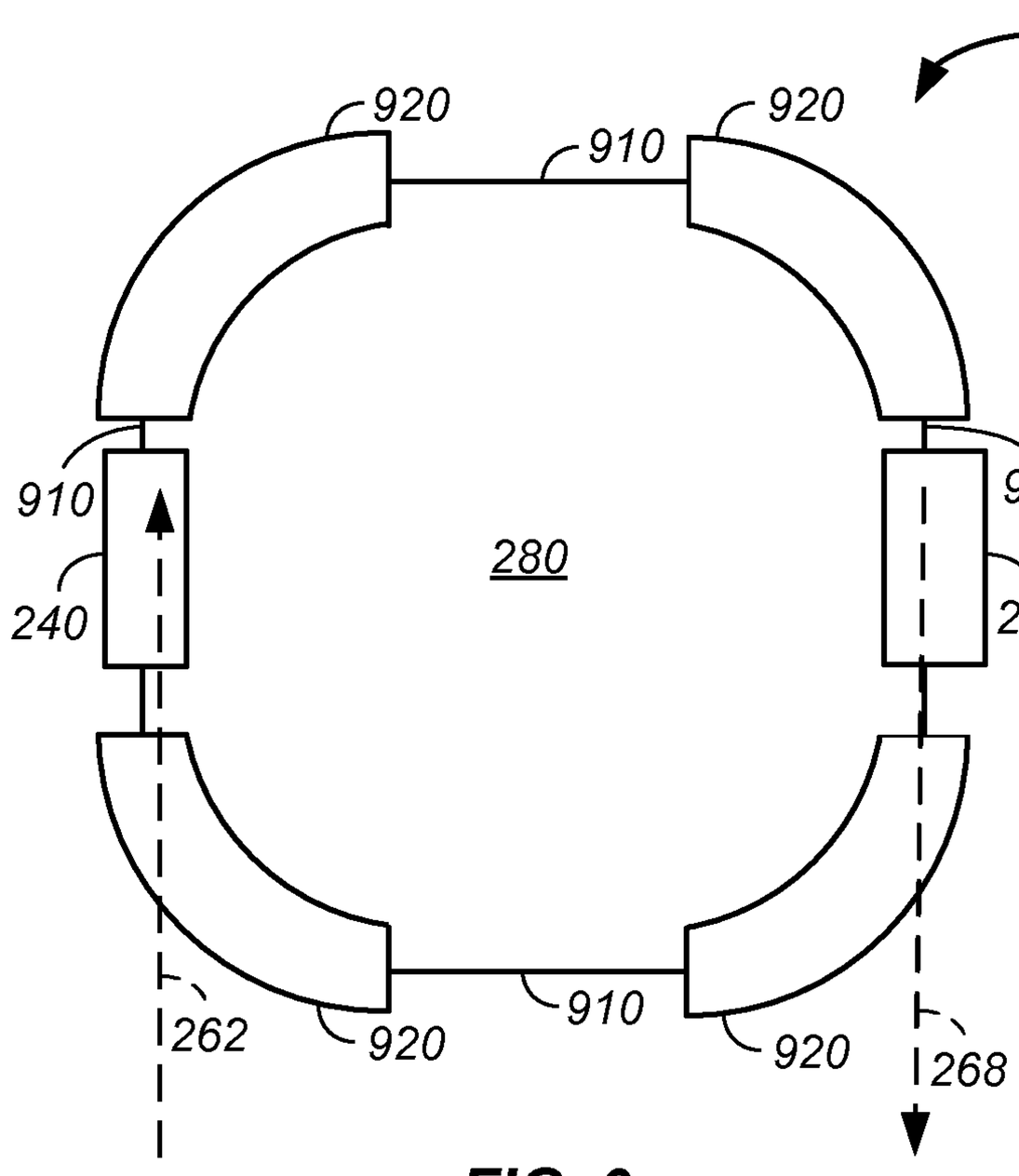
130
920
910
920
910
910
280
240
292
262
920
910
920
268

FIG. 9

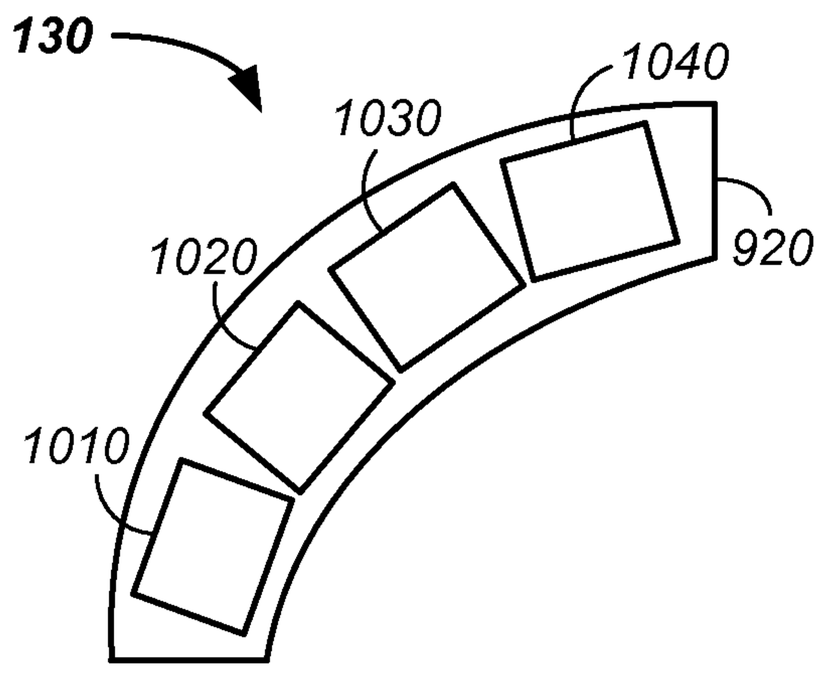
130
1040
1030
1020
920
1010

FIG. 10

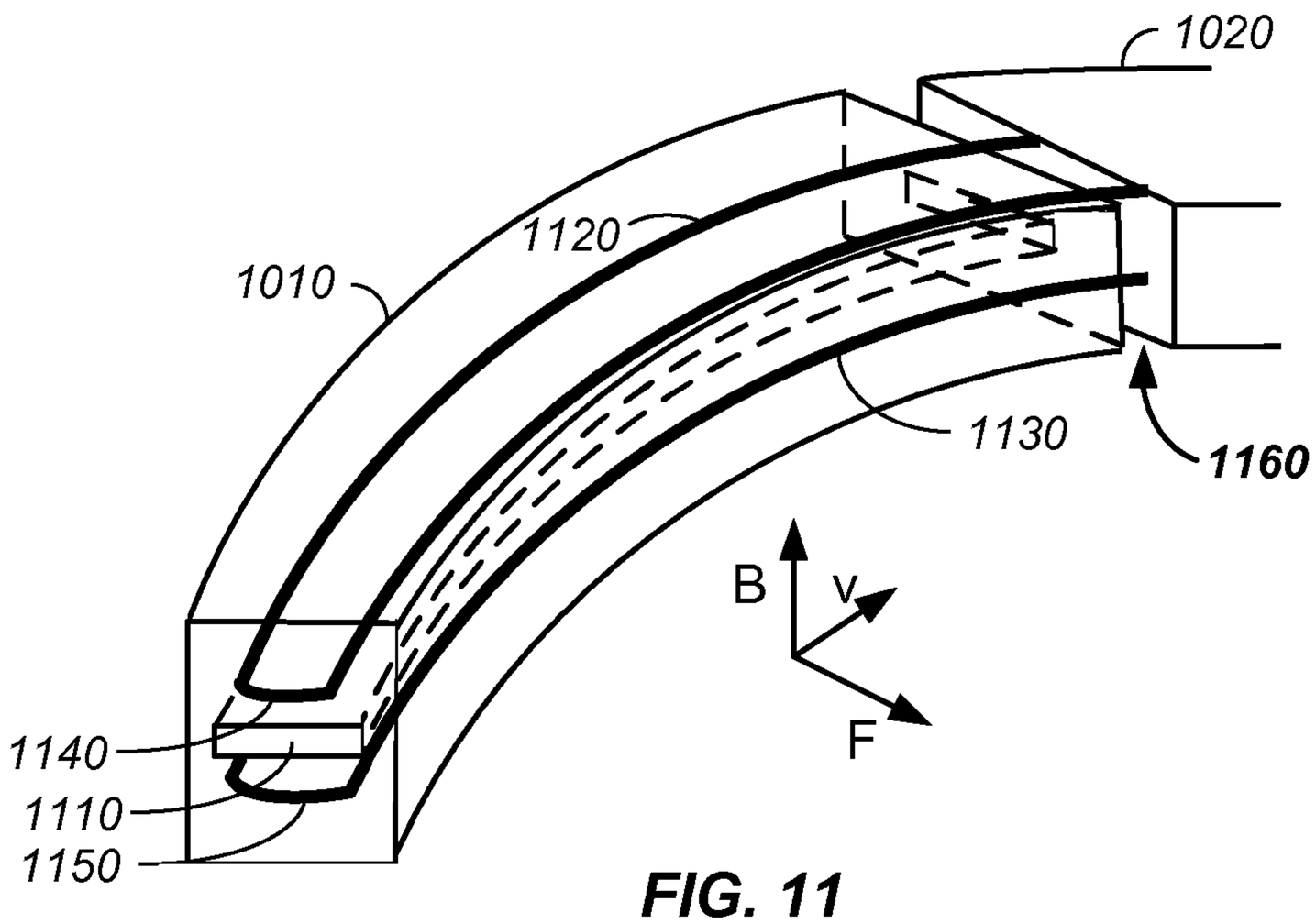
1020
1120
1010
1130
1160
B
v
F
1140
1110
1150

FIG. 11

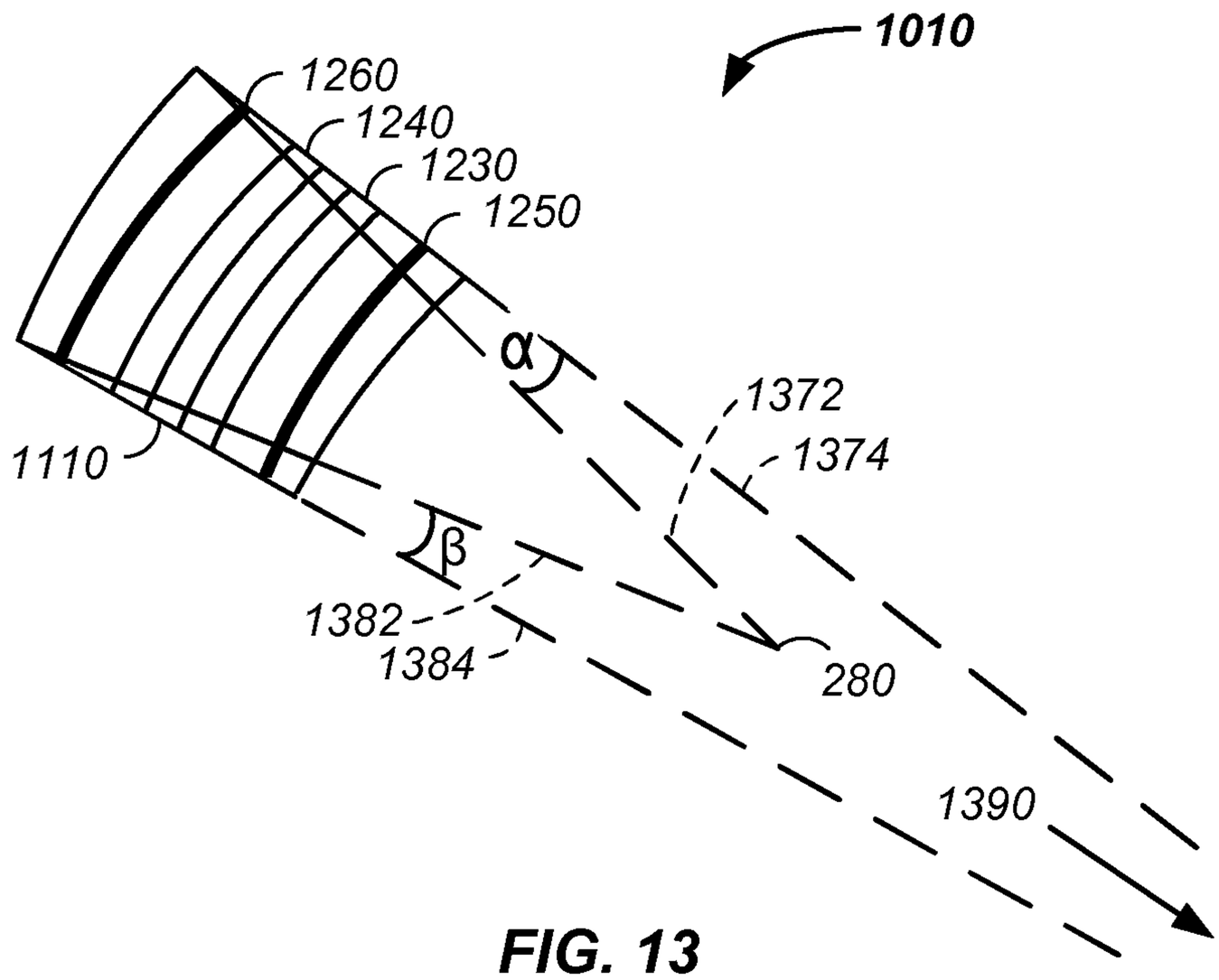
1010
1260
1240
1230
1250
α
1372
1374
1110
β
1382
1384
280
1390

FIG. 13

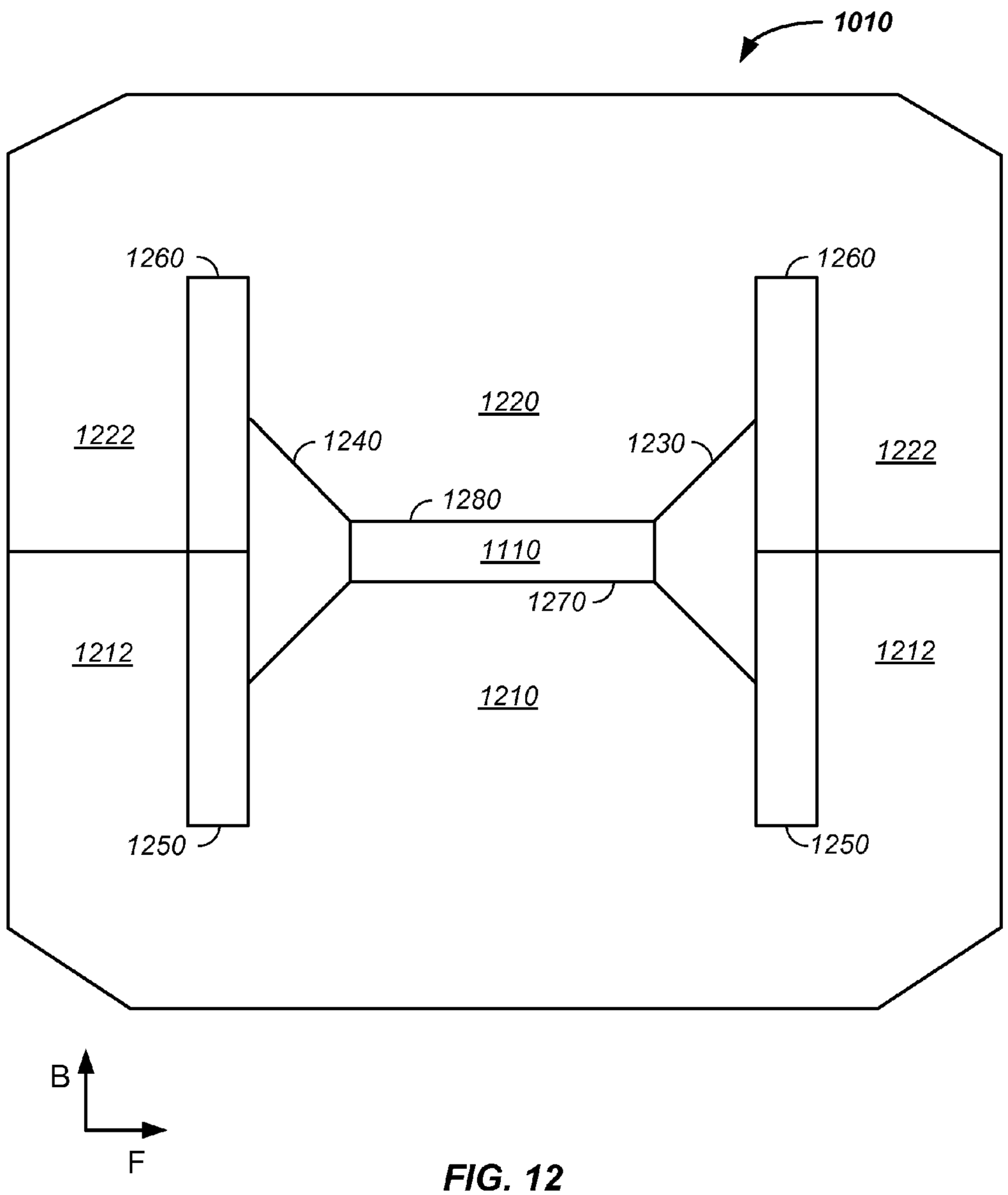
1010
1260
1260
1220
1222
1240
1230
1222
1280
1110
1270
1212
1212
1210
1250
1250
B
F

FIG. 12

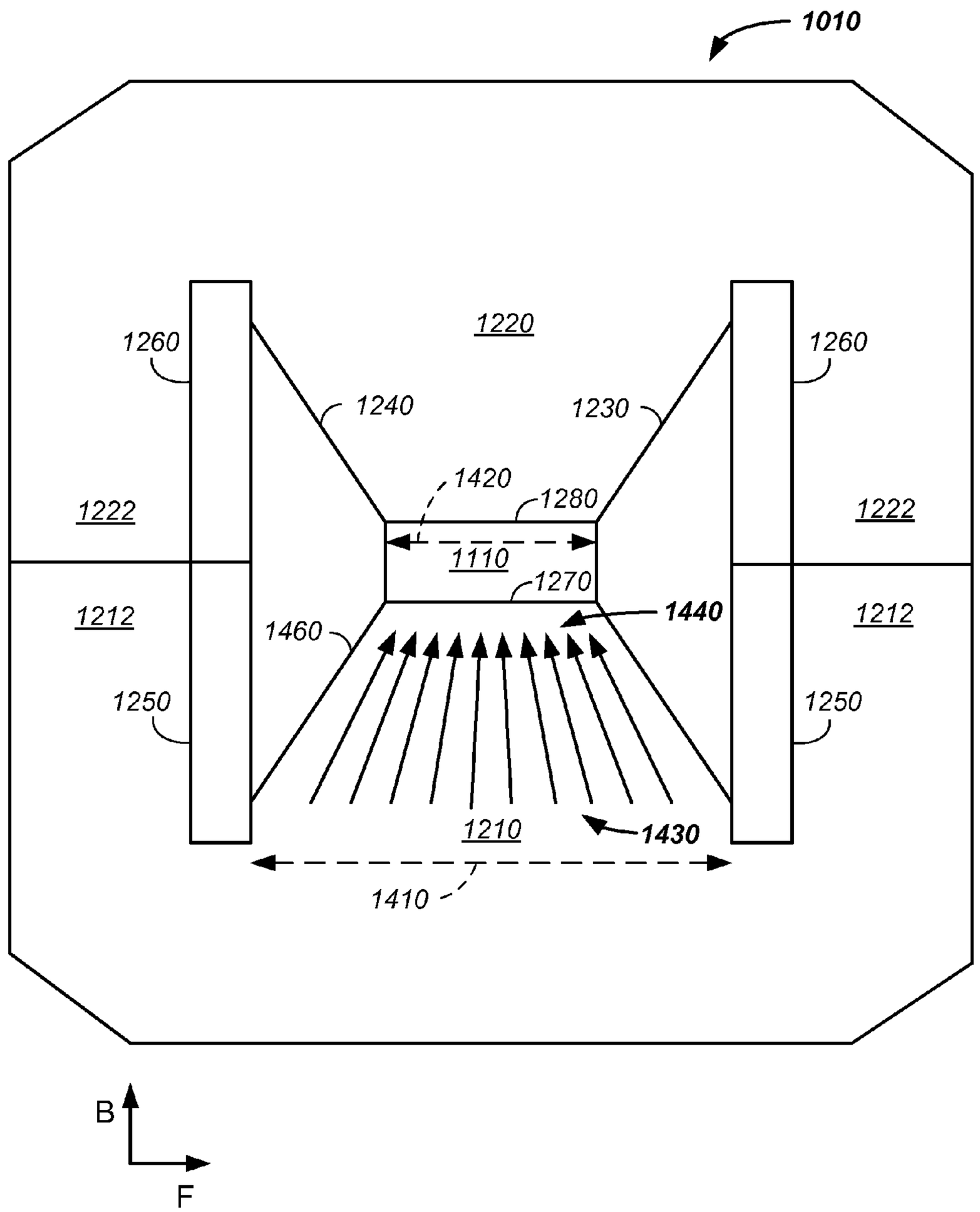
1010
1220
1260
1260
1240
1230
1420
1280
1222
1222
1110
1270
1212
1212
1460
1440
1250
1250
1210
1430
1410
B
F

FIG. 14

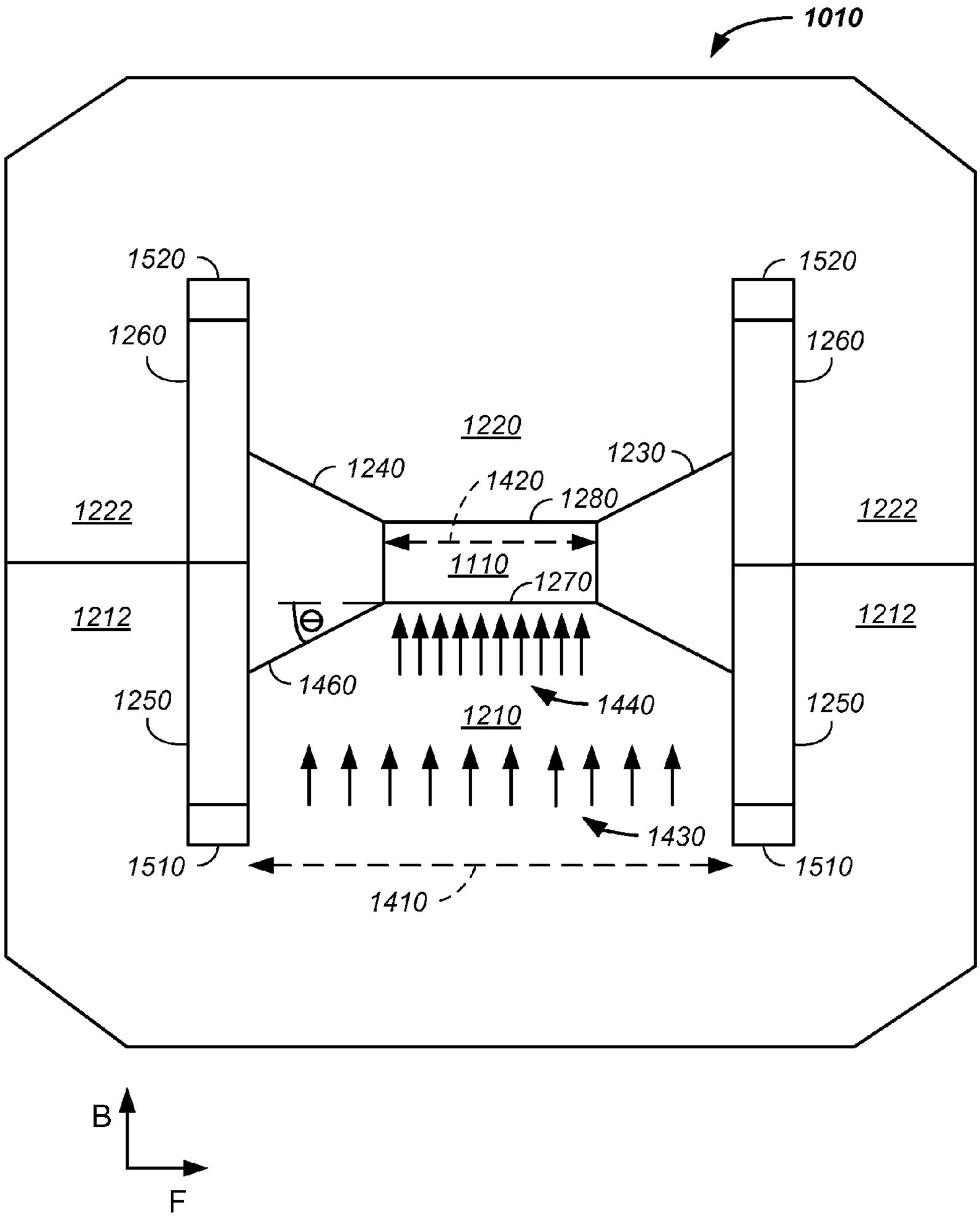
1010
1520
1520
1260
1260
1220
1230
1240
1420
1280
1222
1222
1110
1270
1212
1212
θ
1460
1250
1440
1250
1210
1430
1510
1510
1410
B
F

FIG. 15

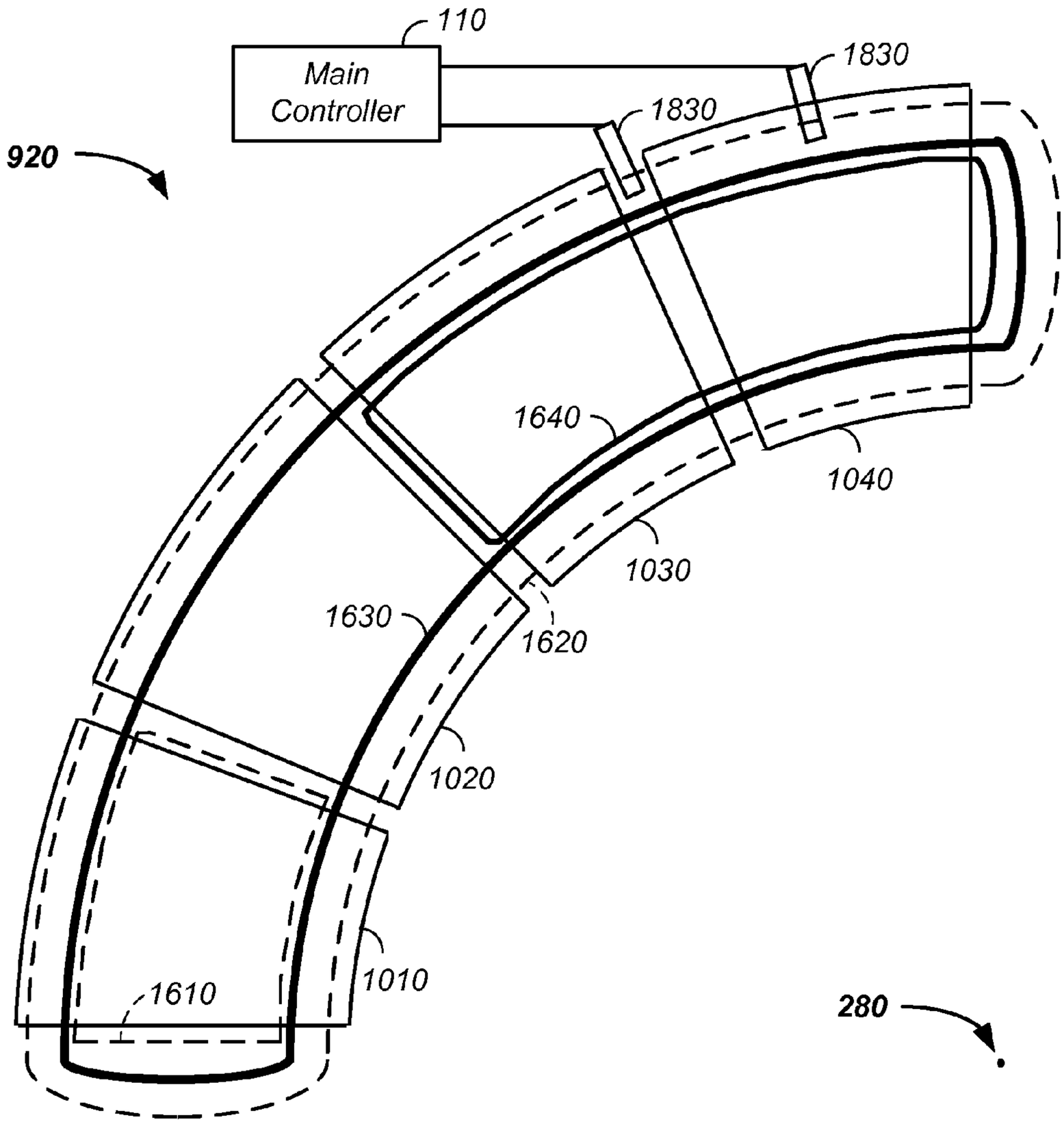
110
Main Controller
1830
1830
920
1640
1040
1030
1630
1620
1020
1610
1010
280

FIG. 16

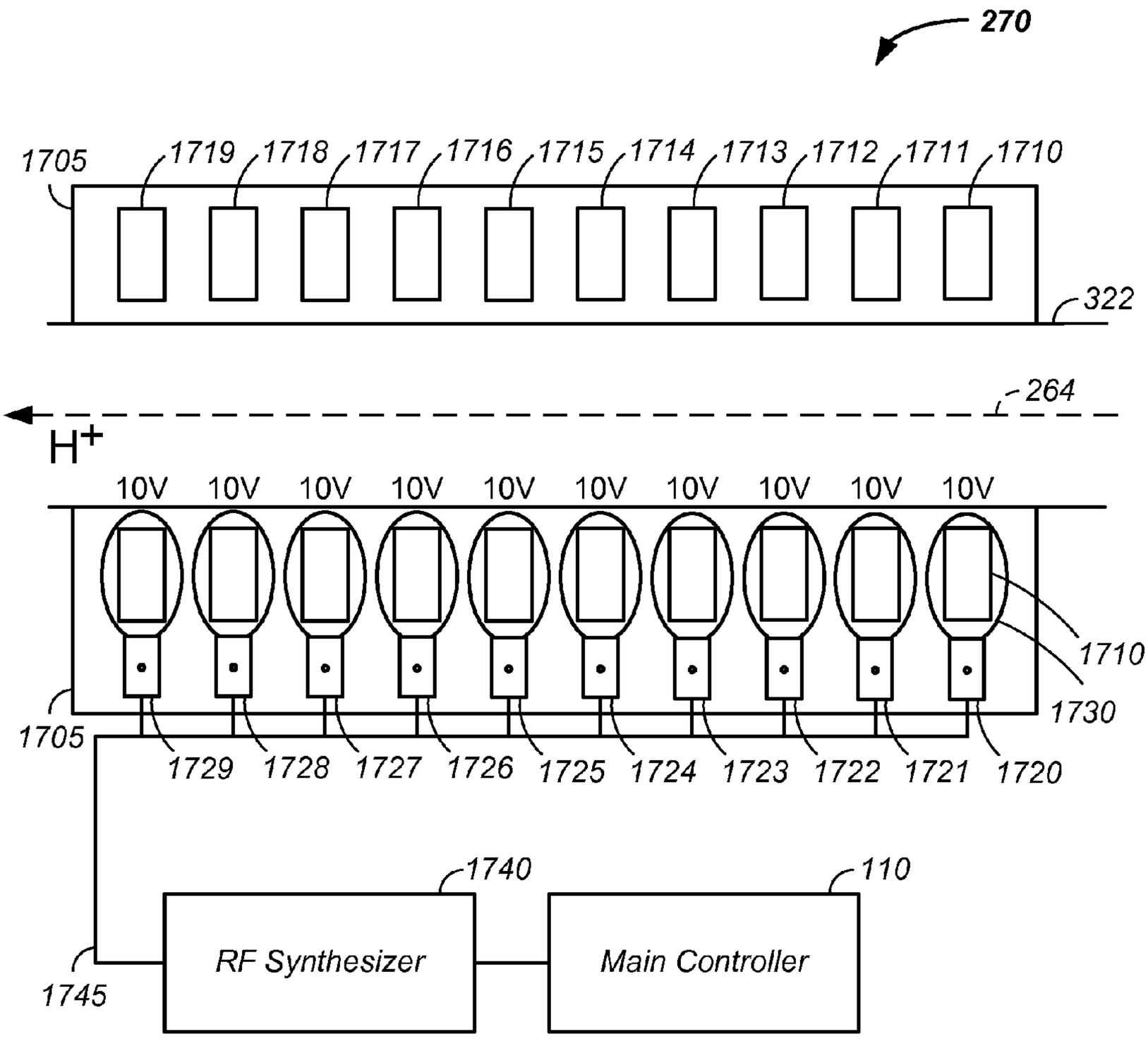

FIG. 17A

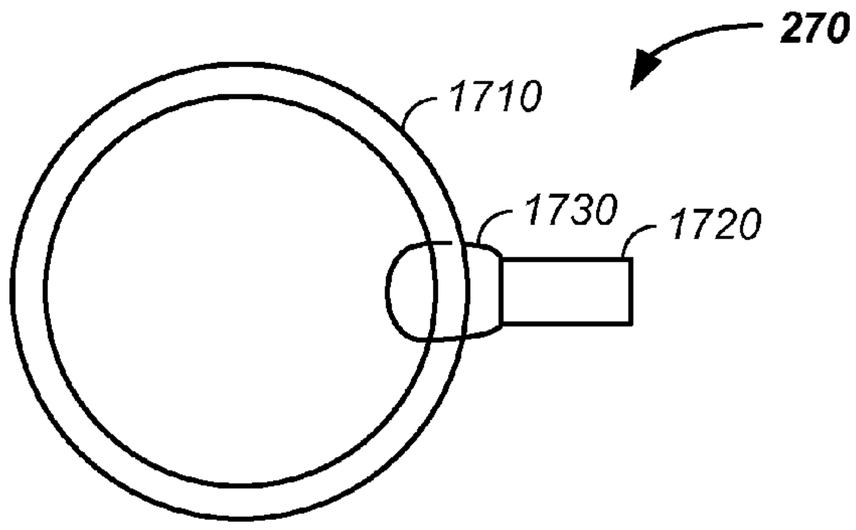

FIG. 17B

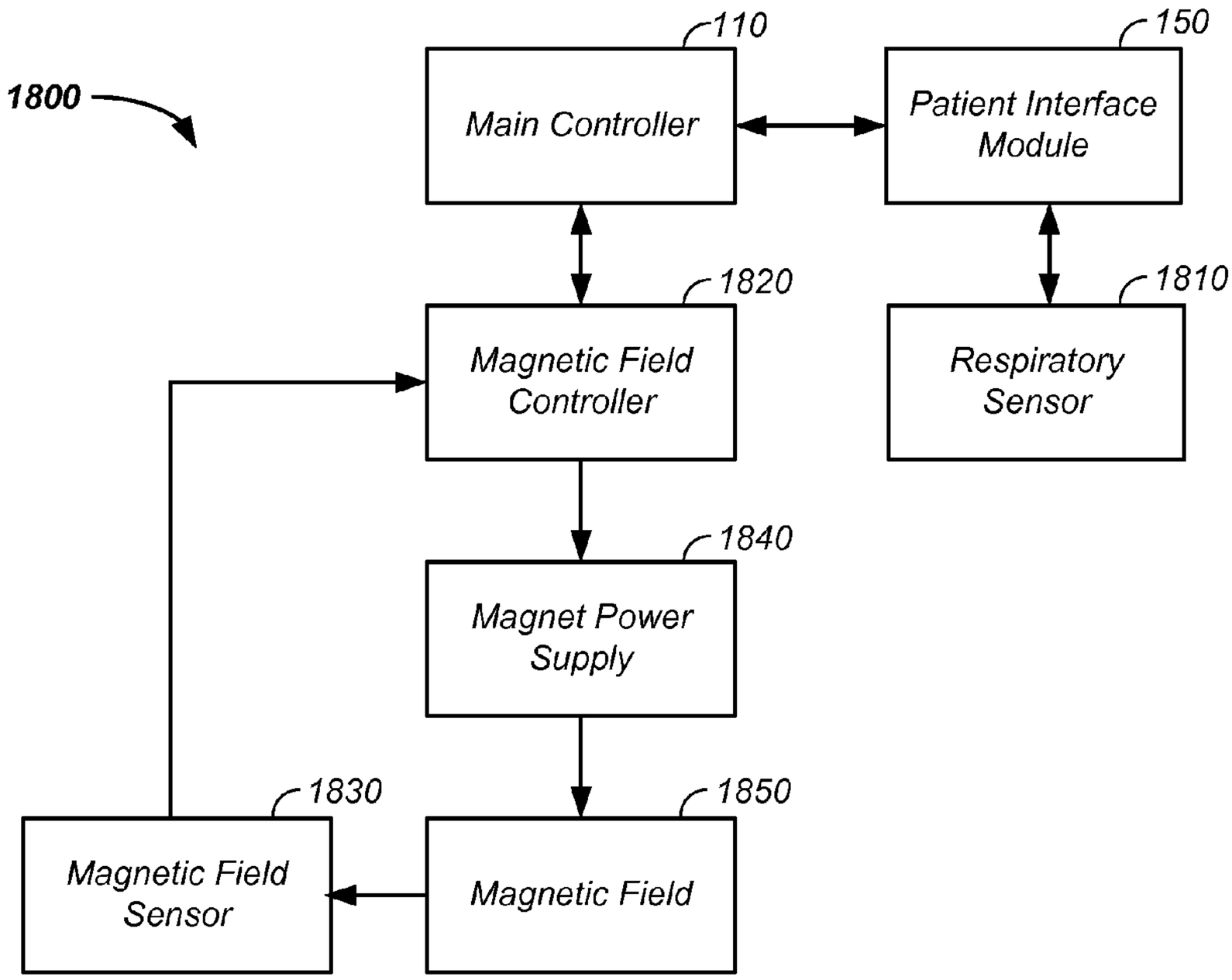
1800
110
Main Controller
150
Patient Interface Module
1820
Magnetic Field Controller
1810
Respiratory Sensor
1840
Magnet Power Supply
1830
Magnetic Field Sensor
1850
Magnetic Field

FIG. 18

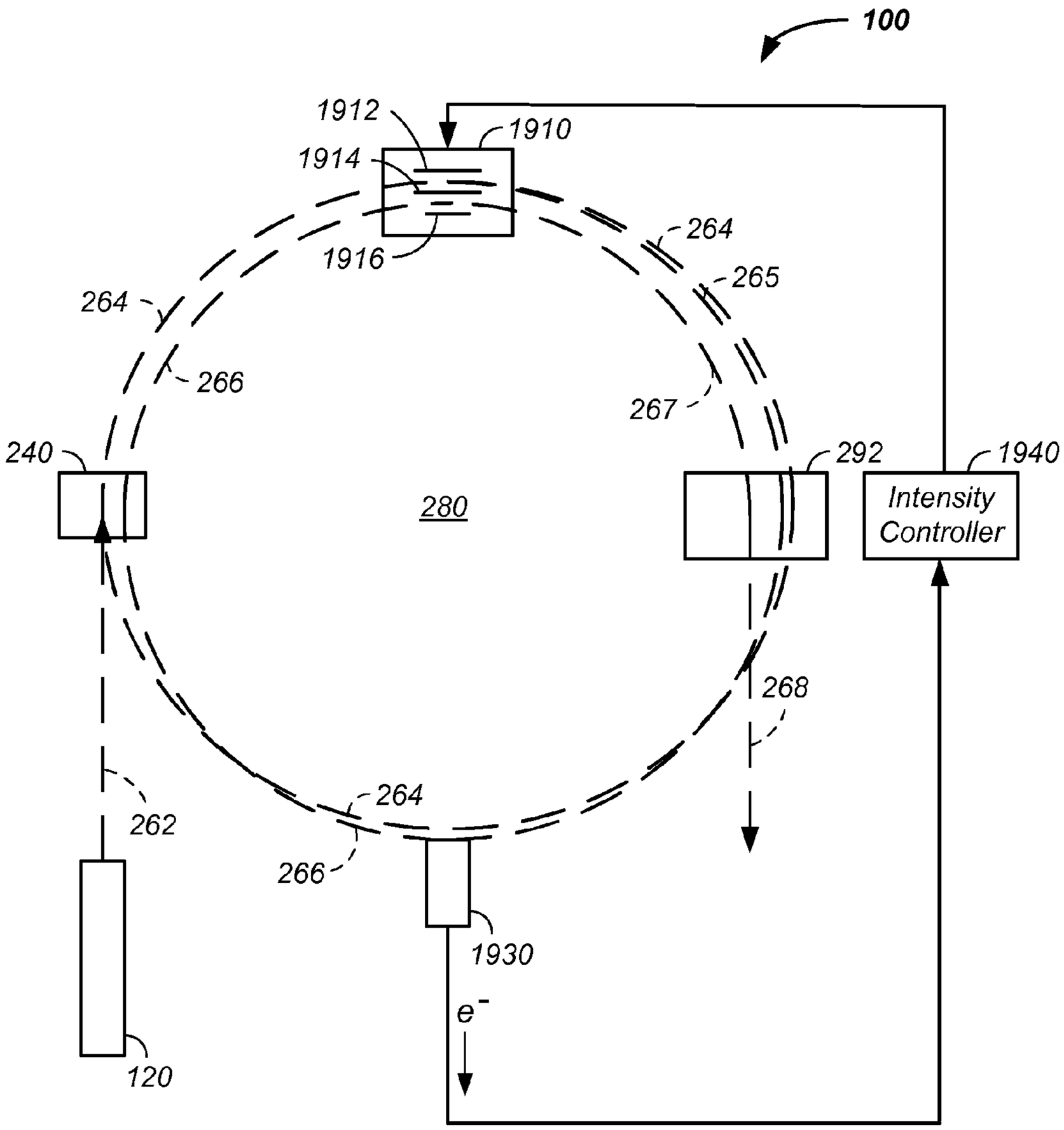
100
1912
1910
1914
1916
264
265
264
266
267
240
292
1940
Intensity Controller
280
268
262
264
266
1930
120
e-

FIG. 19

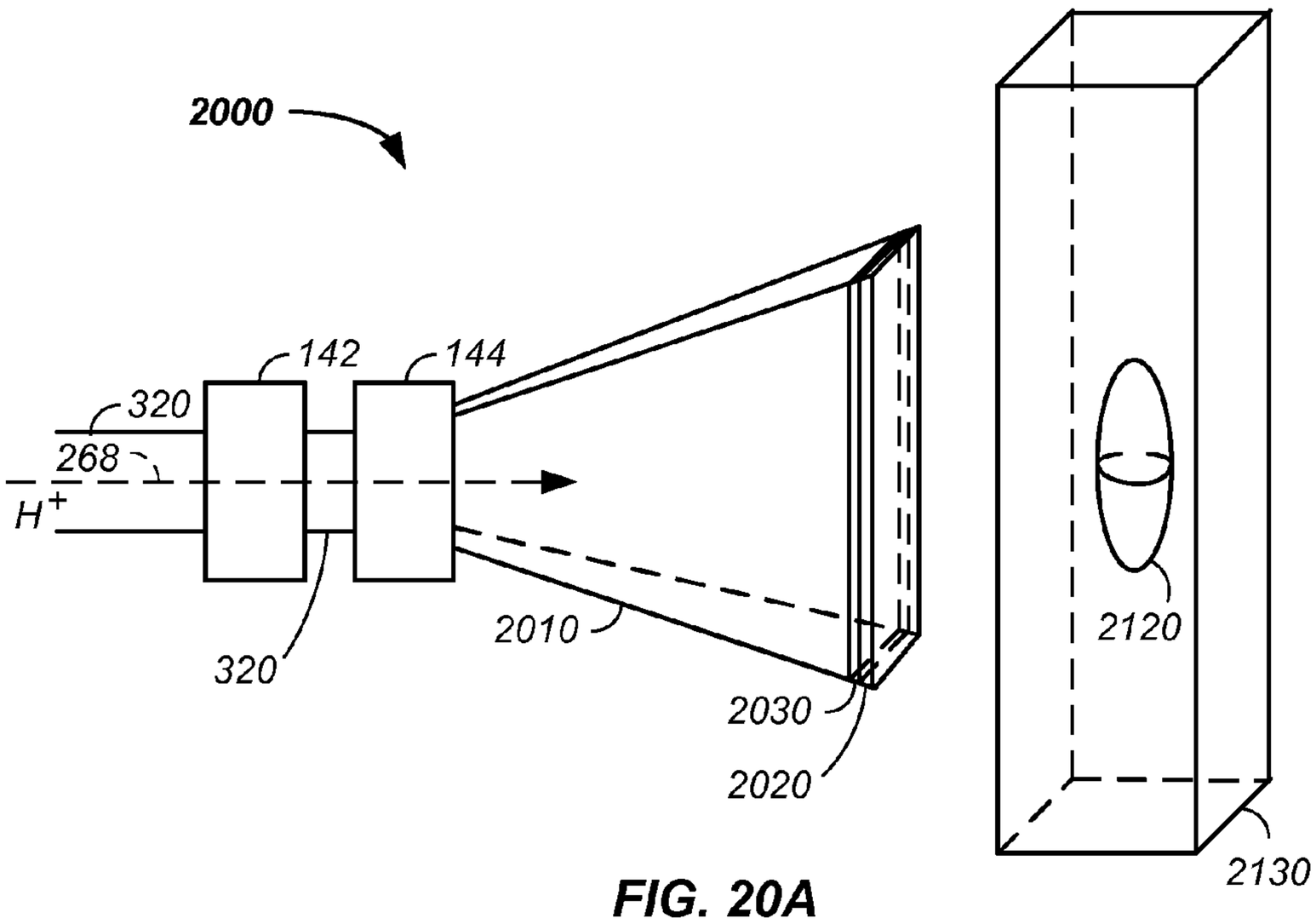

FIG. 20A

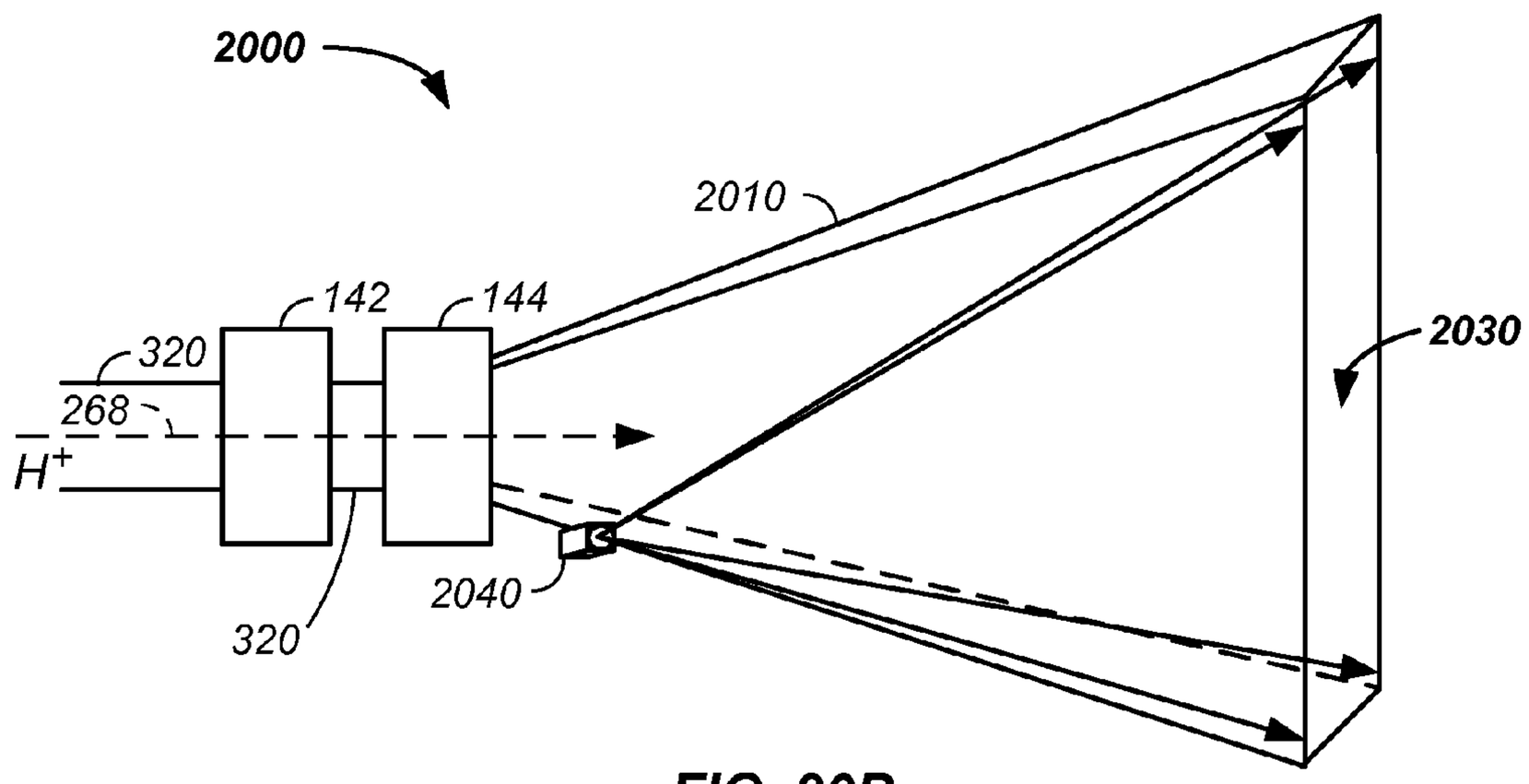

FIG. 20B

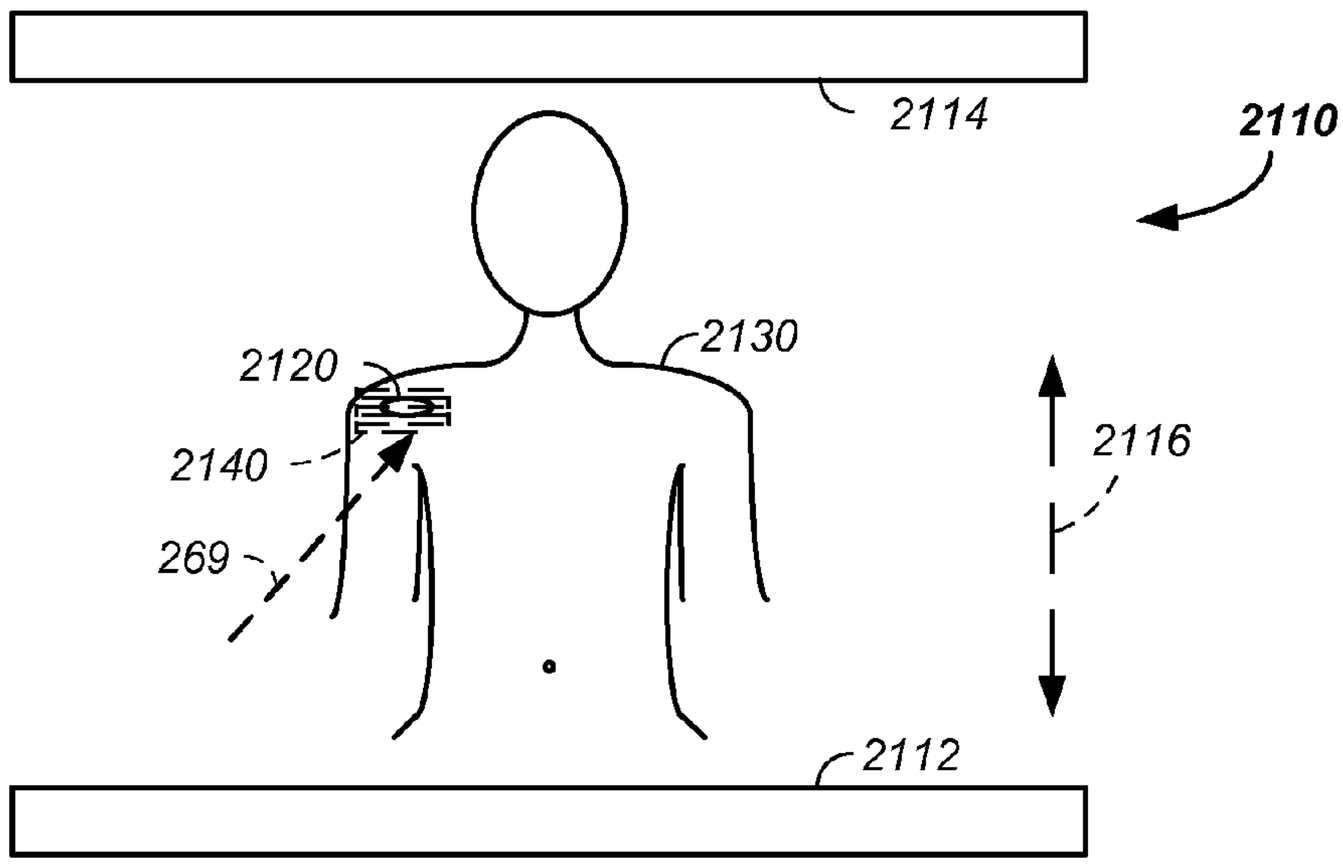

FIG. 21A

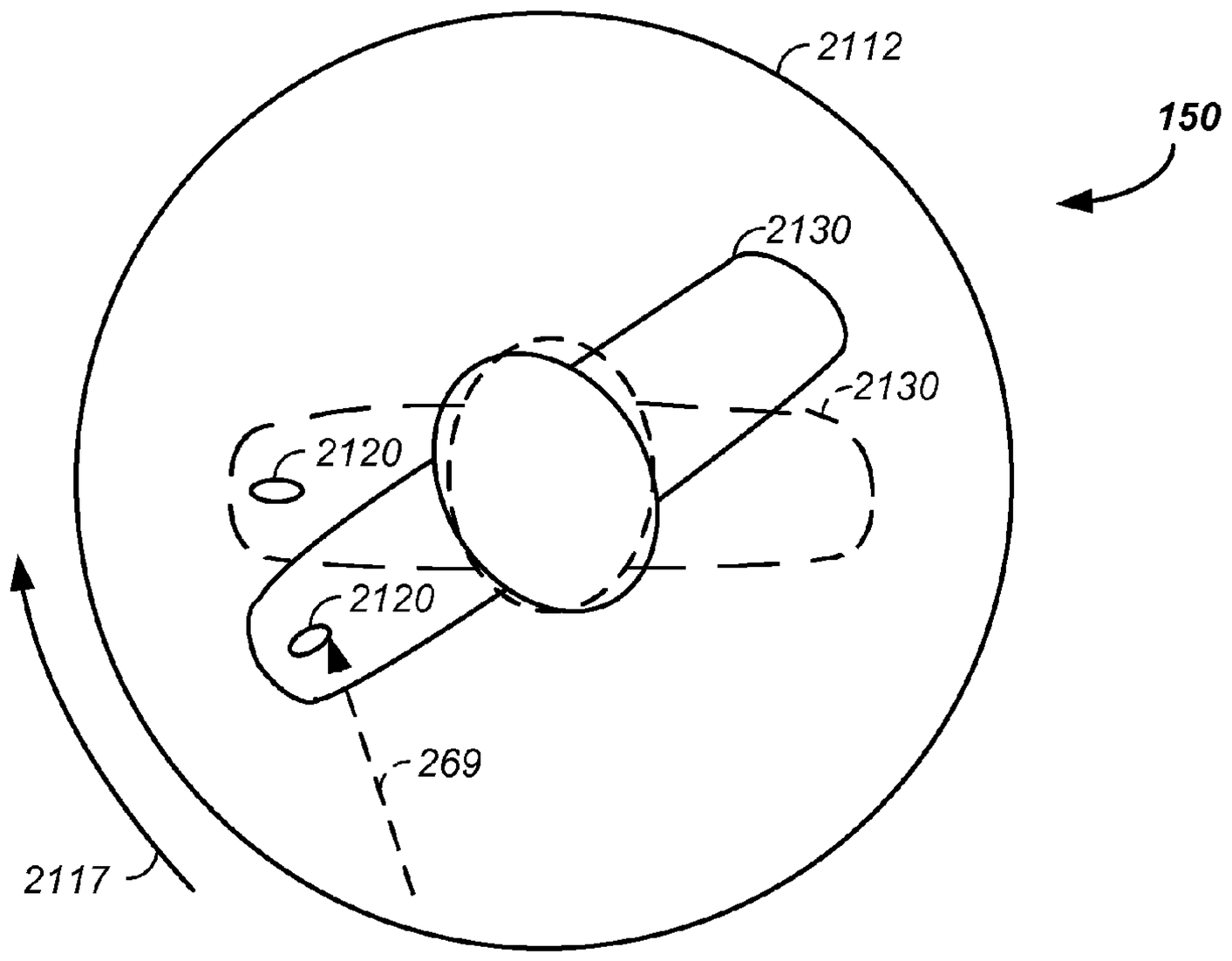

FIG. 21B

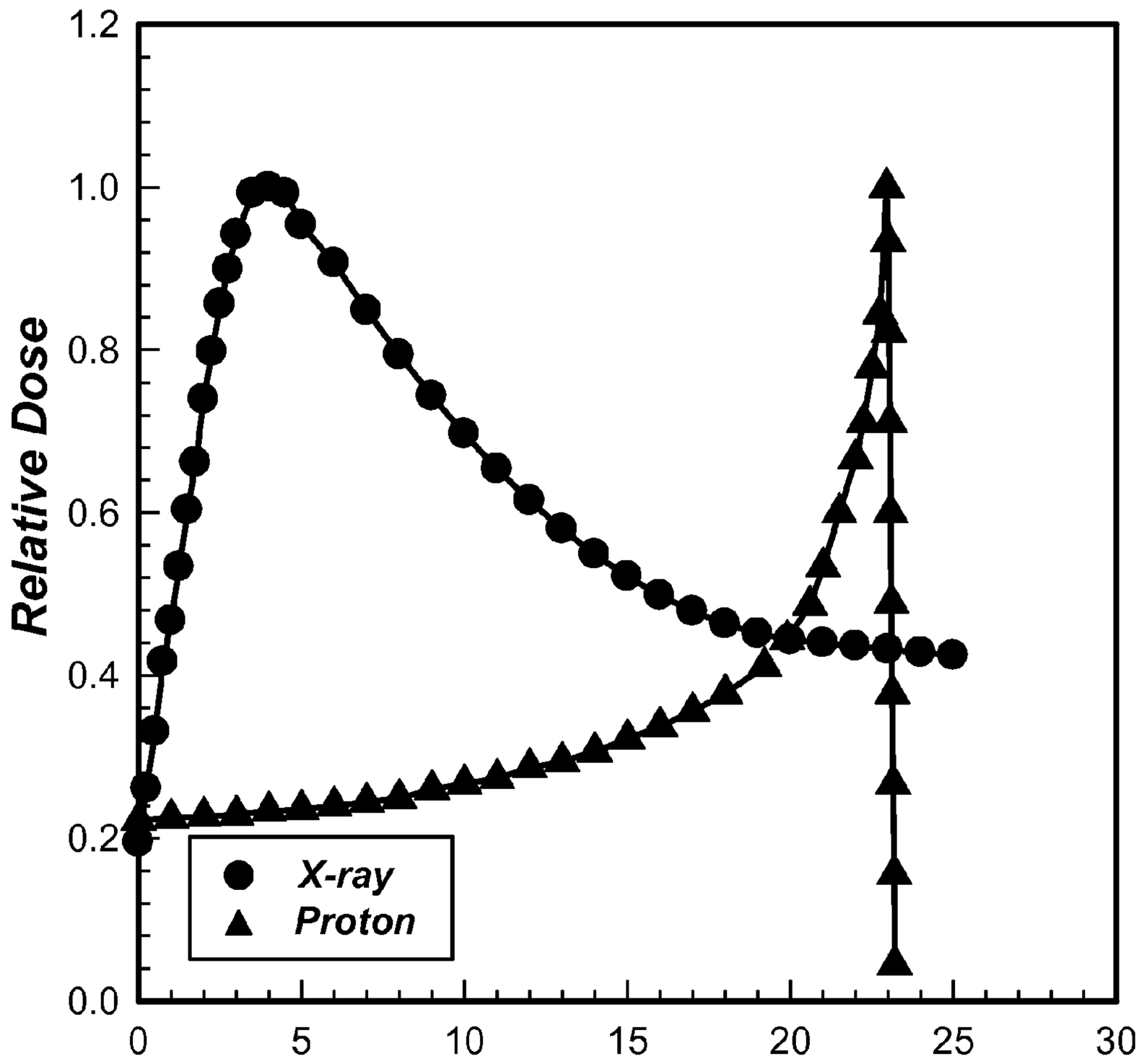
1.2
1.0
0.8
0.6
0.4
0.2
0.0
Relative Dose
X-ray
Proton
0
5
10
15
20
25
30
Depth in Tissue (cm)

FIG. 22

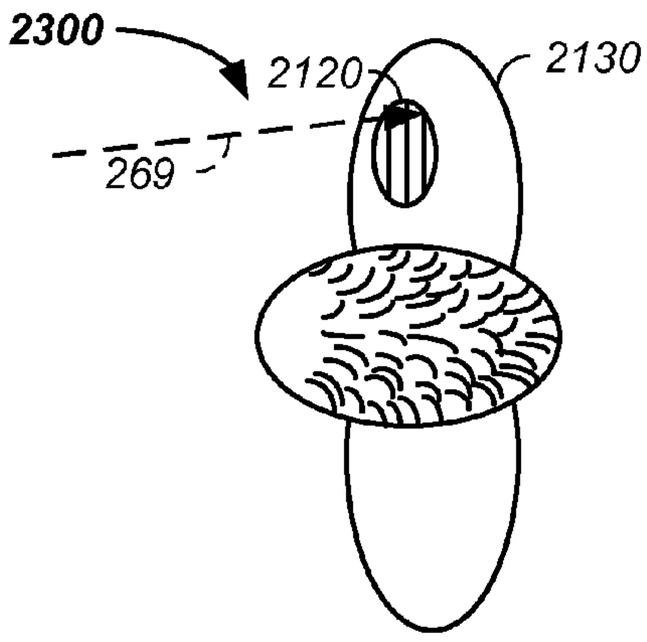

FIG. 23A

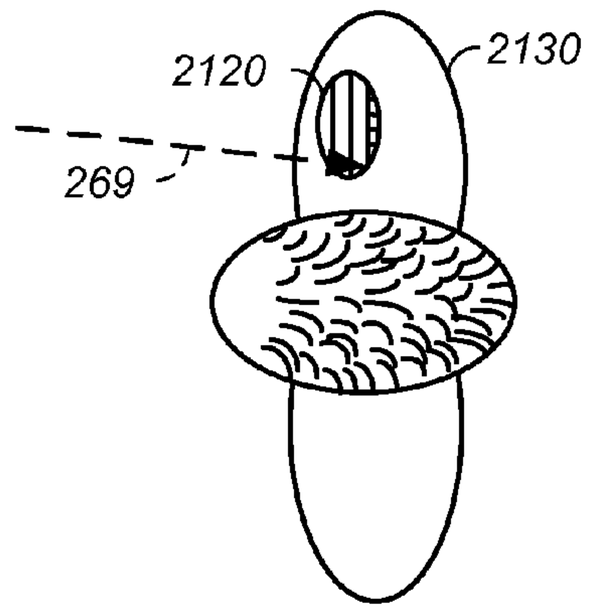

FIG. 23B

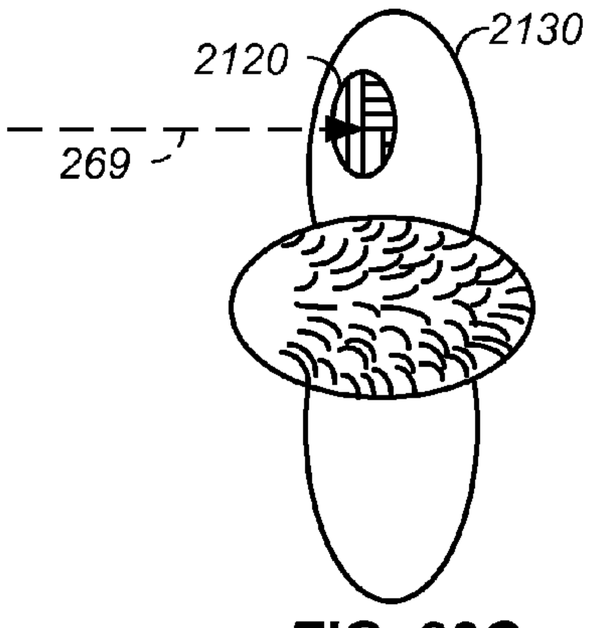

FIG. 23C

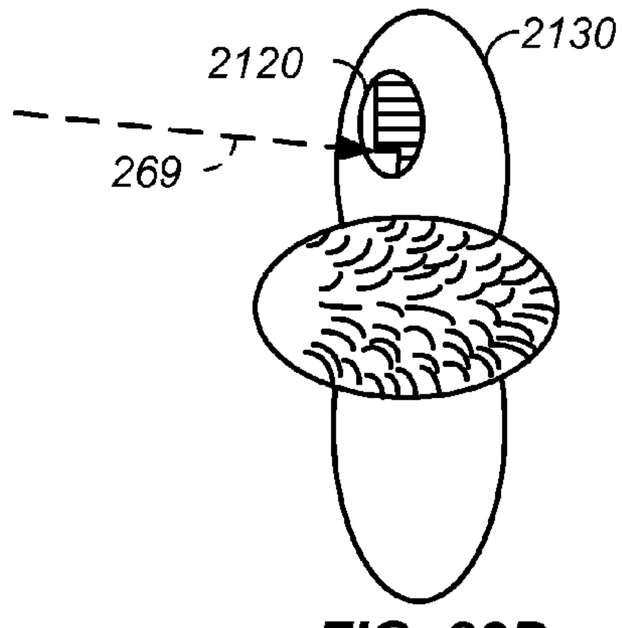

FIG. 23D

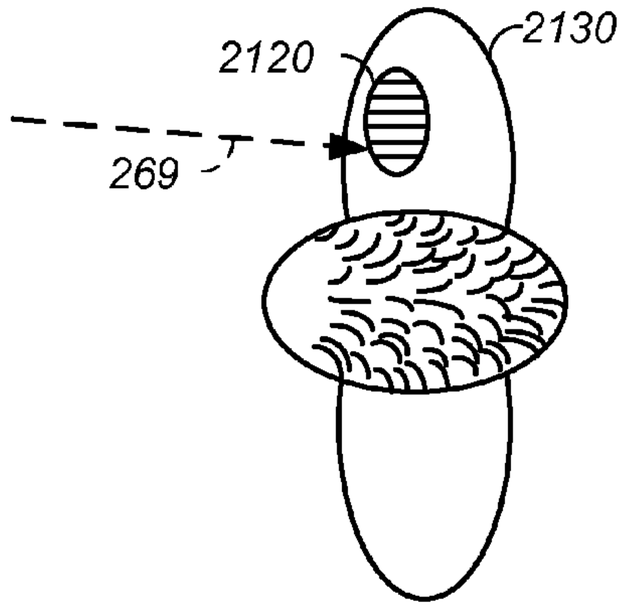

FIG. 23E

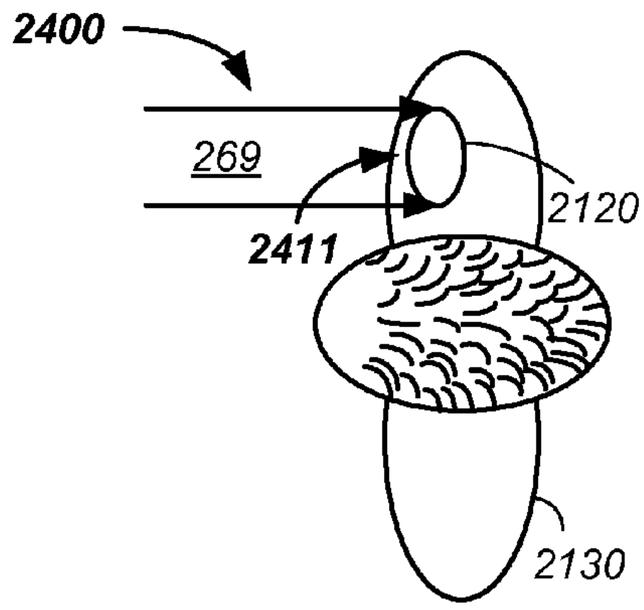

FIG. 24A

FIG. 24B

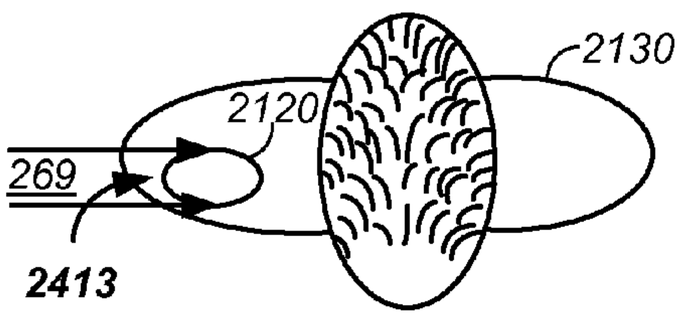

FIG. 24C

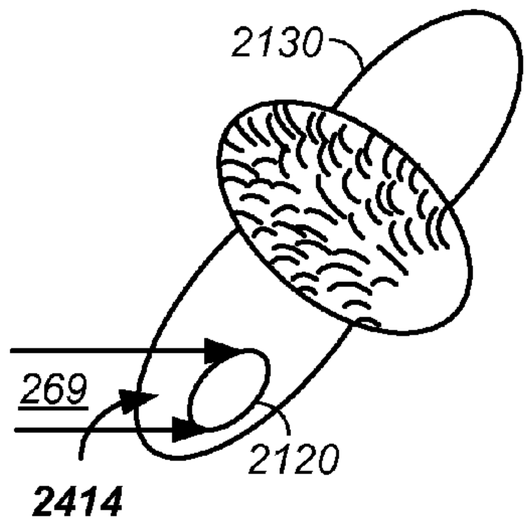

FIG. 24D

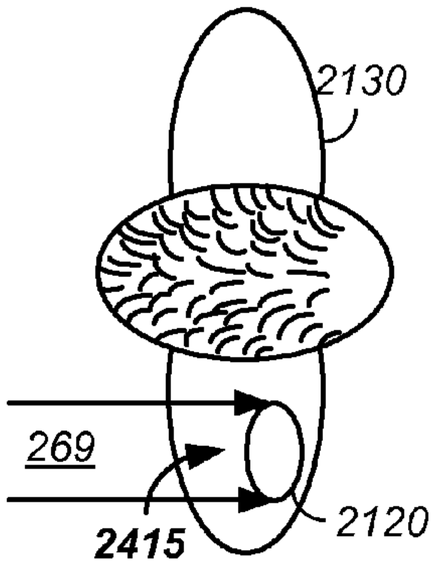

FIG. 24E

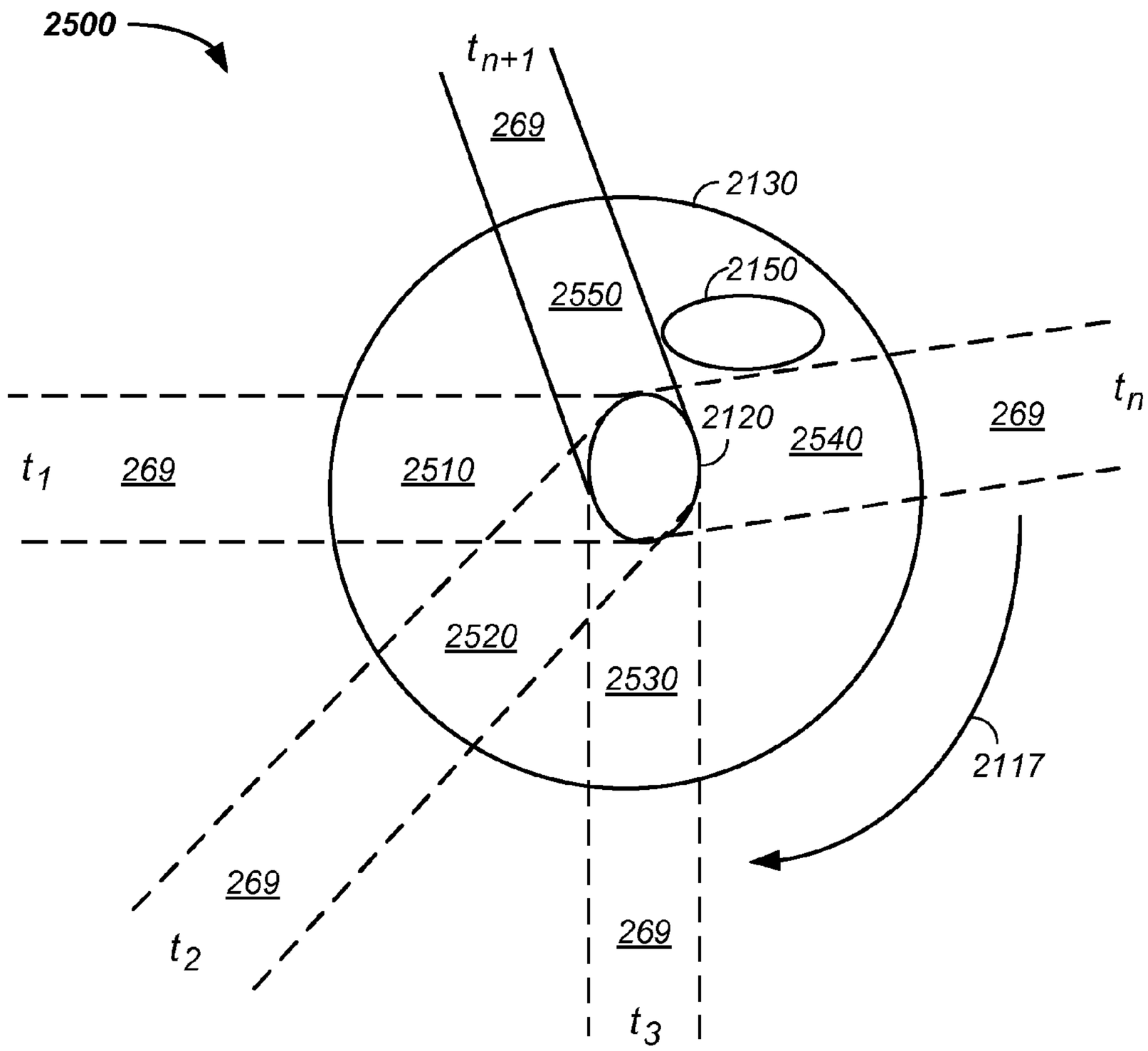
2500
t_{n+1}
269
2130
2150
2550
t_n
269
2120
2540
t_1
269
2510
2520
2530
2117
269
t_2
269
t_3

FIG. 25

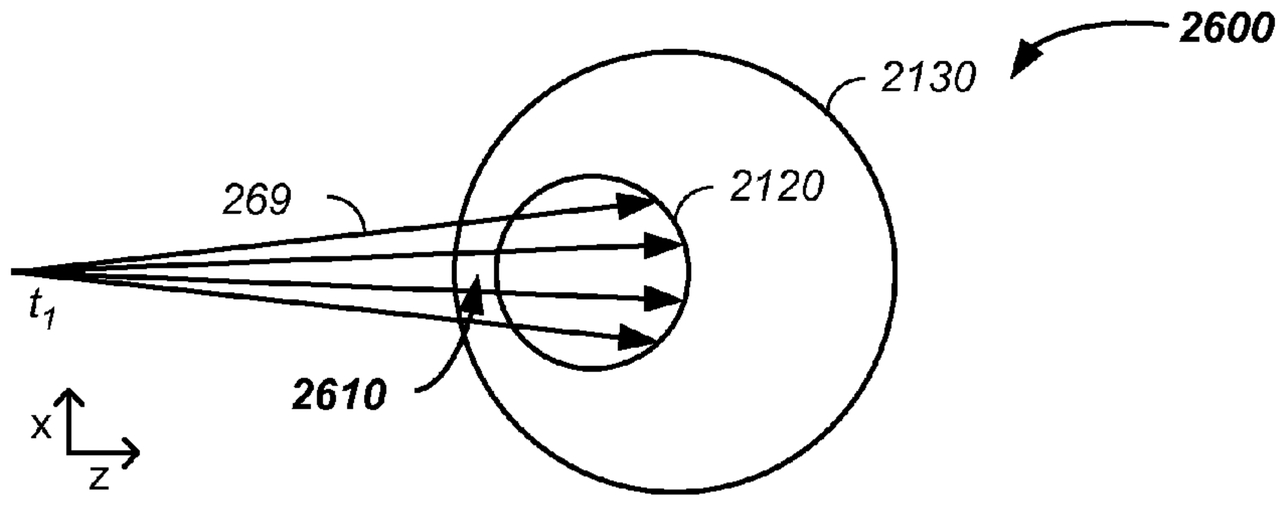

FIG. 26A

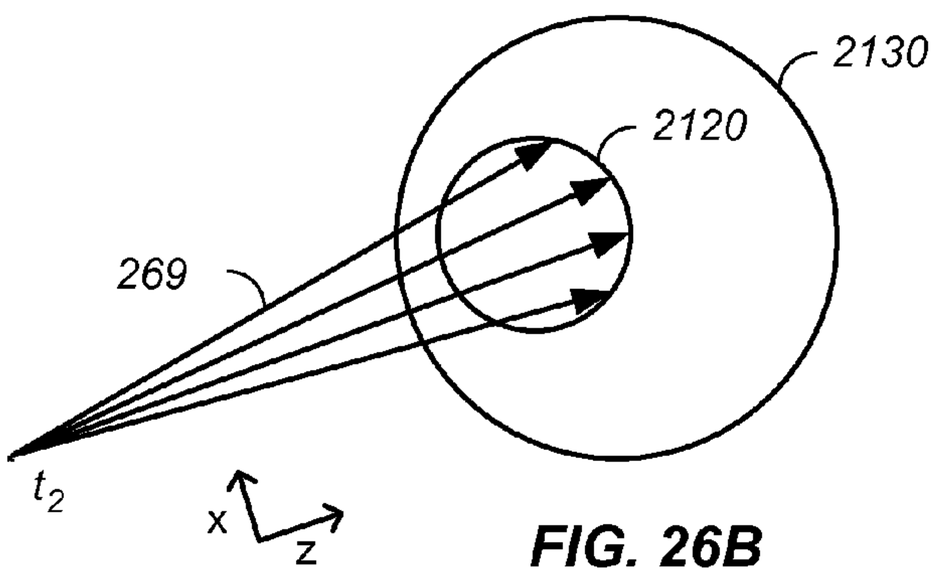

FIG. 26B

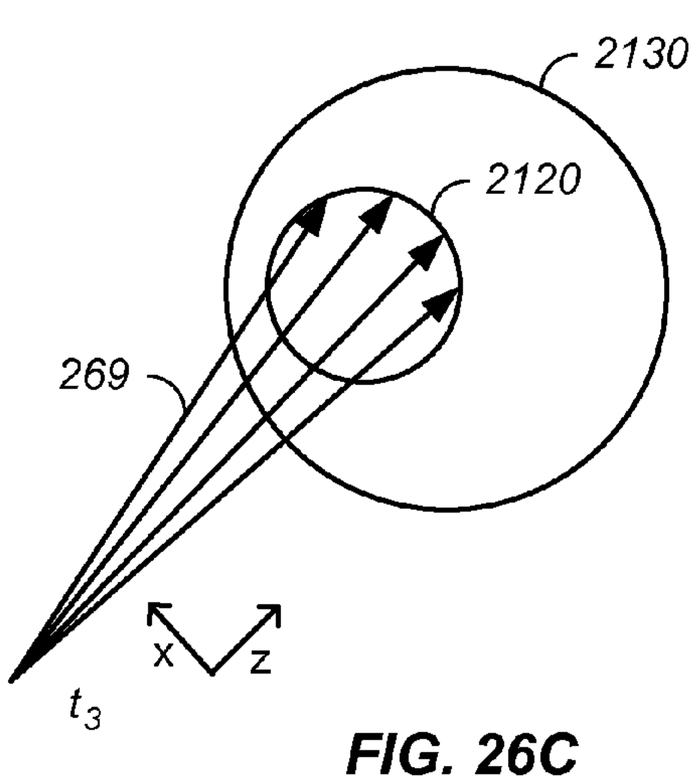

FIG. 26C

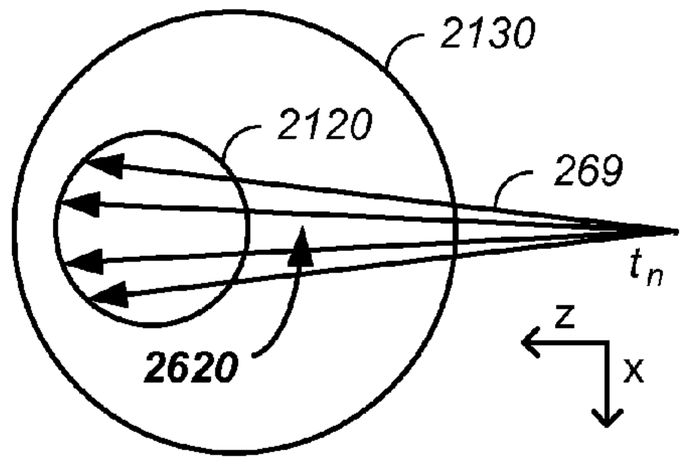

FIG. 26D

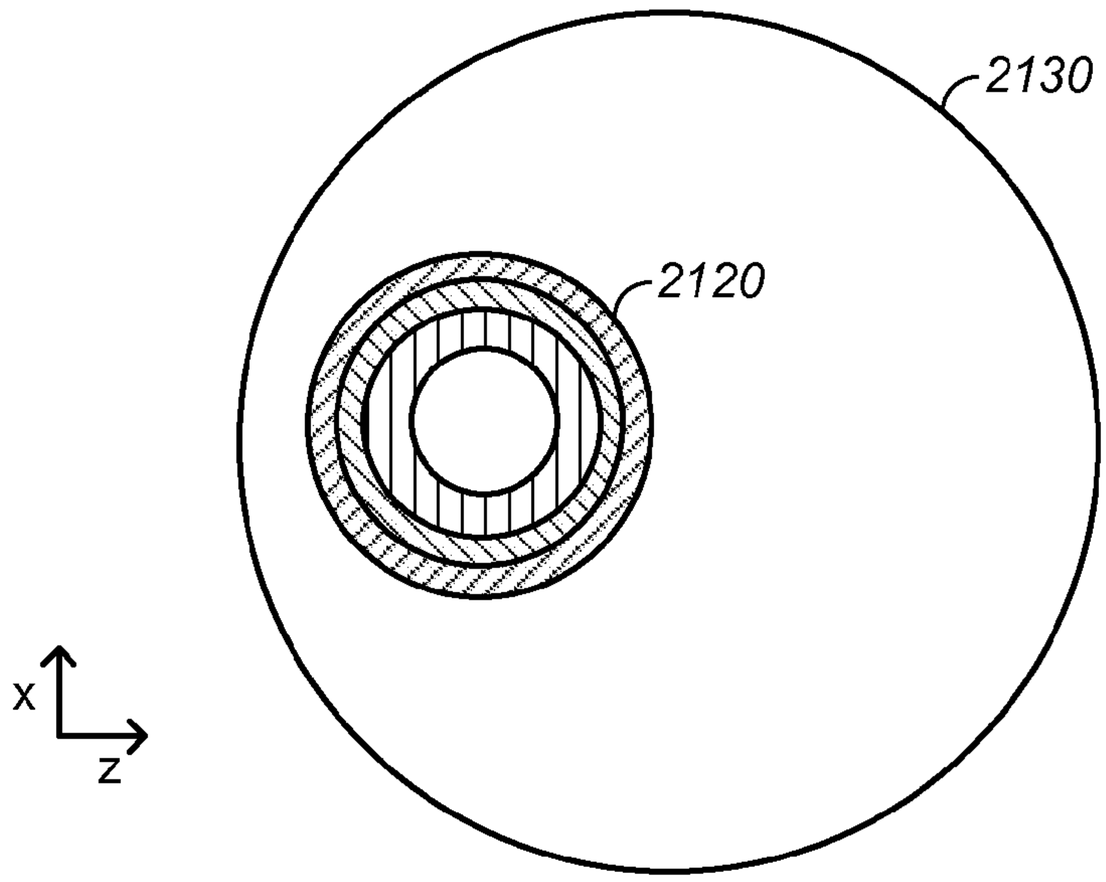

FIG. 26E

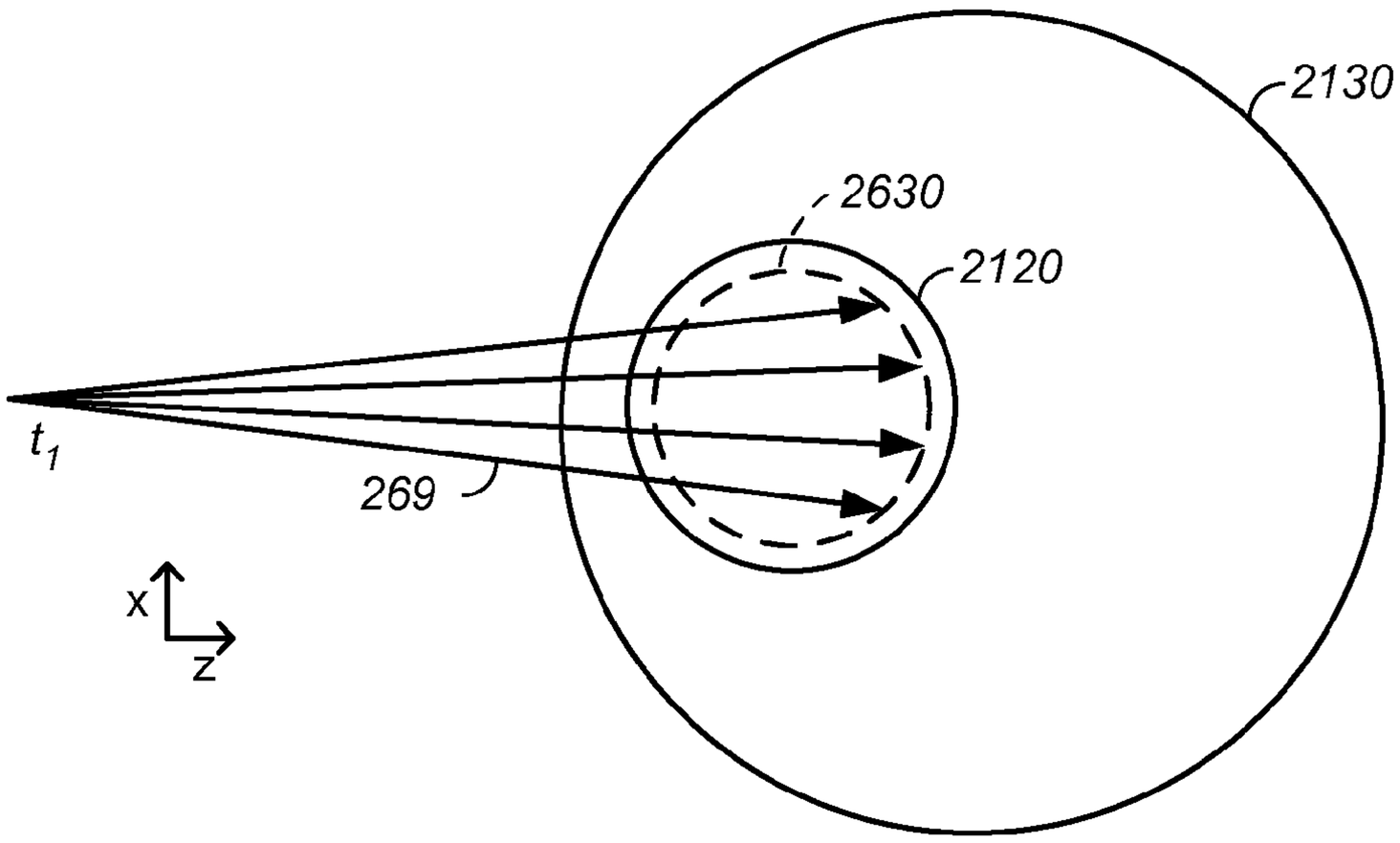

FIG. 26F

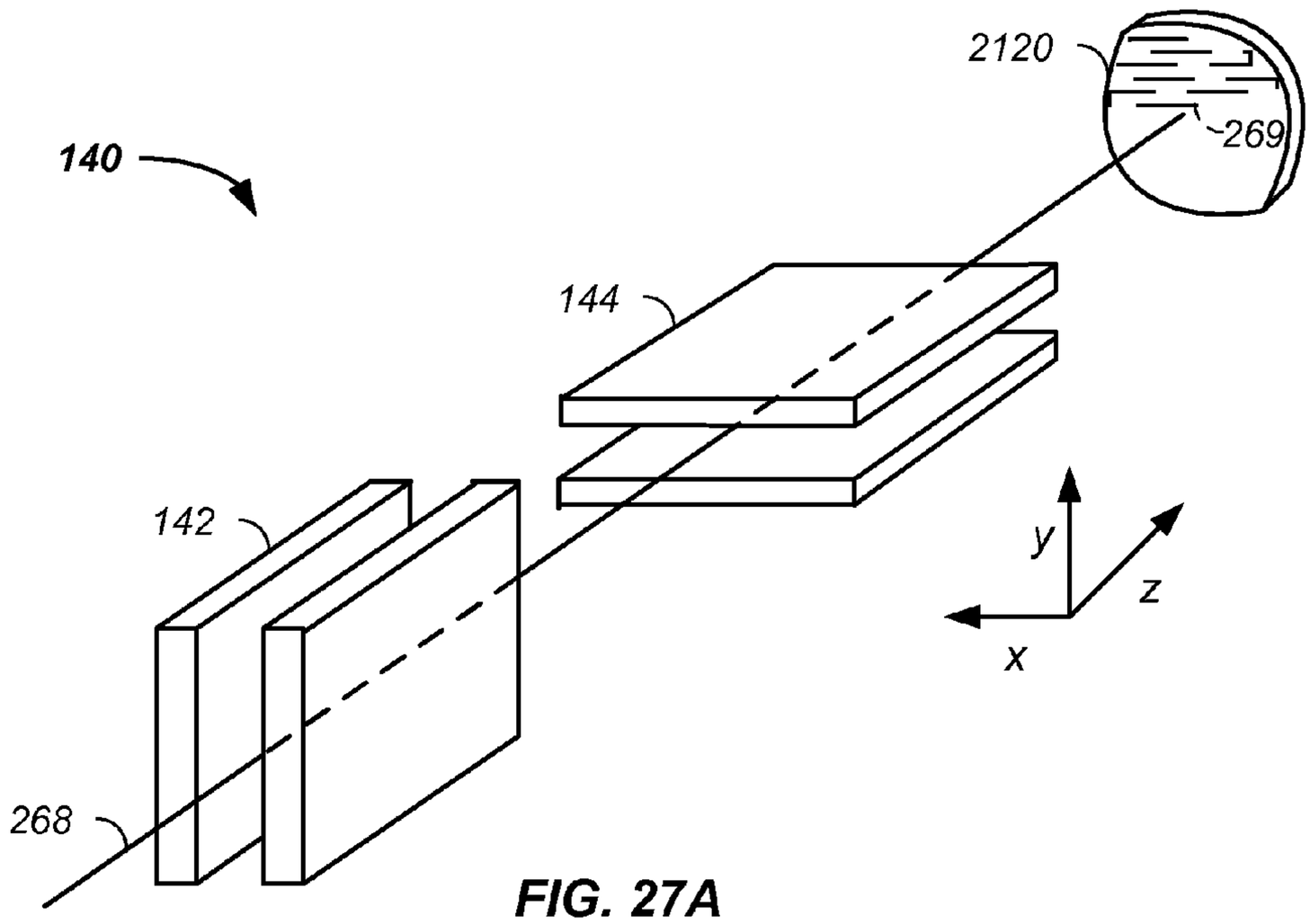

FIG. 27A

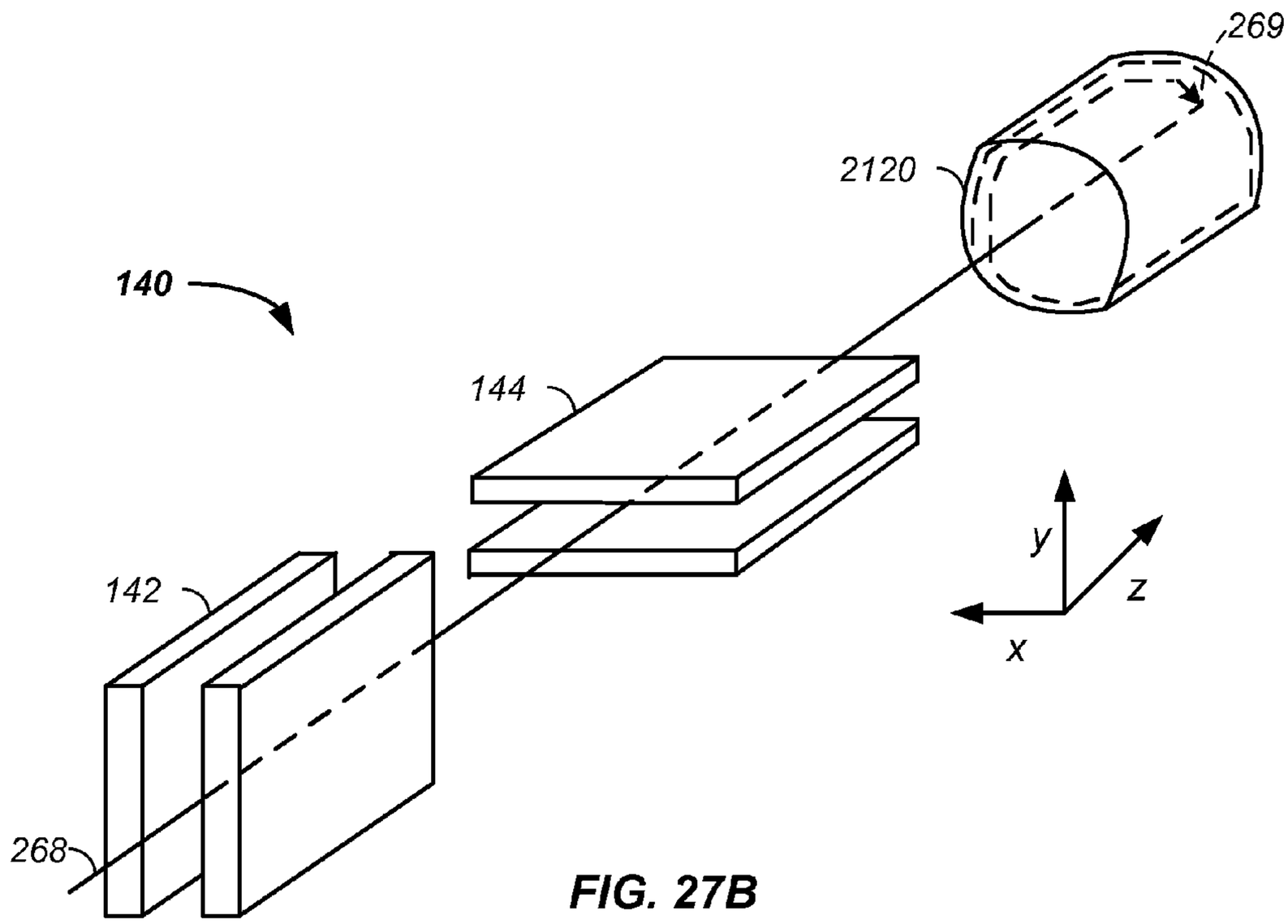

FIG. 27B

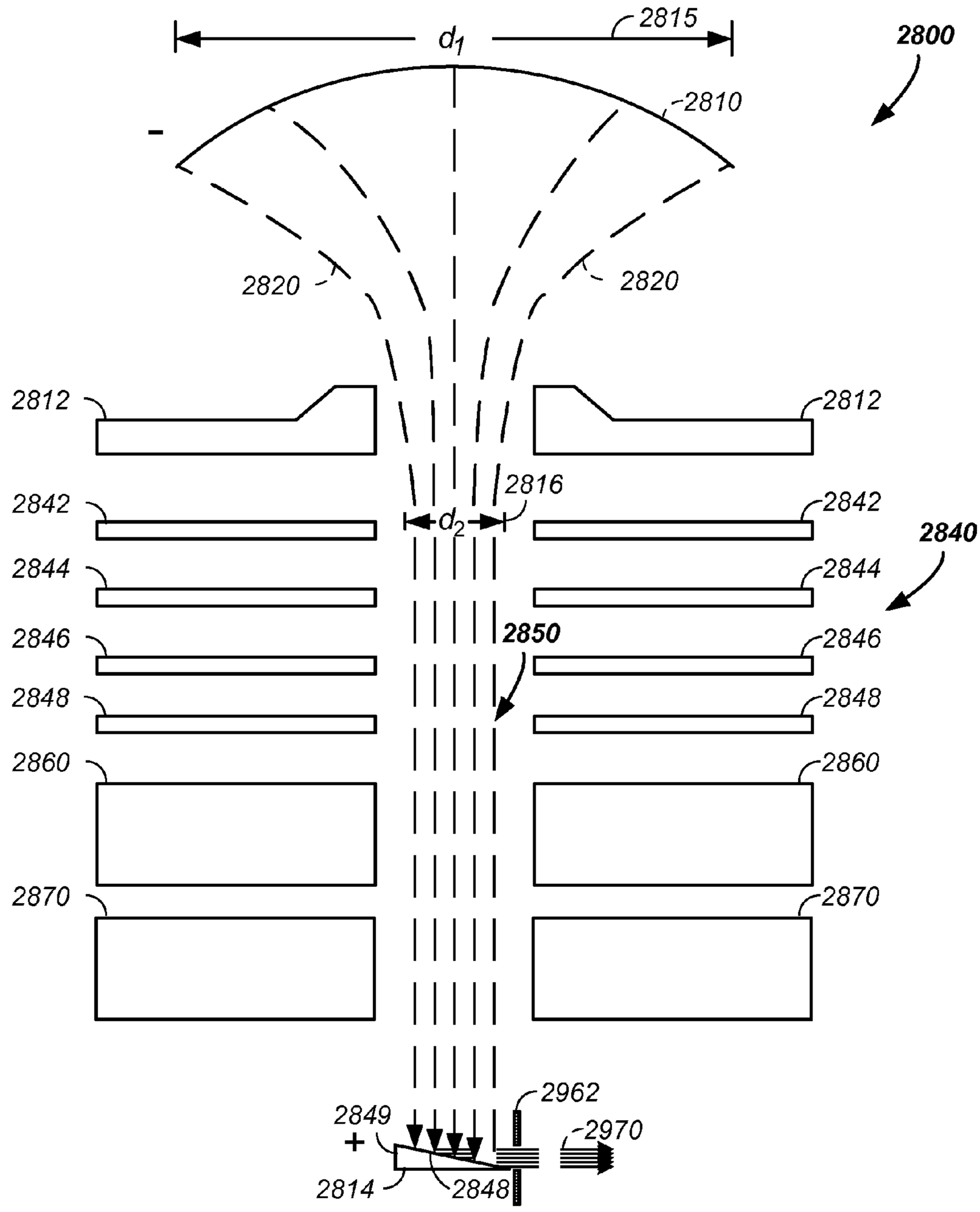
d_1
2815
2800
2810
2820
2820
2812
2812
2816
2842
2842
d_2
2840
2844
2844
2850
2846
2846
2848
2848
2860
2860
2870
2870
2962
2849
2970
2814
2848

FIG. 28

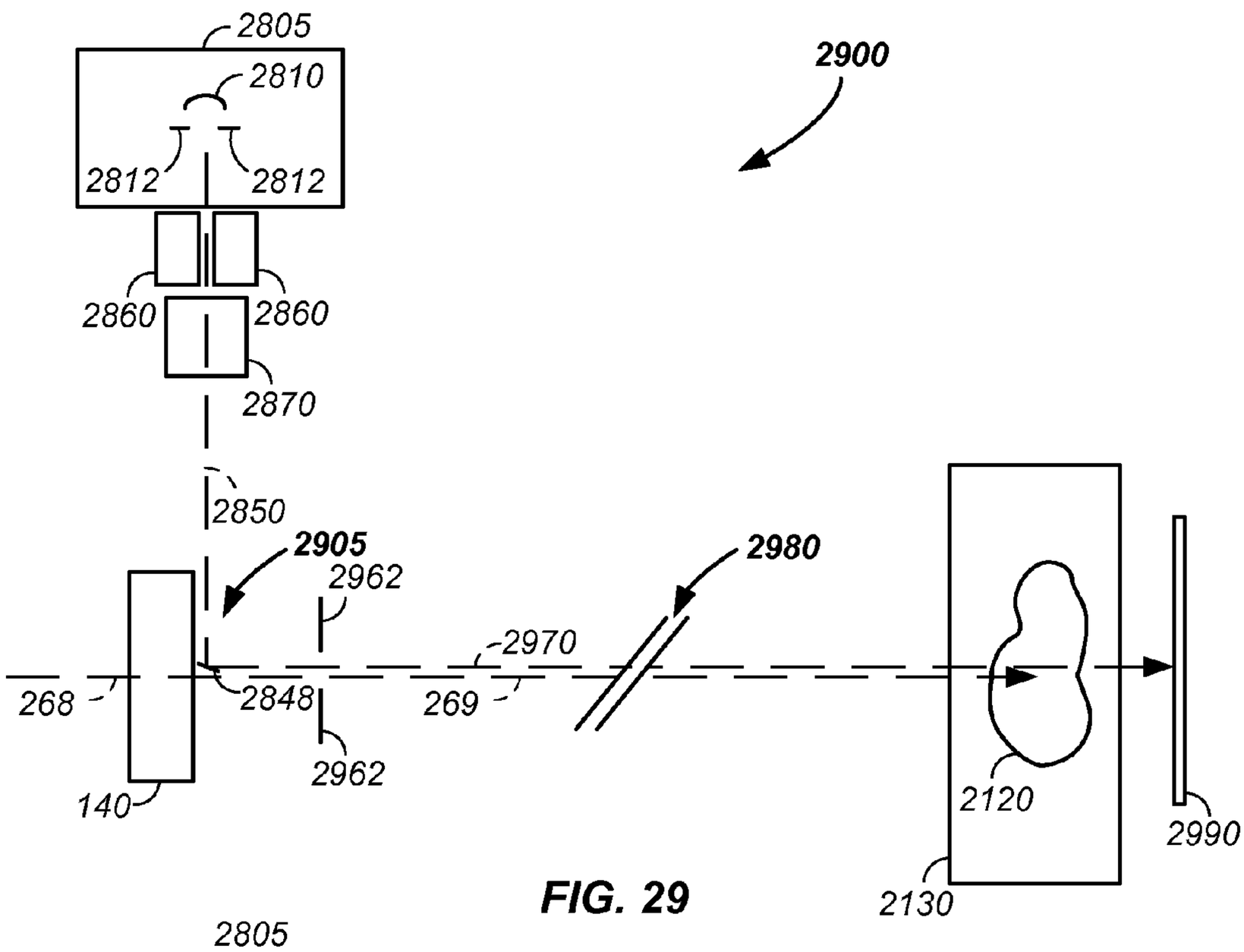
2805
2810
2812
2812
2860
2860
2870
2850
2905
2962
2980
2970
268
2848
269
2962
140
2120
2990
2130
2900

FIG. 29

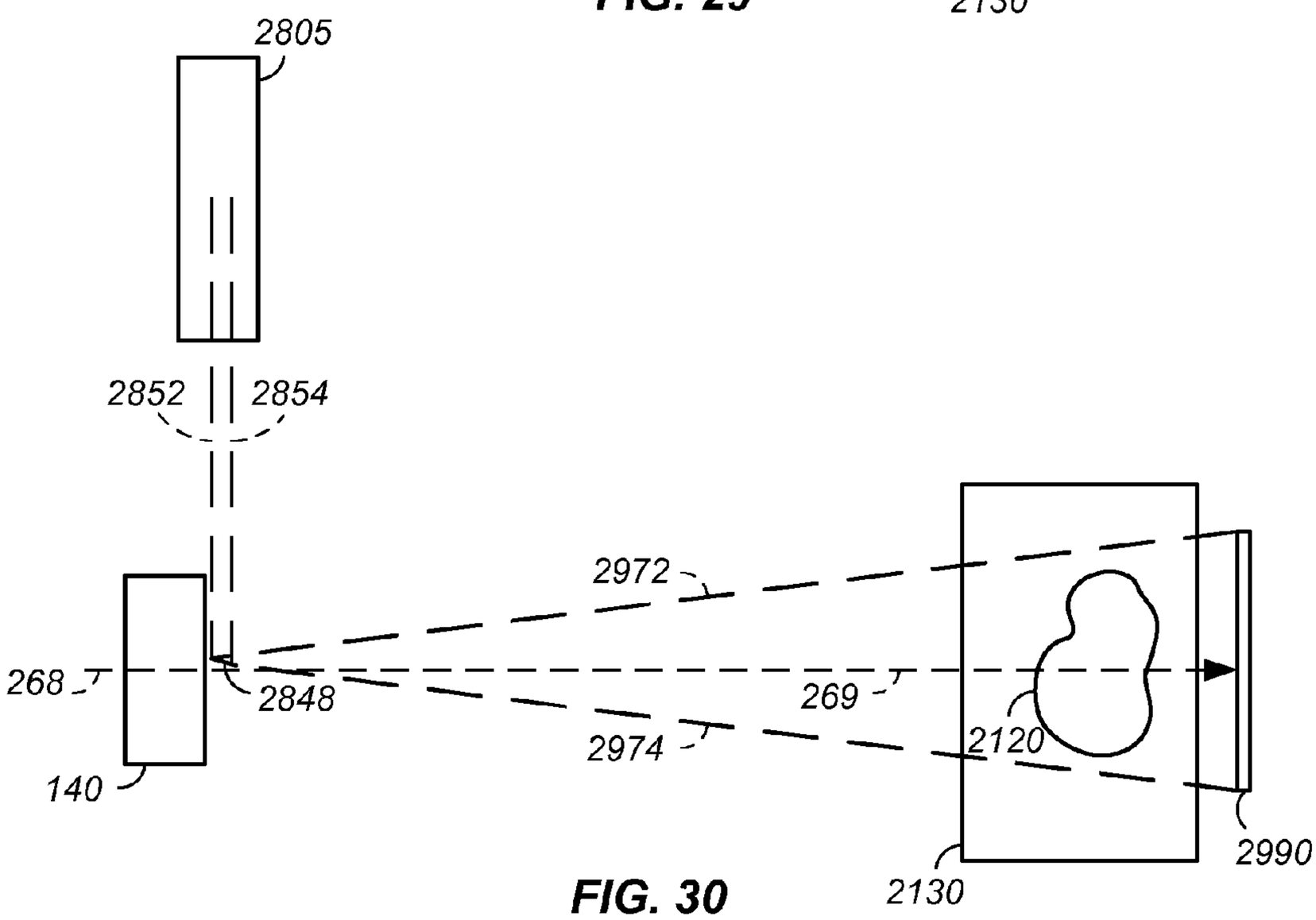
2805
2852
2854
2972
268
2848
269
2974
140
2120
2990
2130

FIG. 30

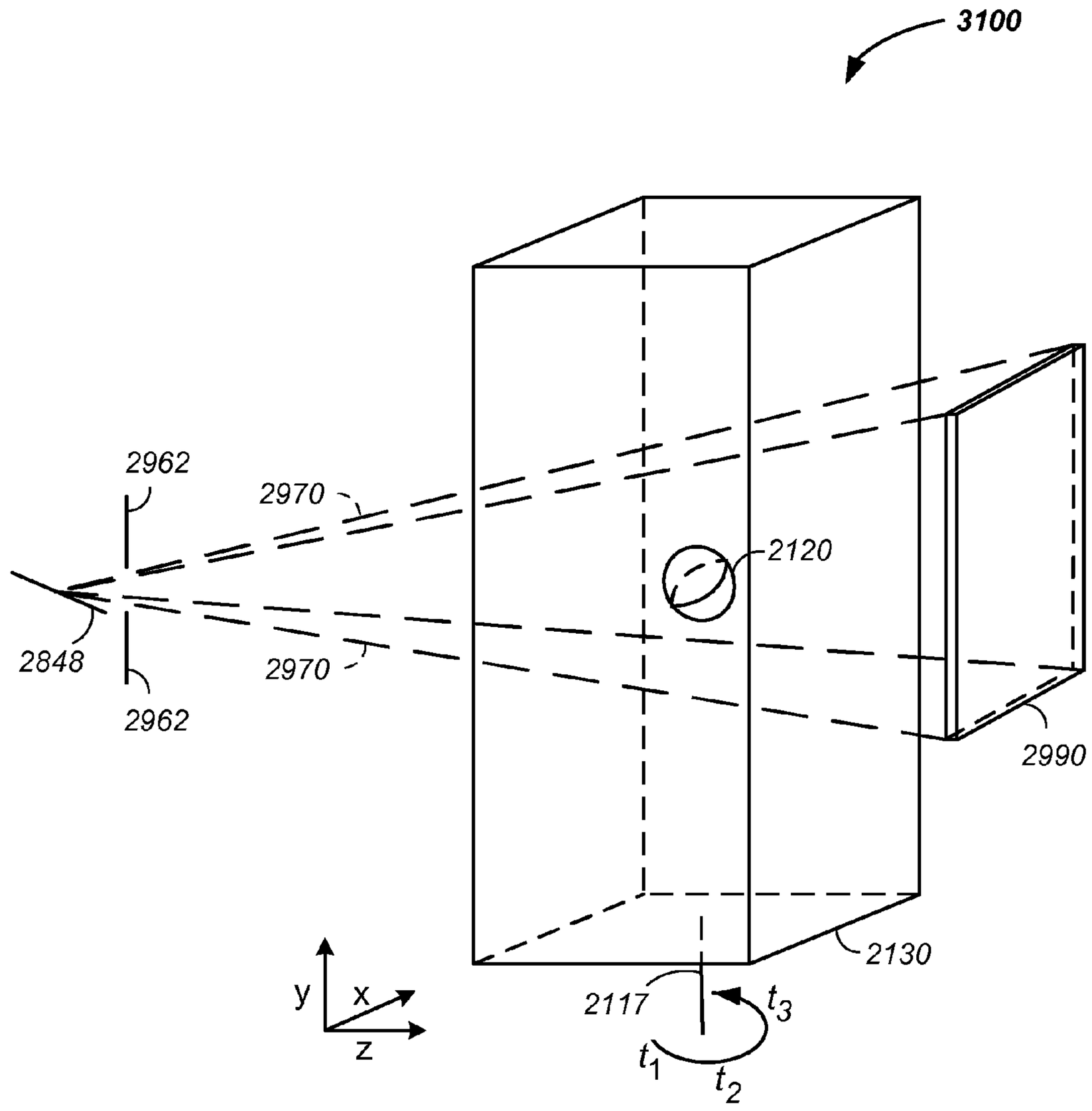

FIG. 31

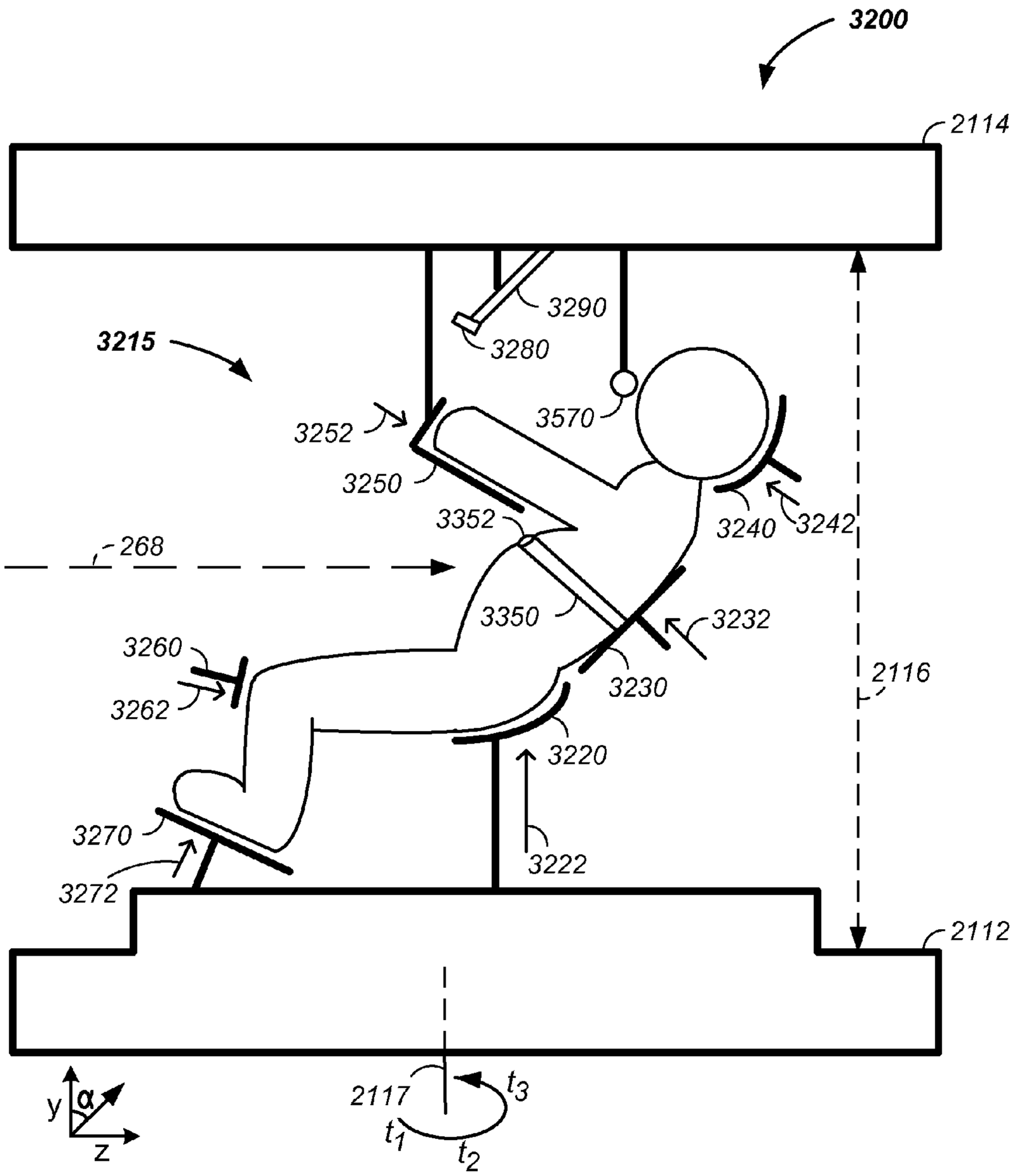
3200
2114
3215
3290
3280
3252
3570
3250
3352
3240
3242
268
3350
3232
3260
3230
2116
3262
3220
3270
3222
3272
2112
2117
t_3
t_1
t_2
y
α
z

FIG. 32

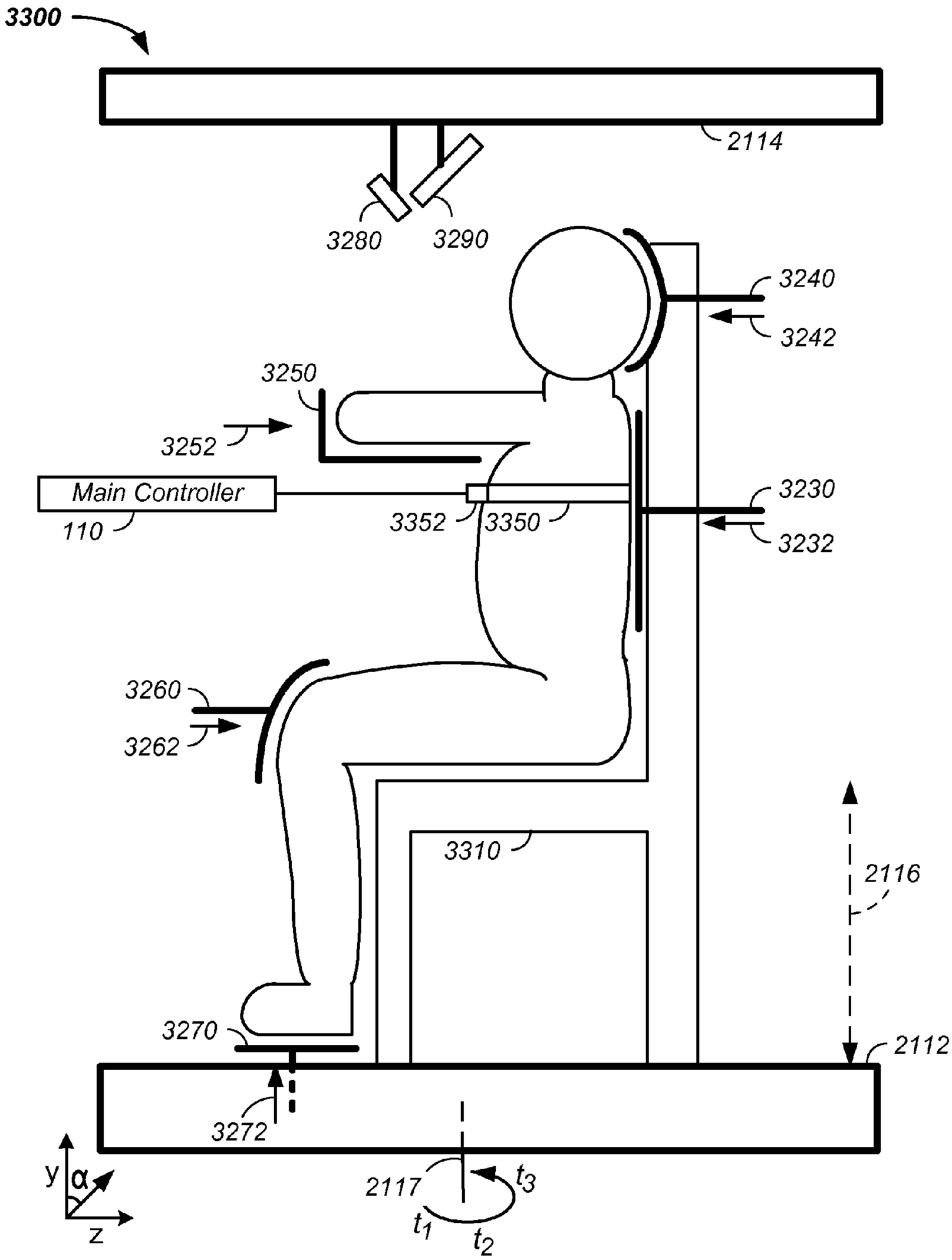
3300
2114
3280
3290
3240
3242
3250
3252
Main Controller
110
3352
3350
3230
3232
3260
3262
3310
2116
3270
2112
3272
y
α
z
2117
t_3
t_1
t_2

FIG. 33

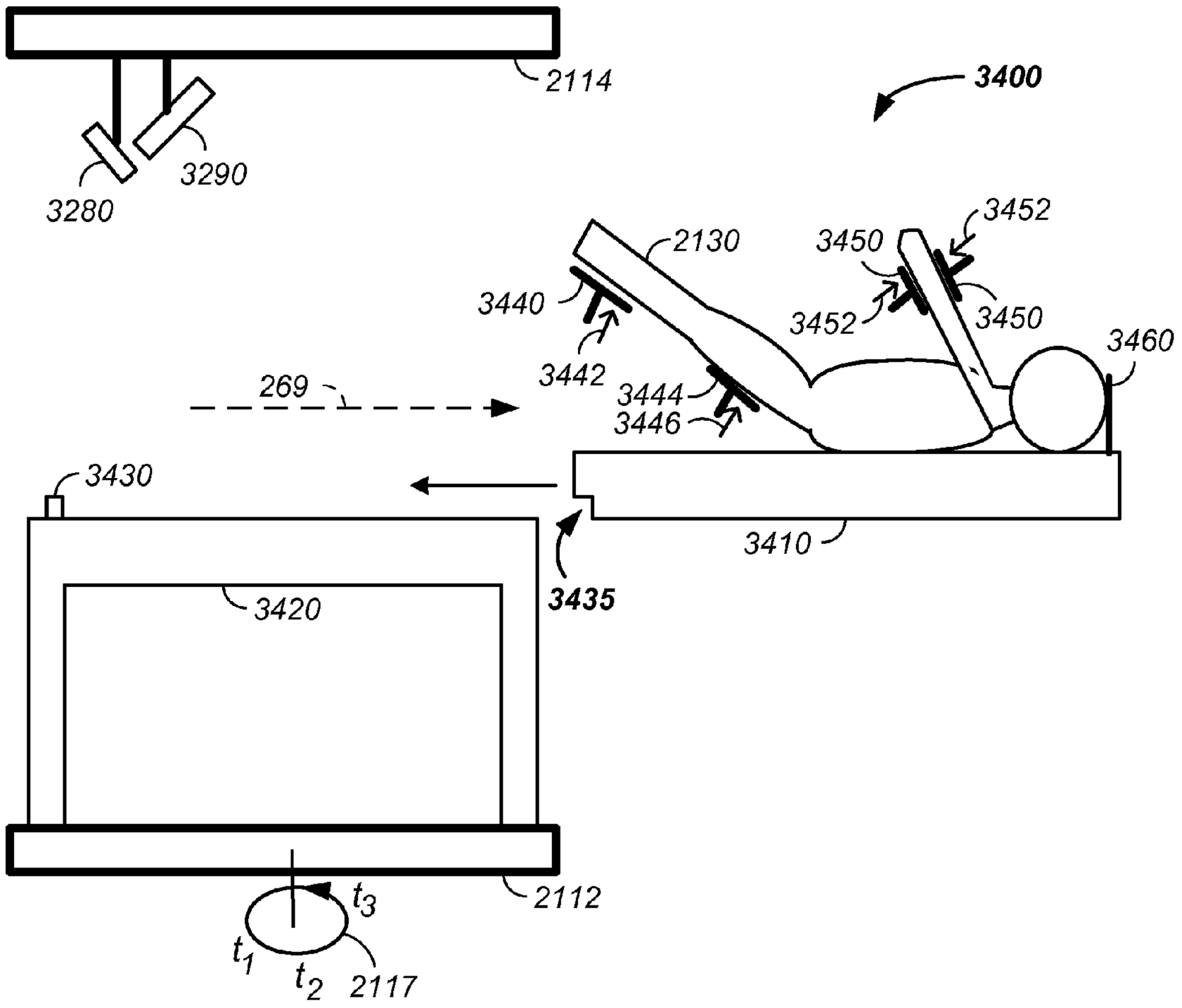
2114
3400
3280
3290
2130
3452
3450
3440
3452
3450
3460
269
3442
3444
3446
3430
3410
3435
3420
2112
t_3
t_1
t_2
2117

FIG. 34

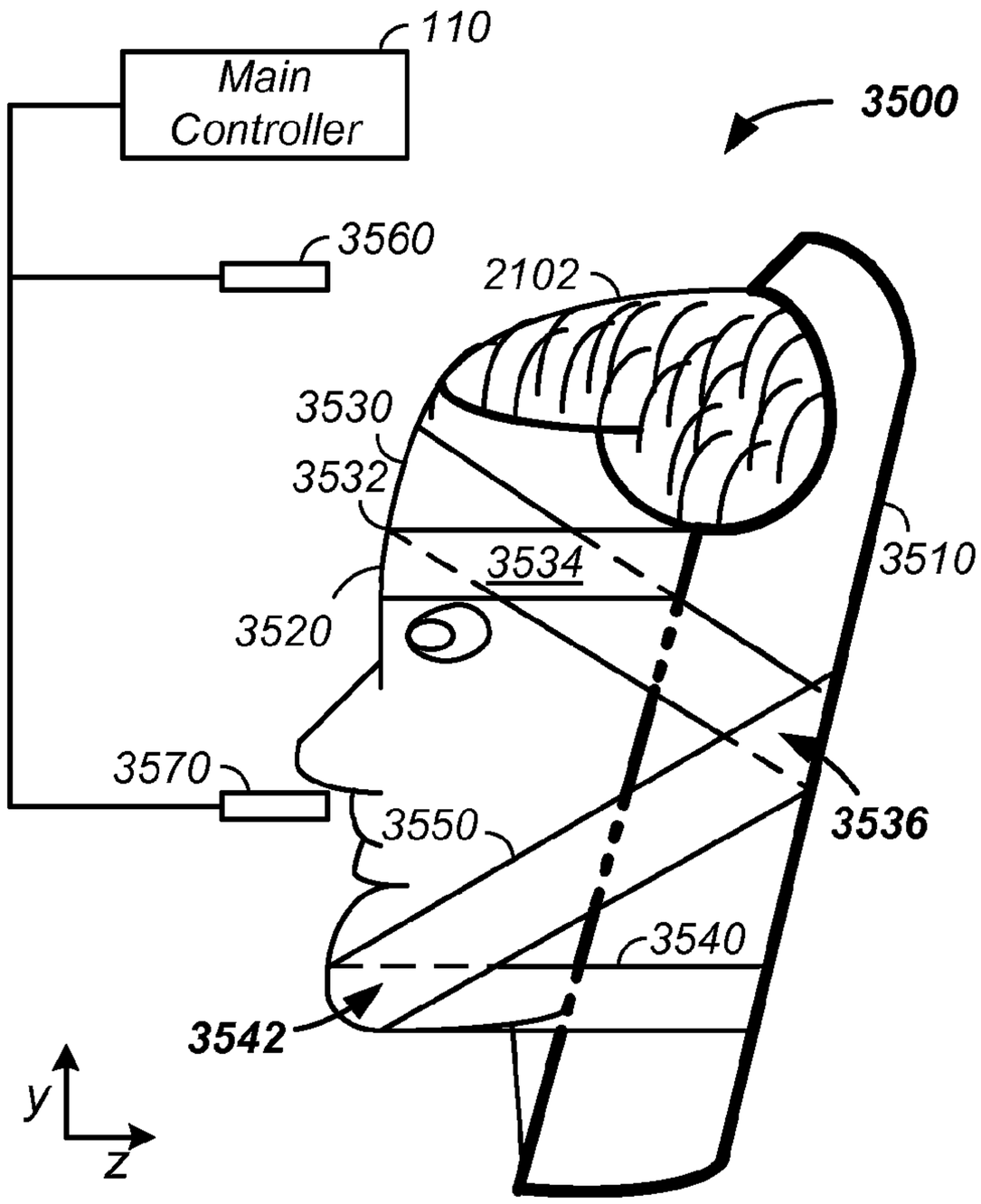
110
Main Controller
3500
3560
2102
3530
3532
3534
3510
3520
3570
3536
3550
3540
3542
y
z

FIG. 35

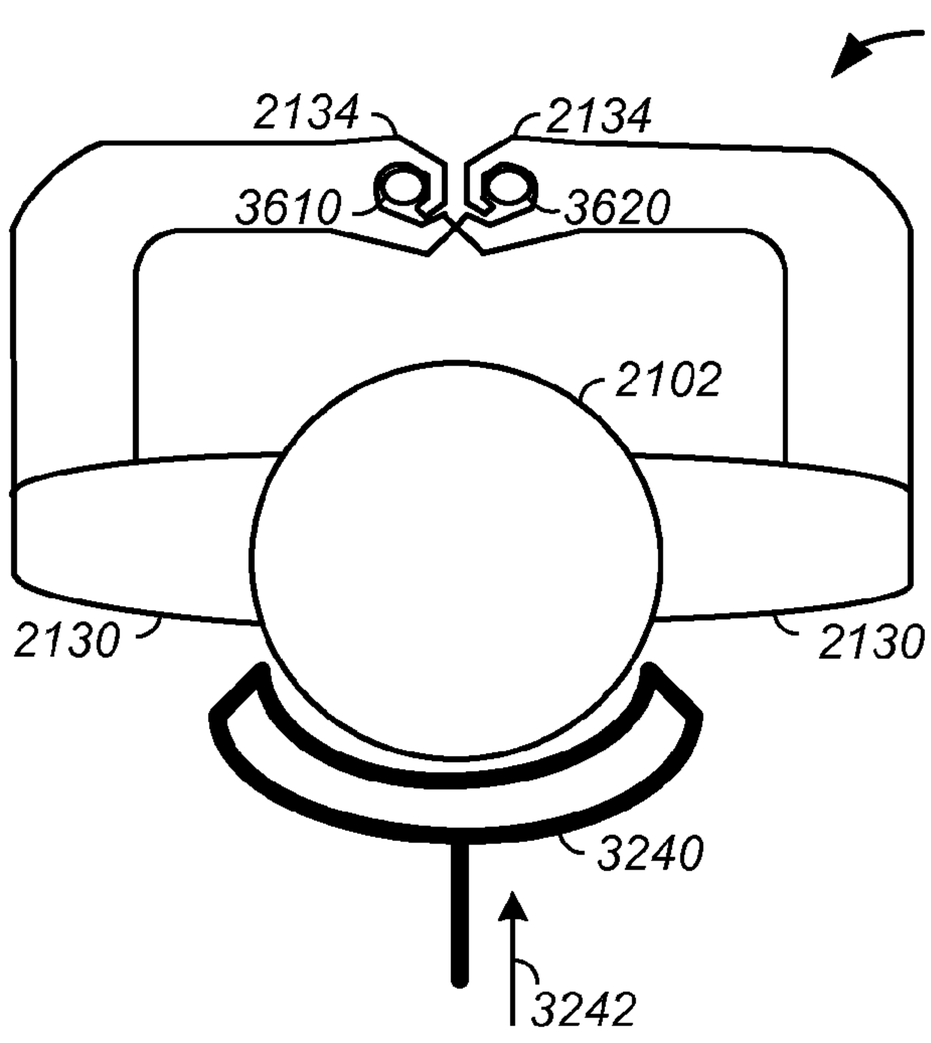
3250
2134
2134
3610
3620
2102
2130
2130
3240
3242

FIG. 36

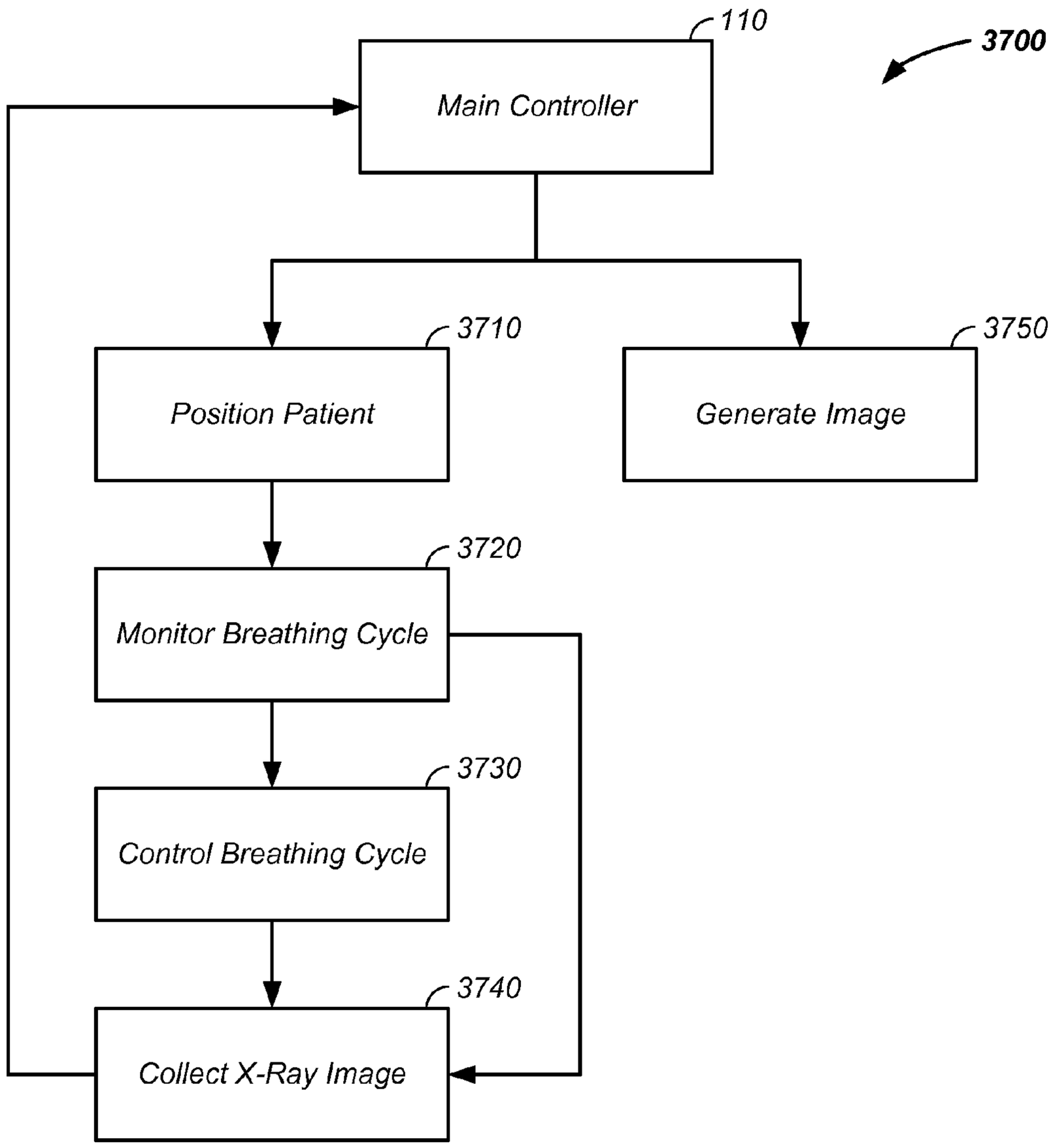
110
3700
Main Controller
3710
Position Patient
3750
Generate Image
3720
Monitor Breathing Cycle
3730
Control Breathing Cycle
3740
Collect X-Ray Image

FIG. 37

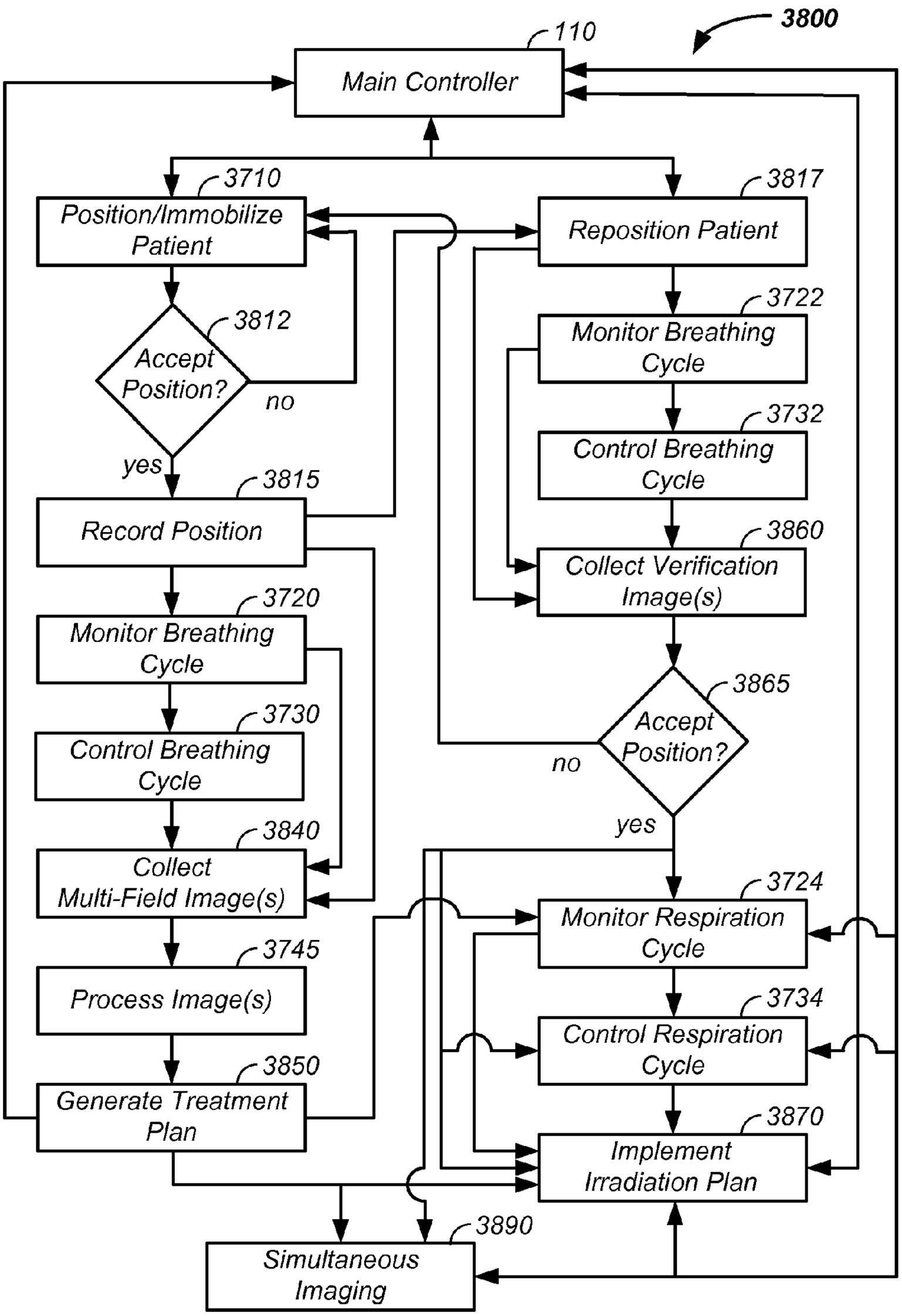
3800
110
Main Controller
3710
Position/Immobilize Patient
3812
Accept Position?
no
yes
3815
Record Position
3720
Monitor Breathing Cycle
3730
Control Breathing Cycle
3840
Collect Multi-Field Image(s)
3745
Process Image(s)
3850
Generate Treatment Plan
3817
Reposition Patient
3722
Monitor Breathing Cycle
3732
Control Breathing Cycle
3860
Collect Verification Image(s)
3865
Accept Position?
no
yes
3724
Monitor Respiration Cycle
3734
Control Respiration Cycle
3870
Implement Irradiation Plan
3890
Simultaneous Imaging

FIG. 38

CHARGED PARTICLE CANCER THERAPY DOSE DISTRIBUTION METHOD AND APPARATUS

CROSS-REFERENCES TO RELATED APPLICATIONS

This application is a divisional of U.S. patent application Ser. No. 12/687,387 filed Jan. 14, 2010, which is a continuation-in-part of U.S. patent application Ser. No. 12/425,683 filed Apr. 17, 2009, which claims the benefit of:

U.S. provisional patent application No. 61/055,395 filed May 22, 2008;
U.S. provisional patent application No. 61/137,574 filed Aug. 1, 2008;
U.S. provisional patent application No. 61/192,245 filed Sep. 17, 2008;
U.S. provisional patent application No. 61/055,409 filed May 22, 2008;
U.S. provisional patent application No. 61/203,308 filed Dec. 22, 2008;
U.S. provisional patent application No. 61/188,407 filed Aug. 11, 2008;
U.S. provisional patent application No. 61/188,406 filed Aug. 11, 2008;
U.S. provisional patent application No. 61/189,815 filed Aug. 25, 2008;
U.S. provisional patent application No. 61/201,731 filed Dec. 15, 2008;
U.S. provisional patent application No. 61/205,362 filed Jan. 12, 2009;
U.S. provisional patent application No. 61/134,717 filed Jul. 14, 2008;
U.S. provisional patent application No. 61/134,707 filed Jul. 14, 2008;
U.S. provisional patent application No. 61/201,732 filed Dec. 15, 2008;
U.S. provisional patent application No. 61/198,509 filed Nov. 7, 2008;
U.S. provisional patent application No. 61/134,718 filed Jul. 14, 2008;
U.S. provisional patent application No. 61/190,613 filed Sep. 2, 2008;
U.S. provisional patent application No. 61/191,043 filed Sep. 8, 2008;
U.S. provisional patent application No. 61/192,237 filed Sep. 17, 2008;
U.S. provisional patent application No. 61/201,728 filed Dec. 15, 2008;
U.S. provisional patent application No. 61/190,546 filed Sep. 2, 2008;
U.S. provisional patent application No. 61/189,017 filed Aug. 15, 2008;
U.S. provisional patent application No. 61/198,248 filed Nov. 5, 2008;
U.S. provisional patent application No. 61/198,508 filed Nov. 7, 2008;
U.S. provisional patent application No. 61/197,971 filed Nov. 3, 2008;
U.S. provisional patent application No. 61/199,405 filed Nov. 17, 2008;
U.S. provisional patent application No. 61/199,403 filed Nov. 17, 2008; and
U.S. provisional patent application No. 61/199,404 filed Nov. 17, 2008, all of which are incorporated herein in their entirety by this reference thereto.

BACKGROUND OF THE INVENTION

1. Field of the Invention

This invention relates generally to treatment of solid cancers. More particularly, the invention relates to a charged particle cancer therapy dose distribution method and apparatus optionally used in combination with beam injection, acceleration, extraction, and/or targeting methods and apparatus.

2. Discussion of the Prior Art

Cancer

Proton therapy systems typically include: a beam generator, an accelerator, and a beam transport system to move the resulting accelerated protons to a plurality of treatment rooms where the protons are delivered to a tumor in a patient's body.

Proton therapy works by aiming energetic ionizing particles, such as protons accelerated with a particle accelerator, onto a target tumor. These particles damage the DNA of cells, ultimately causing their death. Cancerous cells, because of their high rate of division and their reduced ability to repair damaged DNA, are particularly vulnerable to attack on their DNA.

Due to their relatively enormous size, protons scatter less easily than X-rays or gamma rays in the tissue and there is very little lateral dispersion. Hence, the proton beam stays focused on the tumor shape without much lateral damage to surrounding tissue. All protons of a given energy have a certain range, defined by the Bragg peak, and the dosage delivery to tissue ratio is maximum over just the last few millimeters of the particle's range. The penetration depth depends on the energy of the particles, which is directly related to the speed to which the particles were accelerated by the proton accelerator. The speed of the proton is adjustable to the maximum rating of the accelerator. It is therefore possible to focus the cell damage due to the proton beam at the very depth in the tissues where the tumor is situated. Tissues situated before the Bragg peak receive some reduced dose and tissues situated after the peak receive none.

Problem

There exists in the art of charged particle irratiation therapy a need for efficient, even, accurate, and precise delivery of Bragg profile energy to a tumor. More particularly, there exists a need to deliver an effective and uniform radiation dose to all positions of a tumor while minimizing radiation dosage to surrounding tissue. Still further, there exists a need in the art to control the charged particle cancer therapy system in terms of patient translation position, patient rotation position, specified energy, specified intensity, and/or timing of charged particle delivery relative to a patient position. Preferably, the system would operate in conjunction with a negative ion beam source, synchrotron, and/or targeting method apparatus.

SUMMARY OF THE INVENTION

The invention comprises a method and apparatus for efficient radiation dosage delivery to a tumor. The method and apparatus preferably operates in conjunction with a multi-field charged particle cancer therapy method and apparatus timed to patient respiration used in combination with charged particle beam injection, particle beam acceleration and extraction, multi-axis charged particle beam control, and/or targeting methods and apparatus.

DESCRIPTION OF THE FIGURES

FIG. **1** illustrates component connections of a charged particle beam therapy system;

FIG. **2** illustrates a charged particle therapy system;

FIG. **3** illustrates an ion beam generation system;

FIG. **4** illustrates a negative ion beam source;

FIG. **5** illustrates an ion beam focusing system;

FIGS. **6** A-D illustrate focusing electrodes about a negative ion beam path;

FIG. **7**A illustrates a negative ion beam path vacuum system; FIG. **7**B illustrates a support structure; and FIG. **7**C illustrates a foil;

FIG. **8** is a particle beam therapy control flowchart;

FIG. **9** illustrates straight and turning sections of a synchrotron

FIG. **10** illustrates bending magnets of a synchrotron;

FIG. **11** provides a perspective view of a bending magnet;

FIG. **12** illustrates a cross-sectional view of a bending magnet;

FIG. **13** illustrates a cross-sectional view of a bending magnet;

FIG. **14** illustrates magnetic field concentration in a bending magnet;

FIG. **15** illustrates correction coils in a bending magnet;

FIG. **16** illustrates a magnetic turning section of a synchrotron;

FIGS. **17**A and B illustrate an RF accelerator and an RF accelerator subsystem, respectively;

FIG. **18** illustrates a magnetic field control system;

FIG. **19** illustrates a charged particle extraction and intensity control system;

FIGS. **20** A and B illustrate proton beam position verification systems;

FIG. **21** illustrates a patient positioning system from: (A) a front view and (B) a top view;

FIG. **22** provides X-ray and proton beam dose distributions;

FIGS. **23** A-E illustrate controlled scanning and depth of focus irradiation;

FIGS. **24** A-E illustrate multi-field irradiation;

FIG. **25** illustrates dose efficiency enhancement via use of multi-field irradiation;

FIGS. **26** A-C and E illustrate distal irradiation of a tumor from varying rotational directions and FIG. **26** D illustrates integrated radiation resulting from distal radiation;

FIG. **27** illustrates multi-dimensional scanning of a charged particle beam spot scanning system operating on: (A) a 2-D slice or (B) a 3-D volume of a tumor;

FIG. **28** illustrates an electron gun source used in generating X-rays coupled with a particle beam therapy system;

FIG. **29** illustrates an X-ray source proximate a particle beam path;

FIG. **30** illustrates an expanded X-ray beam path;

FIG. **31** provides an X-ray tomography system;

FIG. **32** illustrates a semi-vertical patient positioning system;

FIG. **33** provides an example of a sitting patient positioning system;

FIG. **34** illustrates a laying patient positioning system;

FIG. **35** illustrates a head restraint system;

FIG. **36** illustrates hand and head supports;

FIG. **37** provides a method of coordinating X-ray collection with patient respiration; and

FIG. **38** illustrates a patient positioning, immobilization, and repositioning system.

DETAILED DESCRIPTION OF THE INVENTION

The invention relates generally to treatment of solid cancers. More particularly, a method and apparatus for efficient radiation dose delivery to a tumor is described. Preferably, radiation is delivered through an entry point into the tumor and Bragg peak energy is targeted to a distal or far side of the tumor from an ingress point. Delivering Bragg peak energy to the distal side of the tumor from the ingress point is repeated from multiple rotational directions. Beam intensity is proportional to radiation dose delivery efficiency. The multi-field irradiation process with energy levels targeting the far side of the tumor from each irradiation direction provides even and efficient charged particle radiation dose delivery to the tumor. Preferably, the charged particle therapy is timed to patient respiration via control of charged particle beam injection, acceleration, extraction, and/or targeting methods and apparatus.

In one embodiment, a multi-field charged particle cancer therapy method and apparatus with energy levels delivering radiation to the far side of the tumor is coordinated with patient respiration via use of feedback sensors used to monitor and/or control patient respiration. Preferably, the charged particle therapy is performed on a patient in a partially immobilized and repositionable position and proton delivery is timed to patient respiration via control of charged particle beam injection, acceleration, extraction, and/or targeting methods and apparatus.

Used in combination with the invention, novel design features of a charged particle beam cancer therapy system are described. Particularly, a negative ion beam source with novel features in the negative ion source, ion source vacuum system, ion beam focusing lens, and tandem accelerator is described. Additionally, the synchrotron includes: turning magnets, edge focusing magnets, magnetic field concentration magnets, winding and correction coils, flat magnetic field incident surfaces, and extraction elements, which minimize the overall size of the synchrotron, provide a tightly controlled proton beam, directly reduce the size of required magnetic fields, directly reduce required operating power, and allow continual acceleration of protons in a synchrotron even during a process of extracting protons from the synchrotron. The ion beam source system and synchrotron are preferably computer integrated with a patient imaging system and a patient interface including respiration monitoring sensors and patient positioning elements. Further, the system is integrated with intensity control of a charged particle beam, acceleration, extraction, and/or targeting method and apparatus. More particularly, intensity, energy, and timing control of a charged particle stream of a synchrotron is coordinated with patient positioning and tumor treatment. The synchrotron control elements allow tight control of the charged particle beam, which compliments the tight control of patient positioning to yield efficient treatment of a solid tumor with reduced tissue damage to surrounding healthy tissue. In addition, the system reduces the overall size of the synchrotron, provides a tightly controlled proton beam, directly reduces the size of required magnetic fields, directly reduces required operating power, and allows continual acceleration of protons in a synchrotron even during a process of extracting protons from the synchrotron. All of these systems are preferably used in conjunction with an X-ray system capable of collecting X-rays of a patient: (1) in a positioning, immobilization, and automated repositioning system for proton treatment; (2) at a specified moment of the patient's respiration cycle; and (3) using coordinated translation and rotation of the patient. Combined, the systems provide for efficient, accurate, and precise noninvasive tumor treatment with minimal damage to surrounding healthy tissue.

In various embodiments, the charged particle cancer therapy system incorporates any of:

an injection system having a central magnetic member and a magnetic field separating high and low temperature plasma regions;
a dual vacuum system creating a first partial pressure region on a plasma generation system side of a foil in a tandem accelerator and a second lower partial pressure region on the synchrotron side of the foil;
a negative ion beam focusing system having a conductive mesh axially crossing the negative ion beam;
a synchrotron having four straight sections and four turning sections;
a synchrotron having no hexapole magnets;
four bending magnets in each turning section of the synchrotron;
a winding coil wrapping multiple bending magnets;
a plurality of bending magnets that are beveled and charged particle focusing in each turning section;
a magnetic field concentrating geometry approaching the gap through which the charged particles travel;
correction coils for rapid magnetic field changes;
magnetic field feedback sensors providing signal to the correction coils;
integrated RF-amplifier microcircuits providing currents through loops about accelerating coils;
low density foil for charged particle extraction;
a feedback sensor for measuring particle extraction allowing intensity control;
a synchrotron independently controlling charged particle energy and intensity;
a layer, after synchrotron extraction and before the tumor, for imaging the particle beam x-, y-axis position;
a rotatable platform for turning the subject allowing multi-field imaging and/or multi-field proton therapy;
a radiation plan dispersing ingress Bragg profile energy 360 degrees about the tumor;
a long lifetime X-ray source;
an X-ray source proximate the charged particle beam path;
a multi-field X-ray system;
positioning, immobilizing, and repositioning systems;
respiratory sensors;
simultaneous and independent control of:
proton beam energy
x-axis proton beam control;
y-axis proton beam control;
proton intensity control;
patient translation; and
patient rotation; and
a system timing charged particle therapy to one or more of:
patient translation;
patient rotation; and
patient respiration.

Charged Particle Beam Therapy

Throughout this document, a charged particle beam therapy system, such as a proton beam, hydrogen ion beam, or carbon ion beam, is described. Herein, the charged particle beam therapy system is described using a proton beam. However, the aspects taught and described in terms of a proton beam are not intended to be limiting to that of a proton beam and are illustrative of a charged particle beam system. Any of the techniques described herein are equally applicable to any charged particle beam system.

Referring now to FIG. **1**, a charged particle beam system **100** is illustrated. The charged particle beam preferably comprises a number of subsystems including any of: a main controller **110**; an injection system **120**; a synchrotron **130** that typically includes: (1) an accelerator system **132** and (2) an extraction system **134**; a scanning/targeting/delivery system **140**; a patient interface module **150**; a display system **160**; and/or an imaging system **170**.

An exemplary method of use of the charged particle beam system **100** is provided. The main controller **110** controls one or more of the subsystems to accurately and precisely deliver protons to a tumor of a patient. For example, the main controller **110** obtains an image, such as a portion of a body and/or of a tumor, from the imaging system **170**. The main controller **110** also obtains position and/or timing information from the patient interface module **150**. The main controller **110** then optionally controls the injection system **120** to inject a proton into a synchrotron **130**. The synchrotron typically contains at least an accelerator system **132** and an extraction system **134**. The main controller preferably controls the proton beam within the accelerator system, such as by controlling speed, trajectory, and timing of the proton beam. The main controller then controls extraction of a proton beam from the accelerator through the extraction system **134**. For example, the controller controls timing, energy, and/or intensity of the extracted beam. The controller **110** also preferably controls targeting of the proton beam through the scanning/targeting/delivery system **140** to the patient interface module **150**. One or more components of the patient interface module **150**, such as translational and rotational position of the patient, are preferably controlled by the main controller **110**. Further, display elements of the display system **160** are preferably controlled via the main controller **110**. Displays, such as display screens, are typically provided to one or more operators and/or to one or more patients. In one embodiment, the main controller **110** times the delivery of the proton beam from all systems, such that protons are delivered in an optimal therapeutic manner to the tumor of the patient.

Herein, the main controller **110** refers to a single system controlling the charged particle beam system **100**, to a single controller controlling a plurality of subsystems controlling the charged particle beam system **100**, or to a plurality of individual controllers controlling one or more sub-systems of the charged particle beam system **100**.

Referring now to FIG. **2**, an illustrative exemplary embodiment of one version of the charged particle beam system **100** is provided. The number, position, and described type of components is illustrative and non-limiting in nature. In the illustrated embodiment, the injection system **120** or ion source or charged particle beam source generates protons. The protons are delivered into a vacuum tube that runs into, through, and out of the synchrotron. The generated protons are delivered along an initial path **262**. Focusing magnets **230**, such as quadrupole magnets or injection quadrupole magnets, are used to focus the proton beam path. A quadrupole magnet is a focusing magnet. An injector bending magnet **232** bends the proton beam toward the plane of the synchrotron **130**. The focused protons having an initial energy are introduced into an injector magnet **240**, which is preferably an injection Lamberson magnet. Typically, the initial beam path **262** is along an axis off of, such as above, a circulating plane of the synchrotron **130**. The injector bending magnet **232** and injector magnet **240** combine to move the protons into the synchrotron **130**. Main bending magnets, dipole magnets, or circulating magnets **250** are used to turn the protons along a circulating beam path **264**. A dipole magnet is a bending magnet. The main bending magnets **250** bend the initial beam path **262** into a circulating beam path **264**. In this example, the main bending magnets **250** or circulating magnets are represented as four sets of four magnets to maintain the circulating beam path **264** into a stable circulating beam path. However, any number of magnets or sets of magnets are optionally used to move the protons around a single orbit in the circulation

process. The protons pass through an accelerator **270**. The accelerator accelerates the protons in the circulating beam path **264**. As the protons are accelerated, the fields applied by the magnets are increased. Particularly, the speed of the protons achieved by the accelerator **270** are synchronized with magnetic fields of the main bending magnets **250** or circulating magnets to maintain stable circulation of the protons about a central point or region **280** of the synchrotron. At separate points in time the accelerator **270**/main bending magnet **250** combination is used to accelerate and/or decelerate the circulating protons while maintaining the protons in the circulating path or orbit. An extraction element of the inflector/deflector system **290** is used in combination with a Lamberson extraction magnet **292** to remove protons from their circulating beam path **264** within the synchrotron **130**. One example of a deflector component is a Lamberson magnet. Typically the deflector moves the protons from the circulating plane to an axis off of the circulating plane, such as above the circulating plane. Extracted protons are preferably directed and/or focused using an extraction bending magnet **237** and extraction focusing magnets **235**, such as quadrupole magnets along a transport path **268** into the scanning/targeting/delivery system **140**. Two components of a scanning system **140** or targeting system typically include a first axis control **142**, such as a vertical control, and a second axis control **144**, such as a horizontal control. In one embodiment, the first axis control **142** allows for about 100 mm of vertical or y-axis scanning of the proton beam **268** and the second axis control **144** allows for about 700 mm of horizontal or x-axis scanning of the proton beam **268**. A nozzle system **146** is used for imaging the proton beam and/or as a vacuum barrier between the low pressure beam path of the synchrotron and the atmosphere. Protons are delivered with control to the patient interface module **150** and to a tumor of a patient. All of the above listed elements are optional and may be used in various permutations and combinations. Each of the above listed elements are further described, infra.

Ion Beam Generation System

An ion beam generation system generates a negative ion beam, such as a hydrogen anion or H^- beam; preferably focuses the negative ion beam; converts the negative ion beam to a positive ion beam, such as a proton or H^+ beam; and injects the positive ion beam **262** into the synchrotron **130**. Portions of the ion beam path are preferably under partial vacuum. Each of these systems are further described, infra.

Referring now to FIG. **3**, an exemplary ion beam generation system **300** is illustrated. As illustrated, the ion beam generation system **300** has four major subsections: a negative ion source **310**, a first partial vacuum system **330**, an optional ion beam focusing system **350**, and a tandem accelerator **390**.

Still referring to FIG. **3**, the negative ion source **310** preferably includes an inlet port **312** for injection of hydrogen gas into a high temperature plasma chamber **314**. In one embodiment, the plasma chamber includes a magnetic material **316**, which provides a magnetic field **317** between the high temperature plasma chamber **314** and a low temperature plasma region on the opposite side of the magnetic field barrier. An extraction pulse is applied to a negative ion extraction electrode **318** to pull the negative ion beam into a negative ion beam path **319**, which proceeds through the first partial vacuum system **330**, through the ion beam focusing system **350**, and into the tandem accelerator **390**.

Still referring to FIG. **3**, the first partial vacuum system **330** is an enclosed system running from the hydrogen gas inlet port **312** to a foil **395** in the tandem accelerator **390**. The foil **395** is preferably sealed directly or indirectly to the edges of the vacuum tube **320** providing for a higher pressure, such as about 10^{-5} torr, to be maintained on the first partial vacuum system **330** side of the foil **395** and a lower pressure, such as about 10^{-7} torr, to be maintained on the synchrotron side of the foil **390**. By only pumping first partial vacuum system **330** and by only semi-continuously operating the ion beam source vacuum based on sensor readings, the lifetime of the semi-continuously operating pump is extended. The sensor readings are further described, infra.

Still referring to FIG. **3**, the first partial vacuum system **330** preferably includes: a first pump **332**, such as a continuously operating pump and/or a turbo molecular pump; a large holding volume **334**; and a semi-continuously operating pump **336**. Preferably, a pump controller **340** receives a signal from a pressure sensor **342** monitoring pressure in the large holding volume **334**. Upon a signal representative of a sufficient pressure in the large holding volume **334**, the pump controller **340** instructs an actuator **345** to open a valve **346** between the large holding volume and the semi-continuously operating pump **336** and instructs the semi-continuously operating pump to turn on and pump to atmosphere residual gases out of the vacuum line **320** about the charged particle stream. In this fashion, the lifetime of the semi-continuously operating pump is extended by only operating semi-continuously and as needed. In one example, the semi-continuously operating pump **336** operates for a few minutes every few hours, such as 5 minutes every 4 hours, thereby extending a pump with a lifetime of about 2,000 hours to about 96,000 hours.

Further, by isolating the inlet gas from the synchrotron vacuum system, the synchrotron vacuum pumps, such as turbo molecular pumps can operate over a longer lifetime as the synchrotron vacuum pumps have fewer gas molecules to deal with. For example, the inlet gas is primarily hydrogen gas but may contain impurities, such as nitrogen and carbon dioxide. By isolating the inlet gases in the negative ion source system **310**, first partial vacuum system **330**, ion beam focusing system **350**, and negative ion beam side of the tandem accelerator **390**, the synchrotron vacuum pumps can operate at lower pressures with longer lifetimes, which increases operating efficiency of the synchrotron **130**.

Still referring to FIG. **3**, the optimal ion beam focusing system **350** preferably includes two or more electrodes where one electrode of each electrode pair partially obstructs the ion beam path with conductive paths **372**, such as a conductive mesh. In the illustrated example, two ion beam focusing system sections are illustrated, a two electrode ion beam focusing section **360** and a three electrode ion beam focusing section **370**. For a given electrode pair, electric field lines, running between the conductive mesh of a first electrode and a second electrode, provide inward forces focusing the negative ion beam. Multiple such electrode pairs provide multiple negative ion beam focusing regions. Preferably the two electrode ion focusing section **360**, electrode ion focusing section **370**, and second three electrode ion focusing section are placed after the negative ion source and before the tandem accelerator and/or cover a space of about 0.5, 1, or 2 meters along the ion beam path **319**. Ion beam focusing systems are further described, infra.

Still referring to FIG. **3**, the tandem accelerator **390** preferably includes a foil **395**, such as a carbon foil. The negative ions in the negative ion beam path **319** are converted to positive ions, such as protons, and the initial ion beam path **262** results. The foil **395** is preferably sealed directly or indirectly to the edges of the vacuum tube **320** providing for a higher pressure, such as about 10^{-5} torr, to be maintained on the side of the foil **395** having the negative ion beam path **319** and a lower pressure, such as about 10^{-7} torr, to be maintained on the side of the foil **390** having the proton ion beam path

262. Having the foil **395** physically separating the vacuum chamber **320** into two pressure regions allows for a system having fewer and/or smaller pumps to maintain the lower pressure system in the synchrotron **130** as the inlet hydrogen and its residuals are extracted in a separate contained and isolated space by the first partial vacuum system **330**.

Negative Ion Source

An example of the negative ion source **310** is further described herein. Referring now to FIG. **4**, a cross-section of an exemplary negative ion source system **400** is provided. The negative ion beam **319** is created in multiple stages. During a first stage, hydrogen gas is injected into a chamber. During a second stage, a negative ion is created by application of a first high voltage pulse, which creates a plasma about the hydrogen gas to create negative ions. During a third stage, a magnetic field filter is applied to components of the plasma. During a fourth stage, the negative ions are extracted from a low temperature plasma region, on the opposite side of the magnetic field barrier, by application of a second high voltage pulse. Each of the four stages are further described, infra. While the chamber is illustrated as a cross-section of a cylinder, the cylinder is exemplary only and any geometry applies to the magnetic loop containment walls, described infra.

In the first stage, hydrogen gas **440** is injected through the inlet port **312** into a high temperature plasma region **490**. The injection port **312** is open for a short period of time, such as less than about 1, 5, or 10 microseconds to minimize vacuum pump requirements to maintain vacuum chamber **320** requirements. The high temperature plasma region is maintained at reduced pressure by the partial vacuum system **330**. The injection of the hydrogen gas is optionally controlled by the main controller **110**, which is responsive to imaging system **170** information and patient interface module **150** information, such as patient positioning and period in a respiration cycle.

In the second stage, a high temperature plasma region is created by applying a first high voltage pulse across a first electrode **422** and a second electrode **424**. For example a 5 kV pulse is applied for about 20 microseconds with 5 kV at the second electrode **424** and about 0 kV applied at the first electrode **422**. Hydrogen in the chamber is broken, in the high temperature plasma region **490**, into component parts, such as any of: atomic hydrogen, H^0, a proton, H^+, an electron, e^-, and a hydrogen anion, H^-.

In the third stage, the high temperature plasma region **490** is at least partially separated from a low temperature plasma region **492** by the magnetic field **317** or in this specific example a magnetic field barrier **430**. High energy electrons are restricted from passing through the magnetic field barrier **430**. In this manner, the magnetic field barrier **430** acts as a filter between, zone A and zone B, in the negative ion source. Preferably, a central magnetic material **410**, which is an example of the magnetic material **316**, is placed within the high temperature plasma region **490**, such as along a central axis of the high temperature plasma region **490**. Preferably, the first electrode **422** and second electrode **424** are composed of magnetic materials, such as iron. Preferably, the outer walls **450** of the high temperature plasma region, such as cylinder walls, are composed of a magnetic material, such as a permanent magnet, ferric or iron based material, or a ferrite dielectric ring magnet. In this manner a magnetic field loop is created by: the central magnetic material **410**, first electrode **422**, the outer walls **450**, the second electrode **424**, and the magnetic field barrier **430**. Again, the magnetic field barrier **430** restricts high energy electrons from passing through the magnetic field barrier **430**. Low energy electrons interact with atomic hydrogen, H^0, to create a hydrogen anion, H^-, in the low temperature plasma region **492**.

In the fourth stage, a second high voltage pulse or extraction pulse is applied at a third electrode **426**. The second high voltage pulse is preferentially applied during the later period of application of the first high voltage pulse. For example, an extraction pulse of about 25 kV is applied for about the last 5 microseconds of the first creation pulse of about 20 microseconds. The potential difference, of about 20 kV, between the third electrode **426** and second electrode **424** extracts the negative ion, H^-, from the low temperature plasma region **492** and initiates the negative ion beam **319**, from zone B to zone C.

The magnetic field barrier **430** is optionally created in number of ways. An example of creation of the magnetic field barrier **430** using coils is provided. In this example, the elements described, supra, in relation to FIG. **4** are maintained with several differences. First, the magnetic field is created using coils. An isolating material is preferably provided between the first electrode **422** and the cylinder walls **450** as well as between the second electrode **424** and the cylinder walls **450**. The central material **410** and/or cylinder walls **450** are optionally metallic. In this manner, the coils create a magnetic field loop through the first electrode **422**, isolating material, outer walls **450**, second electrode **424**, magnetic field barrier **430**, and the central material **410**. Essentially, the coils generate a magnetic field in place of production of the magnetic field by the magnetic material **410**. The magnetic field barrier **430** operates as described, supra. Generally, any manner that creates the magnetic field barrier **430** between the high temperature plasma region **490** and low temperature plasma region **492** is functionally applicable to the ion beam extraction system **400**, described herein.

Ion Beam Focusing System

Referring now to FIG. **5**, the ion beam focusing system **350** is further described. In this example, three electrodes are used. In this example, a first electrode **510** and third electrode **530** are both negatively charged and each is a ring electrode circumferentially enclosing or at least partially enclosing the negative ion beam path **319**. A second electrode **520** is positively charged and is also a ring electrode at least partially and preferably substantially circumferentially enclosing the negative ion beam path. In addition, the second electrode includes one or more conducting paths **372** running through the negative ion beam path **319**. For example, the conducting paths are a wire mesh, a conducting grid, or a series of substantially parallel conducting lines running across the second electrode. In use, electric field lines run from the conducting paths of the positively charged electrode to the negatively charged electrodes. For example, in use the electric field lines **540** run from the conducting paths **372** in the negative ion beam path **319** to the negatively charged electrodes **510**, **530**. Two ray trace lines **550**, **560** of the negative ion beam path are used to illustrate focusing forces. In the first ray trace line **550**, the negative ion beam encounters a first electric field line at point M. Negatively charged ions in the negative ion beam **550** encounter forces running up the electric field line **572**, illustrated with an x-axis component vector **571**. The x-axis component force vectors **571** alters the trajectory of the first ray trace line to a inward focused vector **552**, which encounters a second electric field line at point N. Again, the negative ion beam **552** encounters forces running up the electric field line **574**, illustrated as having an inward force vector with an x-axis component **573**, which alters the inward focused vector **552** to a more inward focused vector **554**. Similarly, in the second ray trace line **560**, the negative ion beam encounters a first electric field line at point O. Negatively charged ions in

the negative ion beam encounter forces running up the electric field line **576**, illustrated as having a force vector with an x-axis force **575**. The inward force vector **575** alters the trajectory of the second ray trace line **560** to an inward focused vector **562**, which encounters a second electric field line at point P. Again, the negative ion beam encounters forces running up the electric field line **578**, illustrated as having force vector with an x-axis component **577**, which alters the inward focused vector **562** to a more inward focused vector **564**. The net result is a focusing effect on the negative ion beam. Each of the force vectors **572**, **574**, **576**, **578** optionally has x and/or y force vector components resulting in a 3-dimensional focusing of the negative ion beam path. Naturally, the force vectors are illustrative in nature, many electric field lines are encountered, and the focusing effect is observed at each encounter resulting in integral focusing. The example is used to illustrate the focusing effect.

Still referring to FIG. **5**, optionally any number of electrodes are used, such as 2, 3, 4, 5, 6, 7, 8, or 9 electrodes, to focus the negative ion beam path where every other electrode, in a given focusing section, is either positively or negatively charged. For example, three focusing sections are optionally used. In the first ion focusing section **360**, a pair of electrodes is used where the first electrode encountered along the negative ion beam path is negatively charged and the second electrode is positively charged, resulting in focusing of the negative ion beam path. In the second ion focusing section **370**, two pairs of electrodes are used, where a common positively charged electrode with a conductive mesh running through the negatively ion beam path **319** is used. Thus, in the second ion focusing section **370**, the first electrode encountered along the negative ion beam path is negatively charged and the second electrode is positively charged, resulting in focusing of the negative ion beam path. Further, in the second ion focusing section, moving along the negative ion beam path, a second focusing effect is observed between the second positively charged electrode and a third negatively charged electrode. In this example, a third ion focusing section is used that again has three electrodes, which acts in the fashion of the second ion focusing section, describe supra.

Referring now to FIG. **6**, the central region of the electrodes in the ion beam focusing system **350** are further described. Referring now to FIG. **6**A, the central region of the negatively charged ring electrode **510** is preferably void of conductive material. Referring now to FIGS. **6**B-D, the central region of positively charged electrode ring **520** preferably contains conductive paths **372**. Preferably, the conductive paths **372** or conductive material within the positively charged electrode ring **520** blocks about 1, 2, 5, or 10 percent of the area and more preferably blocks about 5 percent of the cross-sectional area of the negative ion beam path **319**. Referring now to FIG. **6**B, one option is a conductive mesh **610**. Referring now to FIG. **6**C, a second option is a series of conductive lines **620** running substantially in parallel across the positively charged electrode ring **520** that surrounds a portion of the negative ion beam path **319**. Referring now to FIG. **6**D, a third option is to have a foil **630** or metallic layer cover all of the cross-sectional area of the negative ion beam path with holes punched through the material, where the holes take up about 90-99 percent and more preferably about 95 percent of the area of the foil. More generally, the pair of electrodes **510**, **520** are configured to provide electric field lines that provide focusing force vectors to the negative ion beam **319** when the ions in the negative ion beam **319** translate through the electric field lines, as described supra.

In an example of a two electrode negative beam ion focusing system having a first cross-sectional diameter, d_1, the negative ions are focused to a second cross-sectional diameter, d_2, where $d_1>d_2$. Similarly, in an example of a three electrode negative beam ion focusing system having a first ion beam cross-sectional diameter, d_1, the negative ions are focused using the three electrode system to a third negative ion beam cross-sectional diameter, d_3, where $d_1>d_3$. For like potentials on the electrodes, the three electrode system provides tighter or stronger focusing compared to the two-electrode system, $d_3<d_2$.

In the examples provided, supra, of a multi-electrode ion beam focusing system, the electrodes are rings. More generally, the electrodes are of any geometry sufficient to provide electric field lines that provide focusing force vectors to the negative ion beam when the ions in the negative ion beam **319** translate through the electric field lines, as described supra. For example, one negative ring electrode is optionally replaced by a number of negatively charged electrodes, such as about 2, 3, 4, 6, 8, 10, or more electrodes placed about the outer region of a cross-sectional area of the negative ion beam probe. Generally, more electrodes are required to converge or diverge a faster or higher energy beam.

In another embodiment, by reversing the polarity of electrodes in the above example, the negative ion beam is made to diverge. Thus, the negative ion beam path **319** is optionally focused and/or expanded using combinations of electrode pairs. For example, if the electrode having the mesh across the negative ion beam path is made negative, then the negative ion beam path is made to defocus. Hence, combinations of electrode pairs are used for focusing and defocusing a negative ion beam path, such as where a first pair includes a positively charged mesh for focusing and a where a second pair includes a negatively charged mesh for defocusing.

Tandem Accelerator

Referring now to FIG. **7**A, the tandem accelerator **390** is further described. The tandem accelerator accelerates ions using a series of electrodes **710**, **711**, **712**, **713**, **714**, **715**. For example, negative ions, such as H^-, in the negative ion beam path are accelerated using a series of electrodes having progressively higher voltages relative to the voltage of the extraction electrode **426**, or third electrode **426**, of the negative ion beam source **310**. For instance, the tandem accelerator **390** optionally has electrodes ranging from the 25 kV of the extraction electrode **426** to about 525 kV near the foil **395** in the tandem accelerator **390**. Upon passing through the foil **395**, the negative ion, H^-, loses two electrons to yield a proton, H^+, according to equation 1.

$$H^- \rightarrow H^+ + 2e^- \quad \text{(eq. 1)}$$

The proton is further accelerated in the tandem accelerator using appropriate voltages at a multitude of further electrodes **713**, **714**, **715**. The protons are then injected into the synchrotron **130** as described, supra.

Still referring to FIG. **7**, the foil **395** in the tandem accelerator **390** is further described. The foil **395** is preferably a very thin carbon film of about 30 to 200 angstroms in thickness. The foil thickness is designed to both: (1) not block the ion beam and (2) allow the transfer of electrons yielding protons to form the proton beam path **262**. The foil **395** is preferably substantially in contact with a support layer **720**, such as a support grid. The support layer **720** provides mechanical strength to the foil **395** to combine to form a vacuum blocking element **725**. The foil **395** blocks nitrogen, carbon dioxide, hydrogen, and other gases from passing and thus acts as a vacuum barrier. In one embodiment, the foil **395** is preferably sealed directly or indirectly to the edges of the vacuum tube **320** providing for a higher pressure, such as about 10^{-5} torr, to be maintained on the side of the foil **395**

having the negative ion beam path **319** and a lower pressure, such as about 10^{-7} torr, to be maintained on the side of the foil **395** having the proton ion beam path **262**. Having the foil **395** physically separating the vacuum chamber **320** into two pressure regions allows for a vacuum system having fewer and/or smaller pumps to maintain the lower pressure system in the synchrotron **130** as the inlet hydrogen and its residuals are extracted in a separate contained and isolated space by the first partial vacuum system **330**. The foil **395** and support layer **720** are preferably attached to the structure **750** of the tandem accelerator **390** or vacuum tube **320** to form a pressure barrier using any mechanical means, such as a metal, plastic, or ceramic ring **730** compressed to the walls with an attachment screw **740**. Any mechanical means for separating and sealing the two vacuum chamber sides with the foil **395** are equally applicable to this system. Referring now to FIG. **7**B and FIG. **7**C, the support structure **720** and foil **395** are individually viewed in the x-, y-plane, respectively.

Referring now to FIG. **8**, another exemplary method of use of the charged particle beam system **100** is provided. The main controller **110**, or one or more sub-controllers, controls one or more of the subsystems to accurately and precisely deliver protons to a tumor of a patient. For example, the main controller sends a message to the patient indicating when or how to breath. The main controller **110** obtains a sensor reading from the patient interface module, such as a temperature breath sensor or a force reading indicative of where in a respiration cycle the subject is. Coordinated at a specific and reproducible point in the respiration cycle, the main controller collects an image, such as a portion of a body and/or of a tumor, from the imaging system **170**. The main controller **110** also obtains position and/or timing information from the patient interface module **150**. The main controller **110** then optionally controls the injection system **120** to inject hydrogen gas into a negative ion beam source **310** and controls timing of extraction of the negative ion from the negative ion beam source **310**. Optionally, the main controller controls ion beam focusing using the ion beam focusing lens system **350**; acceleration of the proton beam with the tandem accelerator **390**; and/or injection of the proton into the synchrotron **130**. The synchrotron typically contains at least an accelerator system **132** and an extraction system **134**. The synchrotron preferably contains one or more of: turning magnets, edge focusing magnets, magnetic field concentration magnets, winding and correction coils, and flat magnetic field incident surfaces, some of which contain elements under control by the main controller **110**. The main controller preferably controls the proton beam within the accelerator system, such as by controlling speed, trajectory, and/or timing of the proton beam. The main controller then controls extraction of a proton beam from the accelerator through the extraction system **134**. For example, the controller controls timing, energy, and/or intensity of the extracted beam. The main controller **110** also preferably controls targeting of the proton beam through the targeting/delivery system **140** to the patient interface module **150**. One or more components of the patient interface module **150** are preferably controlled by the main controller **110**, such as vertical position of the patient, rotational position of the patient, and patient chair positioning/stabilization/immobilization/control elements. Further, display elements of the display system **160** are preferably controlled via the main controller **110**. Displays, such as display screens, are typically provided to one or more operators and/or to one or more patients. In one embodiment, the main controller **110** times the delivery of the proton beam from all systems, such that protons are delivered in an optimal therapeutic manner to the tumor of the patient.

Synchrotron

Herein, the term synchrotron is used to refer to a system maintaining the charged particle beam in a circulating path; however, cyclotrons are alternatively used, albeit with their inherent limitations of energy, intensity, and extraction control. Further, the charged particle beam is referred to herein as circulating along a circulating path about a central point of the synchrotron. The circulating path is alternatively referred to as an orbiting path; however, the orbiting path does not refer a perfect circle or ellipse, rather it refers to cycling of the protons around a central point or region **280**.

Circulating System

Referring now to FIG. **9**, the synchrotron **130** preferably comprises a combination of straight sections **910** and ion beam turning sections **920**. Hence, the circulating path of the protons is not circular in a synchrotron, but is rather a polygon with rounded corners.

In one illustrative embodiment, the synchrotron **130**, which as also referred to as an accelerator system, has four straight elements or sections and four turning sections. Examples of straight sections **910** include the: inflector **240**, accelerator **270**, extraction system **290**, and deflector **292**. Along with the four straight sections are four ion beam turning sections **920**, which are also referred to as magnet sections or turning sections. Turning sections are further described, infra.

Referring still to FIG. **9**, an exemplary synchrotron is illustrated. In this example, protons delivered along the initial proton beam path **262** are inflected into the circulating beam path with the inflector **240** and after acceleration are extracted via a deflector **292** to the beam transport path **268**. In this example, the synchrotron **130** comprises four straight sections **910** and four bending or turning sections **920** where each of the four turning sections use one or more magnets to turn the proton beam about ninety degrees. As is further described, infra, the ability to closely space the turning sections and efficiently turn the proton beam results in shorter straight sections. Shorter straight sections allows for a synchrotron design without the use of focusing quadrupoles in the circulating beam path of the synchrotron. The removal of the focusing quadrupoles from the circulating proton beam path results in a more compact design. In this example, the illustrated synchrotron has about a five meter diameter versus eight meter and larger cross-sectional diameters for systems using a quadrupole focusing magnet in the circulating proton beam path.

Referring now to FIG. **10**, additional description of the first bending or turning section **920** is provided. Each of the turning sections preferably comprise multiple magnets, such as about 2, 4, 6, 8, 10, or 12 magnets. In this example, four turning magnets **1010**, **1020**, **1030**, **1040** in the first turning section **920** are used to illustrate key principles, which are the same regardless of the number of magnets in a turning section **920**. The turning magnets **1010**, **1020**, **1030**, **1040** are particular types of main bending or circulating magnets **250**.

In physics, the Lorentz force is the force on a point charge due to electromagnetic fields. The Lorentz force is given by equation 2 in terms of magnetic fields with the election field terms not included.

$$F=q(v\times B) \qquad \text{(eq. 2)}$$

In equation 2, F is the force in newtons; q is the electric charge in coulombs; B is the magnetic field in Teslas; and v is the instantaneous velocity of the particles in meters per second.

Referring now to FIG. **11**, an example of a single magnet bending or turning section **1010** is expanded. The turning

section includes a gap **1110** through which protons circulate. The gap **1110** is preferably a flat gap, allowing for a magnetic field across the gap **1110** that is more uniform, even, and intense. A magnetic field enters the gap **1110** through a magnetic field incident surface and exits the gap **1110** through a magnetic field exiting surface. The gap **1110** runs in a vacuum tube between two magnet halves. The gap **1110** is controlled by at least two parameters: (1) the gap **1110** is kept as large as possible to minimize loss of protons and (2) the gap **1110** is kept as small as possible to minimize magnet sizes and the associated size and power requirements of the magnet power supplies. The flat nature of the gap **1110** allows for a compressed and more uniform magnetic field across the gap **1110**. One example of a gap dimension is to accommodate a vertical proton beam size of about two centimeters with a horizontal beam size of about five to six centimeters.

As described, supra, a larger gap size requires a larger power supply. For instance, if the gap **1110** size doubles in vertical size, then the power supply requirements increase by about a factor of four. The flatness of the gap **1110** is also important. For example, the flat nature of the gap **1110** allows for an increase in energy of the extracted protons from about 250 to about 330 MeV. More particularly, if the gap **1110** has an extremely flat surface, then the limits of a magnetic field of an iron magnet are reachable. An exemplary precision of the flat surface of the gap **1110** is a polish of less than about 5 microns and preferably with a polish of about 1 to 3 microns. Unevenness in the surface results in imperfections in the applied magnetic field. The polished flat surface spreads unevenness of the applied magnetic field.

Still referring to FIG. **11**, the charged particle beam moves through the gap **1110** with an instantaneous velocity, v. A first magnetic coil **1120** and a second magnetic coil **1130** run above and below the gap **1110**, respectively. Current running through the coils **1120**, **1130** results in a magnetic field, B, running through the single magnet turning section **1010**. In this example, the magnetic field, B, runs upward, which results in a force, F, pushing the charged particle beam inward toward a central point of the synchrotron, which turns the charged particle beam in an arc.

Still referring to FIG. **11**, a portion of an optional second magnet bending or turning section **1020** is illustrated. The coils **1120**, **1130** typically have return elements **1140**, **1150** or turns at the end of one magnet, such as at the end of the first magnet turning section **1010**. The turns **1140**, **1150** take space. The space reduces the percentage of the path about one orbit of the synchrotron that is covered by the turning magnets. This leads to portions of the circulating path where the protons are not turned and/or focused and allows for portions of the circulating path where the proton path defocuses. Thus, the space results in a larger synchrotron. Therefore, the space between magnet turning sections **1160** is preferably minimized. The second turning magnet is used to illustrate that the coils **1120**, **1130** optionally run along a plurality of magnets, such as 2, 3, 4, 5, 6, or more magnets. Coils **1120**, **1130** running across multiple turning section magnets allows for two turning section magnets to be spatially positioned closer to each other due to the removal of the steric constraint of the turns, which reduces and/or minimizes the space **1160** between two turning section magnets.

Referring now to FIGS. **12** and **13**, two illustrative 90 degree rotated cross-sections of single magnet bending or turning sections **1010** are presented. The magnet assembly has a first magnet **1210** and a second magnet **1220**. A magnetic field induced by coils, described infra, runs between the first magnet **1210** to the second magnet **1220** across the gap **1110**. Return magnetic fields run through a first yoke **1212** and second yoke **1222**. The combined cross-section area of the return yokes roughly approximates the cross-sectional area of the first magnet **1210** or second magnet **1220**. The charged particles run through the vacuum tube in the gap **1110**. As illustrated, protons run into FIG. **12** through the gap **1110** and the magnetic field, illustrated as vector B, applies a force F to the protons pushing the protons towards the center of the synchrotron, which is off page to the right in FIG. **12**. The magnetic field is created using windings. A first coil makes up a first winding coil **1250** and a second coil of wire makes up a second winding coil **1260**. Isolating or concentrating gaps **1230**, **1240**, such as air gaps, isolate the iron based yokes from the gap **1110**. The gap **1110** is approximately flat to yield a uniform magnetic field across the gap **1110**, as described supra.

Still referring to FIG. **13**, the ends of a single bending or turning magnet are preferably beveled. Nearly perpendicular or right angle edges of a turning magnet **1010** are represented by dashed lines **1374**, **1384**. The dashed lines **1374**, **1384** intersect at a point **1390** beyond the center of the synchrotron **280**. Preferably, the edge of the turning magnet is beveled at angles alpha, a, and beta, β, which are angles formed by a first line **1372**, **1382** going from an edge of the turning magnet **1010** and the center **280** and a second line **1374**, **1384** going from the same edge of the turning magnet and the intersecting point **1390**. The angle alpha is used to describe the effect and the description of angle alpha applies to angle beta, but angle alpha is optionally different from angle beta. The angle alpha provides an edge focusing effect. Beveling the edge of the turning magnet **1010** at angle alpha focuses the proton beam.

Multiple turning magnets provide multiple magnet edges that each have edge focusing effects in the synchrotron **130**. If only one turning magnet is used, then the beam is only focused once for angle alpha or twice for angle alpha and angle beta. However, by using smaller turning magnets, more turning magnets fit into the turning sections **920** of the synchrotron **130**. For example, if four magnets are used in a turning section **920** of the synchrotron, then for a single turning section there are eight possible edge focusing effect surfaces, two edges per magnet. The eight focusing surfaces yield a smaller cross-sectional beam size, which allows the use of a smaller gap.

The use of multiple edge focusing effects in the turning magnets results in not only a smaller gap **1110**, but also the use of smaller magnets and smaller power supplies. For a synchrotron **130** having four turning sections **920** where each turning sections has four turning magnets and each turning magnet has two focusing edges, a total of thirty-two focusing edges exist for each orbit of the protons in the circulating path of the synchrotron **130**. Similarly, if 2, 6, or 8 magnets are used in a given turning section, or if 2, 3, 5, or 6 turning sections are used, then the number of edge focusing surfaces expands or contracts according to equation 3.

$$TFE = NTS * \frac{M}{NTS} * \frac{FE}{M} \qquad \text{(eq. 3)}$$

where TFE is the number of total focusing edges, NTS is the number of turning sections, M is the number of magnets, and FE is the number of focusing edges. Naturally, not all magnets are necessarily beveled and some magnets are optionally beveled on only one edge.

The inventors have determined that multiple smaller magnets have benefits over fewer larger magnets. For example, the use of 16 small magnets yields 32 focusing edges whereas

the use of 4 larger magnets yields only 8 focusing edges. The use of a synchrotron having more focusing edges results in a circulating path of the synchrotron built without the use of focusing quadrupole magnets. All prior art synchrotrons use quadrupoles in the circulating path of the synchrotron. Further, the use of quadrupoles in the circulating path necessitates additional straight sections in the circulating path of the synchrotron. Thus, the use of quadrupoles in the circulating path of a synchrotron results in synchrotrons having larger diameters, larger circulating beam pathlengths, and/or larger circumferences.

In various embodiments of the system described herein, the synchrotron has any combination of:

- at least 4 and preferably 6, 8, 10, or more edge focusing edges per 90 degrees of turn of the charged particle beam in a synchrotron having four turning sections;
- at least about 16 and preferably about 24, 32, or more edge focusing edges per orbit of the charged particle beam in the synchrotron;
- only 4 turning sections where each of the turning sections includes at least 4 and preferably 8 edge focusing edges;
- an equal number of straight sections and turning sections;
- exactly 4 turning sections;
- at least 4 focusing edges per turning section;
- no quadrupoles in the circulating path of the synchrotron;
- a rounded corner rectangular polygon configuration;
- a circumference of less than 60 meters;
- a circumference of less than 60 meters and 32 edge focusing surfaces; and/or
- any of about 8, 16, 24, or 32 non-quadrupole magnets per circulating path of the synchrotron, where the non-quadrupole magnets include edge focusing edges.

Flat Gap Surface

While the gap surface is described in terms of the first turning magnet **1010**, the discussion applies to each of the turning magnets in the synchrotron. Similarly, while the gap **1110** surface is described in terms of the magnetic field incident surface **670**, the discussion additionally optionally applies to the magnetic field exiting surface **680**.

Referring again to FIG. **12**, the incident magnetic field surface **1270** of the first magnet **1210** is further described. FIG. **12** is not to scale and is illustrative in nature. Local imperfections or unevenness in quality of the finish of the incident surface **1270** results in inhomogeneities or imperfections in the magnetic field applied to the gap **1110**. The magnetic field incident surface **1270** and/or exiting surface **1280** of the first magnet **1210** is preferably about flat, such as to within about a zero to three micron finish polish or less preferably to about a ten micron finish polish. By being very flat, the polished surface spreads the unevenness of the applied magnetic field across the gap **1110**. The very flat surface, such as about 0, 1, 2, 4, 6, 8, 10, 15, or 20 micron finish, allows for a smaller gap size, a smaller applied magnetic field, smaller power supplies, and tighter control of the proton beam cross-sectional area.

Referring now to FIG. **14**, additional optional magnet elements, of the magnet cross-section illustratively represented in FIG. **12**, are described. The first magnet **1210** preferably contains an initial cross-sectional distance **1410** of the iron based core. The contours of the magnetic field are shaped by the magnets **1210**, **1220** and the yokes **1212**, **1222**. The iron based core tapers to a second cross-sectional distance **1420**. The shape of the magnetic field vector **1440** is illustrative only. The magnetic field in the magnet preferentially stays in the iron based core as opposed to the gaps **1230**, **1240**. As the cross-sectional distance decreases from the initial cross-sectional distance **1410** to the final cross-sectional distance **1420**, the magnetic field concentrates. The change in shape of the magnet from the longer distance **1410** to the smaller distance **1420** acts as an amplifier. The concentration of the magnetic field is illustrated by representing an initial density of magnetic field vectors **1430** in the initial cross-section **1410** to a concentrated density of magnetic field vectors **1440** in the final cross-section **1420**. The concentration of the magnetic field due to the geometry of the turning magnets results in fewer winding coils **1250**, **1260** being required and also a smaller power supply to the coils being required.

In one example, the initial cross-section distance **1410** is about fifteen centimeters and the final cross-section distance **1420** is about ten centimeters. Using the provided numbers, the concentration of the magnetic field is about 15/10 or 1.5 times at the incident surface **1270** of the gap **1110**, though the relationship is not linear. The taper **1460** has a slope, such as about 20, 40, or 60 degrees. The concentration of the magnetic field, such as by 1.5 times, leads to a corresponding decrease in power consumption requirements to the magnets.

Referring now to FIG. **15**, an additional example of geometry of the magnet used to concentrate the magnetic field is illustrated. As illustrated in FIG. **14**, the first magnet **1210** preferably contains an initial cross-sectional distance **1410** of the iron based core. The contours of the magnetic field are shaped by the magnets **1210**, **1220** and the yokes **1212**, **1222**. In this example, the core tapers to a second cross-sectional distance **1420** with a smaller angle theta, θ. As described, supra, the magnetic field in the magnet preferentially stays in the iron based core as opposed to the gaps **1230**, **1240**. As the cross-sectional distance decreases from the initial cross-sectional distance **1410** to the final cross-sectional distance **1420**, the magnetic field concentrates. The smaller angle, theta, results in a greater amplification of the magnetic field in going from the longer distance **1410** to the smaller distance **1420**. The concentration of the magnetic field is illustrated by representing an initial density of magnetic field vectors **1430** in the initial cross-section **1410** to a concentrated density of magnetic field vectors **1440** in the final cross-section **1420**. The concentration of the magnetic field due to the geometry of the turning magnets results in fewer winding coils **1250**, **1260** being required and also a smaller power supply to the winding coils **1250**, **1260** being required.

Still referring to FIG. **15**, optional correction coils **1510**, **1520** are illustrated that are used to correct the strength of one or more turning magnets. The correction coils **1520**, **1530** supplement the winding coils **1250**, **1260**. The correction coils **1510**, **1520** have correction coil power supplies that are separate from winding coil power supplies used with the winding coils **1250**, **1260**. The correction coil power supplies typically operate at a fraction of the power required compared to the winding coil power supplies, such as about 1, 2, 3, 5, 7, or 10 percent of the power and more preferably about 1 or 2 percent of the power used with the winding coils **1250**, **1260**. The smaller operating power applied to the correction coils **1510**, **1520** allows for more accurate and/or precise control of the correction coils. The correction coils are used to adjust for imperfection in the turning magnets. Optionally, separate correction coils are used for each turning magnet allowing individual tuning of the magnetic field for each turning magnet, which eases quality requirements in the manufacture of each turning magnet.

Referring now to FIG. **16**, an example of winding coils **1630** and correction coils **1620** about a plurality of turning magnets **1010**, **1020** in an ion beam turning section **920** is illustrated. As illustrated, the winding coils preferably cover **1**, **2**, or **4** turning magnets. One or more high precision magnetic field sensors **1830** are placed into the synchrotron and

are used to measure the magnetic field at or near the proton beam path. For example, the magnetic sensors are optionally placed between turning magnets and/or within a turning magnet, such as at or near the gap **1110** or at or near the magnet core or yoke. The sensors are part of a feedback system to the correction coils, which is optionally run by the main controller. Thus, the system preferably stabilizes the magnetic field in the synchrotron rather than stabilizing the current applied to the magnets. Stabilization of the magnetic field allows the synchrotron to come to a new energy level quickly. This allows the system to be controlled to an operator or algorithm selected energy level with each pulse of the synchrotron and/or with each breath of the patient.

The winding and/or correction coils correct **1**, **2**, **3**, or **4** turning magnets, and preferably correct a magnetic field generated by two turning magnets. A winding or correction coil covering multiple magnets reduces space between magnets as fewer winding or correction coil ends are required, which occupy space. In the illustrated example, a correction coil **1610** winds around a single turning magnet **1010**. In another example, a correction coil **1640** winds around two magnets. In another example, the correction coil **1620** winds around four magnets controlled primarily by a first winding **1630**.

Space **1160** at the end of a turning magnets **1010**, **1040** is optionally further reduced by changing the cross-sectional shape of the winding coils. For example, when the winding coils are running longitudinally along the length of the circulating path or along the length of the turning magnet, the cross-sectional dimension is thick and when the winding coils turn at the end of a turning magnet to run axially across the winding coil, then the cross-sectional area of the winding coils is preferably thin. For example, the cross-sectional area of winding coils as measured by an m×n matrix is 3×2 running longitudinally along the turning magnet and 6×1 running axially at the end of the turning magnet, thereby reducing the width of the coils, n, while keeping the number of coils constant. Preferably, the turn from the longitudinal to axial direction of the winding coil approximates ninety degrees by cutting each winding and welding each longitudinal section to the connecting axial section at about a ninety degree angle. The nearly perpendicular weld further reduces space requirements of the turn in the winding coil, which reduces space in circulating orbit not experiencing focusing and turning forces, which reduces the size of the synchrotron.

Referring now to FIG. **17**A and FIG. **17**B, the accelerator system **270**, such as a radio-frequency (RF) accelerator system, is further described. The accelerator includes a series of coils **1710-1719**, such as iron or ferrite coils, each circumferentially enclosing the vacuum system **320** through which the proton beam **264** passes in the synchrotron **130**. Referring now to FIG. **17**B, the first coil **1710** is further described. A loop of standard wire **1730** completes at least one turn about the first coil **1710**. The loop attaches to a microcircuit **1720**. Referring again to FIG. **17**A, an RF synthesizer **1740**, which is preferably connected to the main controller **110**, provides a low voltage RF signal that is synchronized to the period of circulation of protons in the proton beam path **264**. The RF synthesizer **1740**, microcircuit **1720**, loop **1730**, and coil **1710** combine to provide an accelerating voltage to the protons in the proton beam path **264**. For example, the RF synthesizer **1740** sends a signal to the microcircuit **1720**, which amplifies the low voltage RF signal and yields an acceleration voltage, such as about 10 volts. The actual acceleration voltage for a single microcircuit/loop/coil combination is about 5, 10, 15, or 20 volts, but is preferably about 10 volts. Preferably, the RF-amplifier microcircuit and accelerating coil are integrated.

Still referring to FIG. **17**A, the integrated RF-amplifier microcircuit and accelerating coil presented in FIG. **17**B is repeated, as illustrated as the set of coils **1711-1719** surrounding the vacuum tube **320**. For example, the RF-synthesizer **1740**, under main controller **130** direction, sends an RF-signal to the microcircuits **1720-1729** connected to coils **1710-1719**, respectively. Each of the microcircuit/loop/coil combinations generates a proton accelerating voltage, such as about 10 volts each. Hence, a set of five coil combinations generates about 50 volts for proton acceleration. Preferably about 5 to 20 microcircuit/loop/coil combinations are used and more preferably about 9 or 10 microcircuit/loop/coil combinations are used in the accelerator system **270**.

As a further clarifying example, the RF synthesizer **1740** sends an RF-signal, with a period equal to a period of circulation of a proton about the synchrotron **130**, to a set of ten microcircuit/loop/coil combinations, which results in about 100 volts for acceleration of the protons in the proton beam path **264**. The 100 volts is generated at a range of frequencies, such as at about 1 MHz for a low energy proton beam to about 15 MHz for a high energy proton beam. The RF-signal is optionally set at an integer multiple of a period of circulation of the proton about the synchrotron circulating path. Each of the microcircuit/loop/coil combinations are optionally independently controlled in terms of acceleration voltage and frequency.

Integration of the RF-amplifier microcircuit and accelerating coil, in each microcircuit/loop/coil combination, results in three considerable advantages. First, for synchrotrons, the prior art does not use microcircuits integrated with the accelerating coils but rather uses a set of long cables to provide power to a corresponding set of coils. The long cables have an impedance/resistance, which is problematic for high frequency RF control. As a result, the prior art system is not operable at high frequencies, such as above about 10 MHz. The integrated RF-amplifier microcircuit/accelerating coil system is operable at above about 10 MHz and even 15 MHz where the impedance and/or resistance of the long cables in the prior art systems results in poor control or failure in proton acceleration. Second, the long cable system, operating at lower frequencies, costs about $50,000 and the integrated microcircuit system costs about $1000, which is 50 times less expensive. Third, the microcircuit/loop/coil combinations in conjunction with the RF-amplifier system results in a compact low power consumption design allowing production and use of a proton cancer therapy system in a small space, as described supra, and in a cost effective manner.

Referring now to FIG. **18**, an example is used to clarify the magnetic field control using a feedback loop **1800** to change delivery times and/or periods of proton pulse delivery. In one case, a respiratory sensor **1810** senses the respiration cycle of the subject. The respiratory sensor sends the information to an algorithm in a magnetic field controller **1820**, typically via the patient interface module **150** and/or via the main controller **110** or a subcomponent thereof. The algorithm predicts and/or measures when the subject is at a particular point in the respiration cycle, such as at the bottom of a breath. Magnetic field sensors **1830** are used as input to the magnetic field controller, which controls a magnet power supply **1840** for a given magnetic field **1850**, such as within a first turning magnet **1010** of a synchrotron **130**. The control feedback loop is thus used to dial the synchrotron to a selected energy level and deliver protons with the desired energy at a selected point in time, such as at the bottom of the breath. More particularly, the main controller injects protons into the synchrotron and accelerates the protons in a manner that combined with extraction delivers the protons to the tumor at a selected point

in the respiration cycle. Intensity of the proton beam is also selectable and controllable by the main controller at this stage. The feedback control to the correction coils allows rapid selection of energy levels of the synchrotron that are tied to the patient's respiration cycle. This system is in stark contrast to a system where the current is stabilized and the synchrotron deliver pulses with a period, such as 10 or 20 cycles per second with a fixed period. Optionally, the feedback or the magnetic field design coupled with the correction coils allows for the extraction cycle to match the varying respiratory rate of the patient.

Traditional extraction systems do not allow this control as magnets have memories in terms of both magnitude and amplitude of a sine wave. Hence, in a traditional system, in order to change frequency, slow changes in current must be used. However, with the use of the feedback loop using the magnetic field sensors, the frequency and energy level of the synchrotron are rapidly adjustable. Further aiding this process is the use of a novel extraction system that allows for acceleration of the protons during the extraction process, described infra.

Referring again to FIG. **16**, an example of a winding coil **1630** that covers two turning magnets **1010**, **1020** is provided. Optionally, a first winding coil **1640** covers two magnets and a second winding coil, not illustrated, covers another two magnets. As described, supra, this system reduces space between turning section allowing more magnetic field to be applied per radian of turn. A first correction coil **1610** is illustrated that is used to correct the magnetic field for the first turning magnet **1010**. A second correction coil **1620** is illustrated that is used to correct the magnetic field for a winding coil **1630** about two turning magnets. Individual correction coils for each turning magnet are preferred and individual correction coils yield the most precise and/or accurate magnetic field in each turning section. Particularly, the individual correction coil **1610** is used to compensate for imperfections in the individual magnet of a given turning section. Hence, with a series of magnetic field sensors, corresponding magnetic fields are individually adjustable in a series of feedback loops, via a magnetic field monitoring system, as an independent coil is used for each turning section. Alternatively, a multiple magnet correction coil is used to correct the magnetic field for a plurality of turning section magnets.

Proton Beam Extraction

Referring now to FIG. **19**, an exemplary proton extraction process from the synchrotron **130** is illustrated. For clarity, FIG. **19** removes elements represented in FIG. **2**, such as the turning magnets, which allows for greater clarity of presentation of the proton beam path as a function of time. Generally, protons are extracted from the synchrotron **130** by slowing the protons. As described, supra, the protons were initially accelerated in a circulating path **264**, which is maintained with a plurality of main bending magnets **250**. The circulating path is referred to herein as an original central beamline **264**. The protons repeatedly cycle around a central point in the synchrotron **280**. The proton path traverses through a radio frequency (RF) cavity system **1910**. To initiate extraction, an RF field is applied across a first blade **1912** and a second blade **1914**, in the RF cavity system **1910**. The first blade **1912** and second blade **1914** are referred to herein as a first pair of blades.

In the proton extraction process, an RF voltage is applied across the first pair of blades, where the first blade **1912** of the first pair of blades is on one side of the circulating proton beam path **264** and the second blade **1914** of the first pair of blades is on an opposite side of the circulating proton beam path **264**. The applied RF field applies energy to the circulating charged-particle beam. The applied RF field alters the orbiting or circulating beam path slightly of the protons from the original central beamline **264** to an altered circulating beam path **265**. Upon a second pass of the protons through the RF cavity system, the RF field further moves the protons off of the original proton beamline **264**. For example, if the original beamline is considered as a circular path, then the altered beamline is slightly elliptical. The applied RF field is timed to apply outward or inward movement to a given band of protons circulating in the synchrotron accelerator. Each orbit of the protons is slightly more off axis compared to the original circulating beam path **264**. Successive passes of the protons through the RF cavity system are forced further and further from the original central beamline **264** by altering the direction and/or intensity of the RF field with each successive pass of the proton beam through the RF field.

The RF voltage is frequency modulated at a frequency about equal to the period of one proton cycling around the synchrotron for one revolution or at a frequency than is an integral multiplier of the period of one proton cycling about the synchrotron. The applied RF frequency modulated voltage excites a betatron oscillation. For example, the oscillation is a sine wave motion of the protons. The process of timing the RF field to a given proton beam within the RF cavity system is repeated thousands of times with each successive pass of the protons being moved approximately one micrometer further off of the original central beamline **264**. For clarity, the approximately 1000 changing beam paths with each successive path of a given band of protons through the RF field are illustrated as the altered beam path **265**.

With a sufficient sine wave betatron amplitude, the altered circulating beam path **265** touches or traverses a material **1930**, such as a foil or a sheet of foil. The foil is preferably a lightweight material, such as beryllium, a lithium hydride, a carbon sheet, or a material having low nuclear charge components. Herein, a material of low nuclear charge is a material composed of atoms consisting essentially of atoms having six or fewer protons. The foil is preferably about 10 to 150 microns thick, is more preferably about 30 to 100 microns thick, and is still more preferably about 40 to 60 microns thick. In one example, the foil is beryllium with a thickness of about 50 microns. When the protons traverse through the foil, energy of the protons is lost and the speed of the protons is reduced. Typically, a current is also generated, described infra. Protons moving at a slower speed travel in the synchrotron with a reduced radius of curvature **266** compared to either the original central beamline **264** or the altered circulating path **265**. The reduced radius of curvature **266** path is also referred to herein as a path having a smaller diameter of trajectory or a path having protons with reduced energy. The reduced radius of curvature **266** is typically about two millimeters less than a radius of curvature of the last pass of the protons along the altered proton beam path **265**.

The thickness of the material **1930** is optionally adjusted to created a change in the radius of curvature, such as about ½, 1, 2, 3, or 4 mm less than the last pass of the protons **265** or original radius of curvature **264**. Protons moving with the smaller radius of curvature travel between a second pair of blades. In one case, the second pair of blades is physically distinct and/or is separated from the first pair of blades. In a second case, one of the first pair of blades is also a member of the second pair of blades. For example, the second pair of blades is the second blade **1914** and a third blade **1916** in the RF cavity system **1910**. A high voltage DC signal, such as about 1 to 5 kV, is then applied across the second pair of blades, which directs the protons out of the synchrotron

through an extraction magnet **292**, such as a Lamberson extraction magnet, into a transport path **268**.

Control of acceleration of the charged particle beam path in the synchrotron with the accelerator and/or applied fields of the turning magnets in combination with the above described extraction system allows for control of the intensity of the extracted proton beam, where intensity is a proton flux per unit time or the number of protons extracted as a function of time. For example, when a current is measured beyond a threshold, the RF field modulation in the RF cavity system is terminated or reinitiated to establish a subsequent cycle of proton beam extraction. This process is repeated to yield many cycles of proton beam extraction from the synchrotron accelerator.

Because the extraction system does not depend on any change in magnetic field properties, it allows the synchrotron to continue to operate in acceleration or deceleration mode during the extraction process. Stated differently, the extraction process does not interfere with synchrotron acceleration. In stark contrast, traditional extraction systems introduce a new magnetic field, such as via a hexapole, during the extraction process. More particularly, traditional synchrotrons have a magnet, such as a hexapole magnet, that is off during an acceleration stage. During the extraction phase, the hexapole magnetic field is introduced to the circulating path of the synchrotron. The introduction of the magnetic field necessitates two distinct modes, an acceleration mode and an extraction mode, which are mutually exclusive in time. The herein described system allows for acceleration and/or deceleration of the proton during the extraction step without the use of a newly introduced magnetic field, such as by a hexapole magnet.

Charged Particle Beam Intensity Control

Control of applied field, such as a radio-frequency (RF) field, frequency and magnitude in the RF cavity system **1910** allows for intensity control of the extracted proton beam, where intensity is extracted proton flux per unit time or the number of protons extracted as a function of time.

Referring still to FIG. **19**, when protons in the proton beam hit the material **1930** electrons are given off resulting in a current. The resulting current is converted to a voltage and is used as part of a ion beam intensity monitoring system or as part of an ion beam feedback loop for controlling beam intensity. The voltage is optionally measured and sent to the main controller **110** or to a controller subsystem **1940**. More particularly, when protons in the charged particle beam path pass through the material **1930**, some of the protons lose a small fraction of their energy, such as about one-tenth of a percent, which results in a secondary electron. That is, protons in the charged particle beam push some electrons when passing through material **1930** giving the electrons enough energy to cause secondary emission. The resulting electron flow results in a current or signal that is proportional to the number of protons going through the target material **1930**. The resulting current is preferably converted to voltage and amplified. The resulting signal is referred to as a measured intensity signal.

The amplified signal or measured intensity signal resulting from the protons passing through the material **1930** is preferably used in controlling the intensity of the extracted protons. For example, the measured intensity signal is compared to a goal signal, which is predetermined in an irradiation of the tumor plan. The difference between the measured intensity signal and the planned for goal signal is calculated. The difference is used as a control to the RF generator. Hence, the measured flow of current resulting from the protons passing through the material **1930** is used as a control in the RF generator to increase or decrease the number of protons undergoing betatron oscillation and striking the material **1930**. Hence, the voltage determined off of the material **1930** is used as a measure of the orbital path and is used as a feedback control to control the RF cavity system. Alternatively, the measured intensity signal is not used in the feedback control and is just used as a monitor of the intensity of the extracted protons.

As described, supra, the photons striking the material **1930** is a step in the extraction of the protons from the synchrotron **130**. Hence, the measured intensity signal is used to change the number of protons per unit time being extracted, which is referred to as intensity of the proton beam. The intensity of the proton beam is thus under algorithm control. Further, the intensity of the proton beam is controlled separately from the velocity of the protons in the synchrotron **130**. Hence, intensity of the protons extracted and the energy of the protons extracted are independently variable.

For example, protons initially move at an equilibrium trajectory in the synchrotron **130**. An RF field is used to excite the protons into a betatron oscillation. In one case, the frequency of the protons orbit is about 10 MHz. In one example, in about one millisecond or after about 10,000 orbits, the first protons hit an outer edge of the target material **130**. The specific frequency is dependent upon the period of the orbit. Upon hitting the material **130**, the protons push electrons through the foil to produce a current. The current is converted to voltage and amplified to yield a measured intensity signal. The measured intensity signal is used as a feedback input to control the applied RF magnitude, RF frequency, or RF field. Preferably, the measured intensity signal is compared to a target signal and a measure of the difference between the measured intensity signal and target signal is used to adjust the applied RF field in the RF cavity system **1910** in the extraction system to control the intensity of the protons in the extraction step. Stated again, the signal resulting from the protons striking and/or passing through the material **130** is used as an input in RF field modulation. An increase in the magnitude of the RF modulation results in protons hitting the foil or material **130** sooner. By increasing the RF, more protons are pushed into the foil, which results in an increased intensity, or more protons per unit time, of protons extracted from the synchrotron **130**.

In another example, a detector **1830** external to the synchrotron **130** is used to determine the flux of protons extracted from the synchrotron and a signal from the external detector is used to alter the RF field or RF modulation in the RF cavity system **1910**. Here the external detector generates an external signal, which is used in a manner similar to the measured intensity signal, described in the preceding paragraphs.

In yet another example, when a current from material **130** resulting from protons passing through or hitting material is measured beyond a threshold, the RF field modulation in the RF cavity system is terminated or reinitiated to establish a subsequent cycle of proton beam extraction. This process is repeated to yield many cycles of proton beam extraction from the synchrotron accelerator.

In still yet another embodiment, intensity modulation of the extracted proton beam is controlled by the main controller **110**. The main controller **110** optionally and/or additionally controls timing of extraction of the charged particle beam and energy of the extracted proton beam.

The benefits of the system include a multi-dimensional scanning system. Particularly, the system allows independence in: (1) energy of the protons extracted and (2) intensity of the protons extracted. That is, energy of the protons extracted is controlled by an energy control system and an intensity control system controls the intensity of the extracted

protons. The energy control system and intensity control system are optionally independently controlled. Preferably, the main controller **110** controls the energy control system and the main controller simultaneously controls the intensity control system to yield an extracted proton beam with controlled energy and controlled intensity where the controlled energy and controlled intensity are independently variable. Thus the irradiation spot hitting the tumor is under independent control of:

time;

energy;

intensity;

x-axis position, where the x-axis represents horizontal movement of the proton beam relative to the patient, and

y-axis position, where the y-axis represents vertical movement of the proton beam relative to the patient.

In addition, the patient is optionally independently translated and/or rotated relative to a translational axis of the proton beam at the same time.

Referring now to FIGS. **20** A and B, a proton beam position verification system **2000** is described. A nozzle **2010** provides an outlet for the second reduced pressure vacuum system initiating at the foil **395** of the tandem accelerator **390** and running through the synchrotron **130** to a nozzle foil **2020** covering the end of the nozzle **2010**. The nozzle expands in x-, y-cross-sectional area along the z-axis of the proton beam path **268** to allow the proton beam **268** to be scanned along the x- and y-axes by the vertical control element **142** and horizontal control element **144**, respectively. The nozzle foil **2020** is preferably mechanically supported by the outer edges of an exit port of the nozzle **2010**. An example of a nozzle foil **2020** is a sheet of about 0.1 inch thick aluminum foil. Generally, the nozzle foil separates atmosphere pressures on the patient side of the nozzle foil **2020** from the low pressure region, such as about 10^{-5} to 10^{-7} torr region, on the synchrotron **130** side of the nozzle foil **2020**. The low pressure region is maintained to reduce scattering of the proton beam **264**, **268**.

Still referring to FIG. **20**, the proton beam verification system **2000** is a system that allows for monitoring of the actual proton beam position **268**, **269** in real-time without destruction of the proton beam. The proton beam verification system **2000** preferably includes a proton beam position verification layer **2030**, which is also referred to herein as a coating, luminescent, fluorescent, phosphorescent, radiance, or viewing layer. The verification layer or coating layer **2030** is preferably a coating or thin layer substantially in contact with an inside surface of the nozzle foil **2020**, where the inside surface is on the synchrotron side of the nozzle foil **2020**. Less preferably, the verification layer or coating layer **2030** is substantially in contact with an outer surface of the nozzle foil **2020**, where the outer surface is on the patient treatment side of the nozzle foil **2020**. Preferably, the nozzle foil **2020** provides a substrate surface for coating by the coating layer. Optionally, a binding layer is located between the coating layer **2030** and the nozzle foil **2020**. Optionally a separate coating layer support element, on which the coating **2030** is mounted, is placed anywhere in the proton beam path **268**.

Referring now to FIG. **20**B, the coating **2030** yields a measurable spectroscopic response, spatially viewable by the detector **2040**, as a result of transmission by the proton beam **268**. The coating **2030** is preferably a phosphor, but is optionally any material that is viewable or imaged by a detector where the material changes spectroscopically as a result of the proton beam path **268** hitting or transmitting through the coating **2030**. A detector or camera **2040** views the coating layer **2030** and determines the current position of the proton beam **269** by the spectroscopic differences resulting from protons passing through the coating layer. For example, the camera **2040** views the coating surface **2030** as the proton beam **268** is being scanned by the horizontal **144** and vertical **142** beam position control elements during treatment of the tumor **2120**. The camera **2040** views the current position of the proton beam **269** as measured by spectroscopic response. The coating layer **2030** is preferably a phosphor or luminescent material that glows or emits photons for a short period of time, such as less than 5 seconds for a 50% intensity, as a result of excitation by the proton beam **268**. Optionally, a plurality of cameras or detectors **2040** are used, where each detector views all or a portion of the coating layer **2030**. For example, two detectors **2040** are used where a first detector views a first half of the coating layer and the second detector views a second half of the coating layer. Preferably, at least a portion of the detector **2040** is mounted into the nozzle **2010** to view the proton beam position after passing through the first axis and second axis controllers **142**, **144**. Preferably, the coating layer **2030** is positioned in the proton beam path **268** in a position prior to the protons striking the patient **2130**.

Still referring to FIG. **20**, the main controller **130**, connected to the camera or detector **2040** output, compares the actual proton beam position **269** with the planned proton beam position and/or a calibration reference to determine if the actual proton beam position **269** is within tolerance. The proton beam verification system **2000** preferably is used in at least two phases, a calibration phase and a proton beam treatment phase. The calibration phase is used to correlate, as a function of x-, y-position of the glowing response the actual x-, y-position of the proton beam at the patient interface. During the proton beam treatment phase, the proton beam position is monitored and compared to the calibration and/or treatment plan to verify accurate proton delivery to the tumor **2120** and/or as a proton beam shutoff safety indicator.

Patient Positioning

Referring now to FIG. **21**, the patient is preferably positioned on or within a patient translation and rotation positioning system **2110** of the patient interface module **150**. The patient translation and rotation positioning system **2110** is used to translate the patient and/or rotate the patient into a zone where the proton beam can scan the tumor using a scanning system **140** or proton targeting system, described infra. Essentially, the patient positioning system **2110** performs large movements of the patient to place the tumor near the center of a proton beam path **268** and the proton scanning or targeting system **140** performs fine movements of the momentary beam position **269** in targeting the tumor **2120**. To illustrate, FIG. **21**A shows the momentary proton beam position **269** and a range of scannable positions **2140** using the proton scanning or targeting system **140**, where the scannable positions **2140** are about the tumor **2120** of the patient **2130**. In this example, the scannable positions are scanned along the x- and y-axes; however, scanning is optionally simultaneously performed along the z-axis as described infra. This illustratively shows that the y-axis movement of the patient occurs on a scale of the body, such as adjustment of about 1, 2, 3, or 4 feet, while the scannable region of the proton beam **268** covers a portion of the body, such as a region of about 1, 2, 4, 6, 8, 10, or 12 inches. The patient positioning system and its rotation and/or translation of the patient combines with the proton targeting system to yield precise and/or accurate delivery of the protons to the tumor.

Referring still to FIG. **21**, the patient positioning system **2110** optionally includes a bottom unit **2112** and a top unit **2114**, such as discs or a platform.

Referring now to FIG. **21**A, the patient positioning unit **2110** is preferably y-axis adjustable **2116** to allow vertical

shifting of the patient relative to the proton therapy beam **268**. Preferably, the vertical motion of the patient positioning unit **2110** is about 10, 20, 30, or 50 centimeters per minute. Referring now to FIG. **21**B, the patient positioning unit **2110** is also preferably rotatable **2117** about a rotation axis, such as about the y-axis running through the center of the bottom unit **2112** or about a y-axis running through the tumor **2120**, to allow rotational control and positioning of the patient relative to the proton beam path **268**. Preferably the rotational motion of the patient positioning unit **2110** is about 360 degrees per minute. Optionally, the patient positioning unit rotates about 45, 90, or 180 degrees. Optionally, the patient positioning unit **2110** rotates at a rate of about 45, 90, 180, 360, 720, or 1080 degrees per minute. The rotation of the positioning unit **2117** is illustrated about the rotation axis at two distinct times, t_1 and t_2. Protons are optionally delivered to the tumor **2120** at n times where each of the n times represent a different relative direction of the incident proton beam **269** hitting the patient **2130** due to rotation of the patient **2117** about the rotation axis.

Any of the semi-vertical, sitting, or laying patient positioning embodiments described, infra, are optionally vertically translatable along the y-axis or rotatable about the rotation or y-axis.

Preferably, the top and bottom units **2112**, **2114** move together, such that they rotate at the same rates and translate in position at the same rates. Optionally, the top and bottom units **2112**, **2114** are independently adjustable along the y-axis to allow a difference in distance between the top and bottom units **2112**, **2114**. Motors, power supplies, and mechanical assemblies for moving the top and bottom units **2112**, **2114** are preferably located out of the proton beam path **269**, such as below the bottom unit **2112** and/or above the top unit **2114**. This is preferable as the patient positioning unit **2110** is preferably rotatable about 360 degrees and the motors, power supplies, and mechanical assemblies interfere with the protons if positioned in the proton beam path **269**

Proton Delivery Efficiency

Referring now to FIG. **22**, a common distribution of relative doses for both X-rays and proton irradiation is presented. As shown, X-rays deposit their highest dose near the surface of the targeted tissue and then deposited doses exponentially decrease as a function of tissue depth. The deposition of X-ray energy near the surface is non-ideal for tumors located deep within the body, which is usually the case, as excessive damage is done to the soft tissue layers surrounding the tumor **2120**. The advantage of protons is that they deposit most of their energy near the end of the flight trajectory as the energy loss per unit path of the absorber transversed by a proton increases with decreasing particle velocity, giving rise to a sharp maximum in ionization near the end of the range, referred to herein as the Bragg peak. Furthermore, since the flight trajectory of the protons is variable by increasing or decreasing the initial kinetic energy or initial velocity of the proton, then the peak corresponding to maximum energy is movable within the tissue. Thus z-axis control of the proton depth of penetration is allowed by the acceleration/extraction process, described supra. As a result of proton dose-distribution characteristics, using the algorithm described, infra, a radiation oncologist can optimize dosage to the tumor **2120** while minimizing dosage to surrounding normal tissues.

Herein, the term ingress refers to a place charged particles enter into the patient **2130** or a place of charged particles entering the tumor **2120**. The ingress region of the Bragg energy profile refers to the relatively flat dose delivery portion at shallow depths of the Bragg energy profile. Similarly, herein the terms proximal or the clause proximal region refer to the shallow depth region of the tissue that receives the relatively flat radiation dose delivery portion of the delivered Bragg profile energy. Herein, the term distal refers to the back portion of the tumor located furthest away from the point of origin where the charged particles enter the tumor. In terms of the Bragg energy profile, the Bragg peak is at the distal point of the profile. Herein, the term ventral refers to the front of the patient and the term dorsal refers to the back of the patient. As an example of use, when delivering protons to a tumor in the body, the protons ingress through the healthy tissue and if delivered to the far side of the tumor, the Bragg peak occurs at the distal side of the tumor. For a case where the proton energy is not sufficient to reach the far side of the tumor, the distal point of the Bragg energy profile is the region of furthest penetration into the tumor.

The Bragg peak energy profile shows that protons deliver their energy across the entire length of the body penetrated by the proton up to a maximum penetration depth. As a result, energy is being delivered, in the proximal portion of the Bragg peak energy profile, to healthy tissue, bone, and other body constituents before the proton beam hits the tumor. It follows that the shorter the pathlength in the body prior to the tumor, the higher the efficiency of proton delivery efficiency, where proton delivery efficiency is a measure of how much energy is delivered to the tumor relative to healthy portions of the patient. Examples of proton delivery efficiency include: (1) a ratio of proton energy delivered to the tumor over proton energy delivered to non-tumor tissue; (2) pathlength of protons in the tumor versus pathlength in the non-tumor tissue; and/or (3) damage to a tumor compared to damage to healthy body parts. Any of these measures are optionally weighted by damage to sensitive tissue, such as a nervous system element, heart, brain, or other organ. To illustrate, for a patient in a laying position where the patient is rotated about the y-axis during treatment, a tumor near the heart would at times be treated with protons running through the head-to-heart path, leg-to-heart path, or hip-to-heart path, which are all inefficient compared to a patient in a sitting or semi-vertical position where the protons are all delivered through a shorter chest-to-heart; side-of-body-to-heart, or back-to-heart path. Particularly, compared to a laying position, using a sitting or semi-vertical position of the patient, a shorter pathlength through the body to a tumor is provided to a tumor located in the torso or head, which results in a higher or better proton delivery efficiency.

Herein proton delivery efficiency is separately described from time efficiency or synchrotron use efficiency, which is a fraction of time that the charged particle beam apparatus is in a tumor treating operation mode.

Depth Targeting

Referring now to FIGS. **23** A-E, x-axis scanning of the proton beam is illustrated while z-axis energy of the proton beam undergoes controlled variation **2300** to allow irradiation of slices of the tumor **2120**. For clarity of presentation, the simultaneous y-axis scanning that is performed is not illustrated. In FIG. **23**A, irradiation is commencing with the momentary proton beam position **269** at the start of a first slice. Referring now to FIG. **23**B, the momentary proton beam position is at the end of the first slice. Importantly, during a given slice of irradiation, the proton beam energy is preferably continuously controlled and changed according to the tissue mass and density in front of the tumor **2120**. The variation of the proton beam energy to account for tissue density thus allows the beam stopping point, or Bragg peak, to remain inside the tissue slice. The variation of the proton beam energy during scanning or during x-, y-axes scanning is possible due to the acceleration/extraction techniques, described supra, which allow for acceleration of the proton

beam during extraction. FIGS. **23**C, **23**D, and **23**E show the momentary proton beam position in the middle of the second slice, two-thirds of the way through a third slice, and after finalizing irradiation from a given direction, respectively. Using this approach, controlled, accurate, and precise delivery of proton irradiation energy to the tumor **2120**, to a designated tumor subsection, or to a tumor layer is achieved. Efficiency of deposition of proton energy to tumor, as defined as the ratio of the proton irradiation energy delivered to the tumor relative to the proton irradiation energy delivered to the healthy tissue is further described infra.

Multi-Field Irradiation

It is desirable to maximize efficiency of deposition of protons to the tumor **2120**, as defined by maximizing the ratio of the proton irradiation energy delivered to the tumor **2120** relative to the proton irradiation energy delivered to the healthy tissue. Irradiation from one, two, or three directions into the body, such as by rotating the body about 90 degrees between irradiation sub-sessions results in proton irradiation from the proximal portion of the Bragg peak concentrating into one, two, or three healthy tissue volumes, respectively. It is desirable to further distribute the proximal portion of the Bragg peak energy evenly through the healthy volume tissue surrounding the tumor **2120**.

Multi-field irradiation is proton beam irradiation from a plurality of entry points into the body. For example, the patient **2130** is rotated and the radiation source point is held constant. For example, the patient **2130** is rotated through 360 degrees and proton therapy is applied from a multitude of angles resulting in the ingress or proximal radiation being circumferentially spread about the tumor yielding enhanced proton irradiation efficiency. In one case, the body is rotated into greater than 3, 5, 10, 15, 20, 25, 30, or 35 positions and proton irradiation occurs with each rotation position. Rotation of the patient is preferably performed using the patient positioning system **2110** and/or the bottom unit **2112** or disc, described supra. Rotation of the patient **2130** while keeping the delivery proton beam **268** in a relatively fixed orientation allows irradiation of the tumor **2120** from multiple directions without use of a new collimator for each direction. Further, as no new setup is required for each rotation position of the patient **2130**, the system allows the tumor **2120** to be treated from multiple directions without reseating or positioning the patient, thereby minimizing tumor **2120** regeneration time, increasing the synchrotrons efficiency, and increasing patient throughput.

The patient is optionally centered on the bottom unit **2112** or the tumor **2120** is optionally centered on the bottom unit **2112**. If the patient is centered on the bottom unit **2112**, then the first axis control element **142** and second axis control element **144** are programmed to compensate for the off central axis of rotation position variation of the tumor **2120**.

Referring now to FIGS. **24** A-E, an example of multi-field irradiation **2400** is presented. In this example, five patient rotation positions are illustrated; however, the five rotation positions are discrete rotation positions of about thirty-six rotation positions, where the body is rotated about ten degrees with each position. Referring now to FIG. **24**A, a range of irradiation beam positions **269** is illustrated from a first body rotation position, illustrated as the patient **2130** facing the proton irradiation beam where the tumor receives the bulk of the Bragg profile energy while a first healthy volume **2411** is irradiated by the less intense ingress portion of the Bragg profile energy. Referring now to FIG. **24**B, the patient **2130** is rotated about forty degrees and the irradiation is repeated. In the second position, the tumor **2120** again receives the bulk of the irradiation energy and a second healthy tissue volume **2412** receives the smaller ingress portion of the Bragg profile energy. Referring now to FIGS. **24** C-E, the patient **2130** is rotated a total of about 90, 130, and 180 degrees, respectively. For each of the third, fourth, and fifth rotation positions, the tumor **2120** receives the bulk of the irradiation energy and the third, fourth, and fifth healthy tissue volumes **2413**, **2414**, **1415** receive the smaller ingress portion of the Bragg peak energy, respectively. Thus, the rotation of the patient during proton therapy results in the proximal or ingress energy of the delivered proton energy to be distributed about the tumor **2120**, such as to regions one to five **2411**-**2415**, while along a given axis, at least about 75, 80, 85, 90, or 95 percent of the energy is delivered to the tumor **2120**.

For a given rotation position, all or part of the tumor is irradiated. For example, in one embodiment only a distal section or distal slice of the tumor **2120** is irradiated with each rotation position, where the distal section is a section furthest from the entry point of the proton beam into the patient **2130**. For example, the distal section is the dorsal side of the tumor when the patient **2130** is facing the proton beam and the distal section is the ventral side of the tumor when the patient **2130** is facing away from the proton beam.

Referring now to FIG. **25**, a second example of multi-field irradiation **2500** is presented where the proton source is stationary and the patient **2130** is rotated.

For ease of presentation, the stationary but scanning proton beam path **269** is illustrated as entering the patient **2130** from varying sides at times t_1, t_2, t_3, . . . , t_n, t_{n+1} as the patient is rotated. At a first time, t_1, the ingress side or proximal region of the Bragg peak profile hits a first area, A_1. Again, the proximal end of the Bragg peak profile refers to the relatively shallow depths of tissue where Bragg energy profile energy delivery is relatively flat. The patient is rotated and the proton beam path is illustrated at a second time, t_2, where the ingress energy of the Bragg energy profile hits a second area, A_2. Thus, the low radiation dosage of the ingress region of the Bragg profile energy is delivered to the second area. At a third time, the ingress end of the Bragg energy profile hits a third area, A_3. This rotation and irradiation process is repeated n times, where n is a positive number greater than five and preferably greater than about 10, 20, 30, 100, or 300. As illustrated, at an n^{th} time, t_n, if the patient **2130** is rotated further, the scanning proton beam **269** would hit a sensitive body constituent **2150**, such as the spinal cord or eyes. Irradiation is preferably suspended until the sensitive body constituent is rotated out of the scanning proton beam **269** path. Irradiation is resumed at a time, t_{n+1}, after the sensitive body constituent **2150** is rotated out of the proton beam path. In this manner:

- the distal Bragg peak energy is always within the tumor;
- the radiation dose delivery of the distal region of the Bragg energy profile is spread over the tumor;
- the ingress or proximal region of the Bragg energy profile is distributed in healthy tissue about the tumor **2120**; and
- sensitive body constituents **2150** receive minimal or no proton beam irradiation.

Proton Delivery Efficiency

Herein, charged particle or proton delivery efficiency is radiation dose delivered to the tumor compared to radiation dose delivered to the healthy regions of the patient.

A proton delivery enhancement method is described where proton delivery efficiency is enhanced, optimized, or maximized. In general, multi-field irradiation is used to deliver protons to the tumor from a multitude of rotational directions. From each direction, the energy of the protons is adjusted to target the distal portion of the tumor, where the distal portion

of the tumor is the volume of the tumor furthest from the entry point of the proton beam into the body.

For clarity, the process is described using an example where the outer edges of the tumor are initially irradiated using distally applied radiation through a multitude of rotational positions, such as through 360 degrees. This results in a symbolic or calculated remaining smaller tumor for irradiation. The process is then repeated as many times as necessary on the smaller tumor. However, the presentation is for clarity. In actuality, irradiation from a given rotational angle is performed once with z-axis proton beam energy and intensity being adjusted for the calculated smaller inner tumors during x- and y-axis scanning.

Referring now to FIG. **26**, the proton delivery enhancement method is further described. Referring now to FIG. **26**A, at a first point in time protons are delivered to the tumor **2120** of the patient **2130** from a first direction. From the first rotational direction, the proton beam is scanned **269** across the tumor. As the proton beam is scanned across the tumor the energy of the proton beam is adjusted to allow the Bragg peak energy to target the distal portion of the tumor. Again, distal refers to the back portion of the tumor located furthest away from where the charged particles enter the tumor. As illustrated, the proton beam is scanned along an x-axis across the patient. This process allows the Bragg peak energy to fall within the tumor, for the middle area of the Bragg peak profile to fall in the middle and proximal portion of the tumor, and for the small intensity ingress portion of the Bragg peak to hit healthy tissue. In this manner, the maximum radiation dose is delivered to the tumor or the proton dose efficiency is maximized for the first rotational direction.

After irradiation from the first rotational position, the patient is rotated to a new rotational position. Referring now to FIG. **26**B, the scanning of the proton beam is repeated. Again, the distal portion of the tumor is targeted with adjustment of the proton beam energy to target the Bragg peak energy to the distal portion of the tumor. Naturally, the distal portion of the tumor for the second rotational position is different from the distal portion of the tumor for the first rotational position. Referring now to FIG. **26**C, the distal irradiation is illustrated from a third rotational direction. Referring now to FIG. **26**C, the process of rotating the patient and then irradiating the new distal portion of the tumor is further illustrated at an n^{th} rotational position. Preferably, the process of rotating the patient and scanning along the x- and y-axes with the Z-axes energy targeting the new distal portion of the tumor is repeated, such as with more than 5, 10, 20, or 30 rotational positions or with about 36 rotational positions.

For clarity, FIGS. **26** A-C and FIG. **26** E show the proton beam as having moved, but in actuality, the proton beam is stationary and the patient is rotated, such as via use of rotating the bottom unit **2112** of the patient positioning system **2110**. Also, FIGS. **26** A-C show the proton beam being scanned across the tumor along the x-axis. Though not illustrated for clarity, the proton beam is additionally scanned up and down the tumor along the y-axis of the patient. Combined, the distal portion or volume of the tumor is irradiated along the x- and y-axes with adjustment of the z-axis energy level of the proton beam. In one case, the tumor is scanned along the x-axis and the scanning is repeated along the x-axis for multiple y-axis positions. In another case, the tumor is scanned along the y-axis and the scanning is repeated along the y-axis for multiple x-axis positions. In yet another case, the tumor is scanned by simultaneously adjusting the x- and y-axes so that the distal portion of the tumor is targeted. In all of these cases, the z-axis or energy of the proton beam is adjusted along the contour of the distal portion of the tumor to target the Bragg peak energy to the distal portion of the tumor.

Referring now to FIG. **26**D, after targeting the distal portion of the tumor from multiple directions, such as through 360 degrees, the outer perimeter of the tumor has been strongly irradiated with peak Bragg profile energy, the middle of the Bragg peak energy profile energy has been delivered along an inner edge of the heavily irradiated tumor perimeter, and smaller dosages from the ingress portion of the Bragg energy profile are distributed throughout the tumor and into some healthy tissue. The delivered dosages or accumulated radiation flux levels are illustrated in a cross-sectional area of the tumor **2120** using an iso-line plot. After a first full rotation of the patient, symbolically, the darkest regions of the tumor are nearly fully irradiated and the regions of the tissue having received less radiation are illustrated with a gray scale with the whitest portions having the lowest radiation dose.

Referring now to FIG. **26**E, after completing the distal targeting multi-field irradiation, a smaller inner tumor is defined, where the inner tumor is already partially irradiated. The smaller inner tumor is indicated by the dashed line **2630**. The above process of irradiating the tumor is repeated for the newly defined smaller tumor. The proton dosages to the outer or distal portions of the smaller tumor are adjusted to account for the dosages delivered from other rotational positions. After the second tumor is irradiated, a yet smaller third tumor is defined. The process is repeated until the entire tumor is irradiated at the prescribed or defined dosage.

As described at the onset of this example, the patient is preferably only rotated to each rotational position once. In the above described example, after irradiation of the outer perimeter of the tumor, the patient is rotationally positioned, such as through 360 degrees, and the distal portion of the newest smaller tumor is targeted as described, supra. However, the irradiation dosage to be delivered to the second smaller tumor and each subsequently smaller tumor is known a-priori. Hence, when at a given angle of rotation, the smaller tumor or multiple progressively smaller tumors, are optionally targeted so that the patient is only rotated to the multiple rotational irradiation positions once.

The goal is to deliver a treatment dosage to each position of the tumor, to preferably not exceed the treatment dosage to any position of the tumor, to minimize ingress radiation dosage to healthy tissue, to circumferentially distribute ingress radiation hitting the healthy tissue, and to further minimize ingress radiation dosage to sensitive areas. Since the Bragg energy profile is known, it is possible to calculated the optimal intensity and energy of the proton beam for each rotational position and for each x- and y-axis scanning position. These calculation result in slightly less than threshold radiation dosage to be delivered to the distal portion of the tumor for each rotational position as the ingress dose energy from other positions bring the total dose energy for the targeted position up to the threshold delivery dose.

Referring again to FIG. **26**A and FIG. **26**C, the intensity of the proton beam is preferably adjusted to account for the cross-sectional distance or density of the healthy tissue. An example is used for clarity. Referring now to FIG. **26**A, when irradiating from the first position where the healthy tissue has a small area **2610**, the intensity of the proton beam is preferably increased as relatively less energy is delivered by the ingress portion of the Bragg profile to the healthy tissue. Referring now to FIG. **26**C, in contrast when irradiating from the n^{th} rotational position where the healthy tissue has a large cross-sectional area, the intensity of the proton beam is preferably decreased as a greater fraction the proton dose is delivered to the healthy tissue from this orientation.

In one example, for each rotational position and/or for each z-axis distance into the tumor, the efficiency of proton dose delivery to the tumor is calculated. The intensity of the proton beam is made proportional to the calculated efficiency. Essentially, when the scanning direction has really good efficiency, the intensity is increased and vise-versa. For example, if the tumor is elongated, generally the efficiency of irradiating the distal portion by going through the length of the tumor is higher than irradiating a distal region of the tumor by going across the tumor with the Bragg energy distribution. Generally, in the optimization algorithm:

- distal portions of the tumor are targeted for each rotational position;
- the intensity of the proton beam is largest with the largest cross-sectional area of the tumor;
- intensity is larger when the intervening healthy tissue volume is smallest; and
- intensity is minimized or cut to zero when the intervening healthy tissue volume includes sensitive tissue, such as the spinal cord or eyes.

Using an algorithm so defined, the efficiency of radiation dose delivery to the tumor is maximized. More particularly, the ratio of radiation dose delivered to the tumor versus the radiation dose delivered to surrounding healthy tissue approaches a maximum. Further, integrated radiation dose delivery to each x, y, and z-axis volume of the tumor as a result of irradiation from multiple rotation directions is at or near the preferred dose level. Still further, ingress radiation dose delivery to healthy tissue is circumferentially distributed about the tumor via use of multi-field irradiation where radiation is delivered from a plurality of directions into the body, such as more than 5, 10, 20, or 30 directions.

Multi-Field Irradiation

In one multi-field irradiation example, the particle therapy system with a synchrotron ring diameter of less than six meters includes ability to:

- rotate the patient through about 360 degrees;
- extract radiation in about 0.1 to 10 seconds;
- scan vertically about 100 millimeters;
- scan horizontally about 700 millimeters;
- vary beam energy from about 30 to 330 MeV/second during irradiation;
- vary the proton beam intensity independently of varying the proton beam energy;
- focus the proton beam with a cross-sectional distance from about 2 to 20 millimeters at the tumor; and/or
- complete multi-field irradiation of a tumor in less than about 1, 2, 4, or 6 minutes as measured from the time of initiating proton delivery to the patient **2130**.

Two multi-field irradiation methods are described. In the first method, the main controller **110** rotationally positions the patient **2130** and subsequently irradiates the tumor **2120**. The process is repeated until a multi-field irradiation plan is complete. In the second method, the main controller **110** simultaneously rotates and irradiates the tumor **2120** within the patient **2130** until the multi-field irradiation plan is complete. More particularly, the proton beam irradiation occurs while the patient **2130** is being rotated.

The 3-dimensional scanning system of the proton spot focal point, described herein, is preferably combined with a rotation/raster method. The method includes layer wise tumor irradiation from many directions. During a given irradiation slice, the proton beam energy is continuously changed according to the tissue's density in front of the tumor to result in the beam stopping point, defined by the Bragg peak, always being inside the tumor and inside the irradiated slice. The novel method allows for irradiation from many directions, referred to herein as multi-field irradiation, to achieve the maximal effective dose at the tumor level while simultaneously significantly reducing possible side-effects on the surrounding healthy tissues in comparison to existing methods. Essentially, the multi-field irradiation system distributes dose-distribution at tissue depths not yet reaching the tumor.

Proton Beam Position Control

Referring now to FIGS. **27** A and B, a beam delivery and tissue volume scanning system is illustrated. Presently, the worldwide radiotherapy community uses a method of dose field forming using a pencil beam scanning system. In stark contrast, FIG. **27** illustrates a spot scanning system or tissue volume scanning system. In the tissue volume scanning system, the proton beam is controlled, in terms of transportation and distribution, using an inexpensive and precise scanning system. The scanning system is an active system, where the beam is focused into a spot focal point of about one-half, one, two, or three millimeters in diameter. The focal point is translated along two axes while simultaneously altering the applied energy of the proton beam, which effectively changes the third dimension of the focal point. The system is applicable in combination with the above described rotation of the body, which preferably occurs in-between individual moments or cycles of proton delivery to the tumor. Optionally, the rotation of the body by the above described system occurs continuously and simultaneously with proton delivery to the tumor.

For example, in the illustrated system in FIG. **27**A, the spot is translated horizontally, is moved down a vertical y-axis, and is then back along the horizontal axis. In this example, current is used to control a vertical scanning system having at least one magnet. The applied current alters the magnetic field of the vertical scanning system to control the vertical deflection of the proton beam. Similarly, a horizontal scanning magnet system controls the horizontal deflection of the proton beam. The degree of transport along each axes is controlled to conform to the tumor cross-section at the given depth. The depth is controlled by changing the energy of the proton beam. For example, the proton beam energy is decreased, so as to define a new penetration depth, and the scanning process is repeated along the horizontal and vertical axes covering a new cross-sectional area of the tumor. Combined, the three axes of control allow scanning or movement of the proton beam focal point over the entire volume of the cancerous tumor. The time at each spot and the direction into the body for each spot is controlled to yield the desired radiation does at each sub-volume of the cancerous volume while distributing energy hitting outside of the tumor.

The focused beam spot volume dimension is preferably tightly controlled to a diameter of about 0.5, 1, or 2 millimeters, but is alternatively several centimeters in diameter. Preferred design controls allow scanning in two directions with: (1) a vertical amplitude of about 100 mm amplitude and frequency up to about 200 Hz; and (2) a horizontal amplitude of about 700 mm amplitude and frequency up to about 1 Hz.

In FIG. **27**A, the proton beam is illustrated along a z-axis controlled by the beam energy, the horizontal movement is along an x-axis, and the vertical direction is along a y-axis. The distance the protons move along the z-axis into the tissue, in this example, is controlled by the kinetic energy of the proton. This coordinate system is arbitrary and exemplary. The actual control of the proton beam is controlled in 3-dimensional space using two scanning magnet systems and by controlling the kinetic energy of the proton beam. The use of the extraction system, described supra, allows for different scanning patterns. Particularly, the system allows simultaneous adjustment of the x-, y-, and z-axes in the irradiation of

the solid tumor. Stated again, instead of scanning along an x,y-plane and then adjusting energy of the protons, such as with a range modulation wheel, the system allows for moving along the z-axes while simultaneously adjusting the x- and or y-axes. Hence, rather than irradiating slices of the tumor, the tumor is optionally irradiated in three simultaneous dimensions. For example, the tumor is irradiated around an outer edge of the tumor in three dimensions. Then the tumor is irradiated around an outer edge of an internal section of the tumor. This process is repeated until the entire tumor is irradiated. The outer edge irradiation is preferably coupled with simultaneous rotation of the subject, such as about a vertical y-axis. This system allows for maximum efficiency of deposition of protons to the tumor, as defined as the ratio of the proton irradiation energy delivered to the tumor relative to the proton irradiation energy delivered to the healthy tissue.

Combined, the system allows for multi-axes control of the charged particle beam system in a small space with a small power supply. For example, the system uses multiple magnets where each magnet has at least one edge focusing effect in each turning section of the synchrotron and/or multiple magnets having concentrating magnetic field geometry, as described supra. The multiple edge focusing effects in the circulating beam path of the synchrotron combined with the concentration geometry of the magnets and described extraction system yields a synchrotron having:

- a small circumference system, such as less than about 50 meters;
- a vertical proton beam size gap of about 2 cm;
- corresponding reduced power supply requirements associated with the reduced gap size;
- an extraction system not requiring a newly introduced magnetic field;
- acceleration or deceleration of the protons during extraction; and
- control of z-axis energy during extraction.

The result is a 3-dimensional scanning system, x-, y-, and z-axes control, where the z-axes control resides in the synchrotron and where the z-axes energy is variably controlled during the extraction process inside the synchrotron.

Referring now to FIG. **27**B, an example of a proton scanning or targeting system **140** used to direct the protons to the tumor with 4-dimensional scanning control is provided, where the 4-dimensional scanning control is along the x-, y-, and z-axes along with intensity control, as described supra. A fifth controllable axis is time. A sixth controllable axis is patient rotation. Typically, charged particles traveling along the transport path **268** are directed through a first axis control element **142**, such as a vertical control, and a second axis control element **144**, such as a horizontal control and into a tumor **2120**. As described, supra, the extraction system also allows for simultaneous variation in the z-axis. Further, as described, supra, the intensity or dose of the extracted beam is optionally simultaneously and independently controlled and varied. Thus instead of irradiating a slice of the tumor, as in FIG. **27**A, all four dimensions defining the targeting spot of the proton delivery in the tumor are simultaneously variable. The simultaneous variation of the proton delivery spot is illustrated in FIG. **27**B by the spot delivery path **269**. In the illustrated case, the protons are initially directed around an outer edge of the tumor and are then directed around an inner radius of the tumor. Combined with rotation of the subject about a vertical axis, a multi-field irradiation process is used where a not yet irradiated portion of the tumor is preferably irradiated at the further distance of the tumor from the proton entry point into the body. This yields the greatest percentage of the proton delivery, as defined by the Bragg peak, into the tumor and minimizes damage to peripheral healthy tissue.

Imaging/X-Ray System

Herein, an X-ray system is used to illustrate an imaging system.

Timing

An X-ray is preferably collected either (1) just before or (2) concurrently with treating a subject with proton therapy for a couple of reasons. First, movement of the body, described supra, changes the local position of the tumor in the body relative to other body constituents. If the patient or subject **2130** has an X-ray taken and is then bodily moved to a proton treatment room, accurate alignment of the proton beam to the tumor is problematic. Alignment of the proton beam to the tumor **2120** using one or more X-rays is best performed at the time of proton delivery or in the seconds or minutes immediately prior to proton delivery and after the patient is placed into a therapeutic body position, which is typically a fixed position or partially immobilized position. Second, the X-ray taken after positioning the patient is used for verification of proton beam alignment to a targeted position, such as a tumor and/or internal organ position.

Positioning

An X-ray is preferably taken just before treating the subject to aid in patient positioning. For positioning purposes, an X-ray of a large body area is not needed. In one embodiment, an X-ray of only a local area is collected. When collecting an X-ray, the X-ray has an X-ray path. The proton beam has a proton beam path. Overlaying the X-ray path with the proton beam path is one method of aligning the proton beam to the tumor. However, this method involves putting the X-ray equipment into the proton beam path, taking the X-ray, and then moving the X-ray equipment out of the beam path. This process takes time. The elapsed time while the X-ray equipment moves has a couple of detrimental effects. First, during the time required to move the X-ray equipment, the body moves. The resulting movement decreases precision and/or accuracy of subsequent proton beam alignment to the tumor. Second, the time required to move the X-ray equipment is time that the proton beam therapy system is not in use, which decreases the total efficiency of the proton beam therapy system.

X-Ray Source Lifetime

Preferably, components in the particle beam therapy system require minimal or no maintenance over the lifetime of the particle beam therapy system. For example, it is desirable to equip the proton beam therapy system with an X-ray system having a long lifetime source, such as a lifetime of about 20 years.

In one system, described infra, electrons are used to create X-rays. The electrons are generated at a cathode where the lifetime of the cathode is temperature dependent. Analogous to a light bulb, where the filament is kept in equilibrium, the cathode temperature is held in equilibrium at temperatures at about 200, 500, or 1000 degrees Celsius. Reduction of the cathode temperature results in increased lifetime of the cathode. Hence, the cathode used in generating the electrons is preferably held at as low of a temperature as possible. However, if the temperature of the cathode is reduced, then electron emissions also decrease. To overcome the need for more electrons at lower temperatures, a large cathode is used and the generated electrons are concentrated. The process is analogous to compressing electrons in an electron gun; however, here the compression techniques are adapted to apply to enhancing an X-ray tube lifetime.

Referring now to FIG. **28**, an example of an X-ray generation device **2800** having an enhanced lifetime is provided.

Electrons **2820** are generated at a cathode **2810**, focused with a control electrode **2812**, and accelerated with a series of accelerating electrodes **2840**. The accelerated electrons **2850** impact an X-ray generation source **2848** resulting in generated X-rays that are then directed along an X-ray path **2970** to the subject **2130**. The concentrating of the electrons from a first diameter **2815** to a second diameter **2816** allows the cathode to operate at a reduced temperature and still yield the necessary amplified level of electrons at the X-ray generation source **2848**. In one example, the X-ray generation source **2848** is the anode coupled with the cathode **2810** and/or the X-ray generation source is substantially composed of tungsten.

Still referring to FIG. **28**, a more detailed description of an exemplary X-ray generation device **2800** is described. An anode **2814**/cathode **2810** pair is used to generated electrons. The electrons **2820** are generated at the cathode **2810** having a first diameter **2815**, which is denoted d_1. The control electrodes **2812** attract the generated electrons **2820**. For example, if the cathode is held at about −150 kV and the control electrode is held at about −149 kV, then the generated electrons **2820** are attracted toward the control electrodes **2812** and focused. A series of accelerating electrodes **2840** are then used to accelerate the electrons into a substantially parallel path **2850** with a smaller diameter **2816**, which is denoted d_2. For example, with the cathode held at −150 kV, a first, second, third, and fourth accelerating electrodes **2842**, **2844**, **2846**, **2848** are held at about **−120**, **−90**, **−60**, and −30 kV, respectively. If a thinner body part is to be analyzed, then the cathode **2810** is held at a smaller level, such as about −90 kV and the control electrode, first, second, third, and fourth electrode are each adjusted to lower levels. Generally, the voltage difference from the cathode to fourth electrode is less for a smaller negative voltage at the cathode and vise-versa. The accelerated electrons **2850** are optionally passed through a magnetic lens **2860** for adjustment of beam size, such as a cylindrical magnetic lens. The electrons are also optionally focused using quadrupole magnets **2870**, which focus in one direction and defocus in another direction. The accelerated electrons **2850**, which are now adjusted in beam size and focused strike the X-ray generation source **2848**, such as tungsten, resulting in generated X-rays that pass through an optional blocker **2962** and proceed along an X-ray path **2970** to the subject. The X-ray generation source **2848** is optionally cooled with a cooling element **2849**, such as water touching or thermally connected to a backside of the X-ray generation source **2848**. The concentrating of the electrons from a first diameter **2815** to a second diameter **2816** allows the cathode to operate at a reduced temperature and still yield the necessary amplified level of electrons at the X-ray generation source **2848**.

More generally, the X-ray generation device **2800** produces electrons having initial vectors. One or more of the control electrode **2812**, accelerating electrodes **2840**, magnetic lens **2860**, and quadrupole magnets **2870** combine to alter the initial electron vectors into parallel vectors with a decreased cross-sectional area having a substantially parallel path, referred to as the accelerated electrons **2850**. The process allows the X-ray generation device **2800** to operate at a lower temperature. Particularly, instead of using a cathode that is the size of the electron beam needed, a larger electrode is used and the resulting electrons **2820** are focused and/or concentrated into the required electron beam needed.

As lifetime is roughly an inverse of current density, the concentration of the current density results in a larger lifetime of the X-ray generation device. A specific example is provided for clarity. If the cathode has a fifteen mm radius or d_1 is about 30 mm, then the area (πr^2) is about 225 mm^2 times pi. If the concentration of the electrons achieves a radius of five mm or d_2 is about 10 mm, then the area (πr^2) is about 25 mm^2 times pi. The ratio of the two areas is about nine ($225\pi/25\pi$). Thus, there is about nine times less density of current at the larger cathode compared to the traditional cathode having an area of the desired electron beam. Hence, the lifetime of the larger cathode approximates nine times the lifetime of the traditional cathode, though the actual current through the larger cathode and traditional cathode is about the same. Preferably, the area of the cathode **2810** is about 2, 4, 6, 8, 10, 15, 20, or 25 times that of the cross-sectional area of the substantially parallel electron beam **2850**.

In another embodiment of the invention, the quadrupole magnets **2870** result in an oblong cross-sectional shape of the electron beam **2850**. A projection of the oblong cross-sectional shape of the electron beam **2850** onto the X-ray generation source **2848** results in an X-ray beam **2970** that has a small spot in cross-sectional view, which is preferably substantially circular in cross-sectional shape, that is then passed through the patient **2830**. The small spot is used to yield an X-ray having enhanced resolution at the patient.

Referring now to FIG. **29**, in one embodiment, an X-ray is generated close to, but not in, the proton beam path. A proton beam therapy system and an X-ray system combination **2900** is illustrated in FIG. **29**. The proton beam therapy system has a proton beam **268** in a transport system after the Lamberson extraction magnet **292** of the synchrotron **130**. The proton beam is directed by the scanning/targeting/delivery system **140** to a tumor **2120** of a patient **2130**. The X-ray system **2905** includes an electron beam source **2805** generating an electron beam **2850**. The electron beam is directed to an X-ray generation source **2848**, such as a piece of tungsten. Preferably, the tungsten X-ray source is located about 1, 2, 3, 5, 10, 15, or 20 millimeters from the proton beam path **268**. When the electron beam **2850** hits the tungsten, X-rays are generated in all directions. X-rays are blocked with a port **2962** and are selected for an X-ray beam path **2970**. The X-ray beam path **2970** and proton beam path **268** run substantially in parallel as they progress to the tumor **2120**. The distance between the X-ray beam path **2970** and proton beam path **269** preferably diminishes to near zero and/or the X-ray beam path **2970** and proton beam path **269** overlap by the time they reach the tumor **2120**. Simple geometry shows this to be the case given the long distance, of at least a meter, between the tungsten and the tumor **2120**. The distance is illustrated as a gap **2980** in FIG. **29**. The X-rays are detected at an X-ray detector **2990**, which is used to form an image of the tumor **2120** and/or position of the patient **2130**.

As a whole, the system generates an X-ray beam that lies in substantially the same path as the proton therapy beam. The X-ray beam is generated by striking a tungsten or equivalent material with an electron beam. The X-ray generation source is located proximate to the proton beam path. Geometry of the incident electrons, geometry of the X-ray generation material, and/or geometry of the X-ray beam blocker **262** yield an X-ray beam that runs either substantially in parallel with the proton beam or results in an X-ray beam path that starts proximate the proton beam path an expands to cover and transmit through a tumor cross-sectional area to strike an X-ray detector array or film allowing imaging of the tumor from a direction and alignment of the proton therapy beam. The X-ray image is then used to control the charged particle beam path to accurately and precisely target the tumor, and/or is used in system verification and validation.

Referring now to FIG. **30**, additional geometry of the electron beam path **2850** and X-ray beam path **2970** is illustrated.

Particularly, the electron beam **2850** is shown as an expanded electron beam path **2852**, **2854**. Also, the X-ray beam path **2970** is shown as an expanded X-ray beam path **2972**, **2974**.

Referring now to FIG. **31**, a 3-dimensional (3-D) X-ray tomography system **3100** is presented. In a typical X-ray tomography system, the X-ray source and detector rotationally translate about a stationary subject. In the X-ray tomography system described herein, the X-ray source and detector are stationary and the patient **2130** rotates. The stationary X-ray source allows a system where the X-ray source **2848** is proximate the proton therapy beam path **268**, as described supra. In addition, the rotation of the patient **2130** allows the proton dosage to be distributed around the body, rather than being concentrated on one static entrance side of the body. Further, the 3-D X-ray tomography system allows for simultaneous updates of the tumor position relative to body constituents in real-time during proton therapy treatment of the tumor **2120** in the patient **2130**. The X-ray tomography system is further described, infra.

In a first step of the X-ray tomography system **3100**, the patient **2130** is positioned relative to the X-ray beam path **2970** and proton beam path **268** using a patient semi-immobilization/placement system, described infra. After patient **2130** positioning, a series of reference 2-D X-ray images are collected, on a detector array **2990** or film, of the patient **2130** and tumor **2120** as the subject is rotated about a y-axis **2117**. For example, a series of about 50, 100, 200, or 400 X-ray images of the patient are collected as the patient is rotated. In a second example, an X-ray image is collected with each n degrees of rotation of the patient **2130**, where n is about ½, 1, 2, 3, or 5 degrees of rotation. Preferably, about 200 images are collected during one full rotation of the patient through 360 degrees. Subsequently, using the reference 2-D X-ray images, an algorithm produces a reference 3-D picture of the tumor **2120** relative to the patient's constituent body parts. A tumor **2120** irradiation plan is made using the 3-D picture of the tumor **2120** and the patient's constituent body parts. Creation of the proton irradiation plan is optionally performed after the patient has moved from the X-ray imaging area.

In a second step, the patient **2130** is repositioned relative to the X-ray beam path **2970** and proton beam path **268** using the patient semi-immobilization/placement system. Just prior to implementation of the proton irradiation plan, a few comparative X-ray images of the patient **2130** and tumor **2120** are collected at a limited number of positions using the X-ray tomography system **2600** setup. For example, a single X-ray image is collected with the patient positioned straight on, at angles of plus/minus forty-five degrees, and/or at angles of plus/minus ninety degrees relative to the proton beam path **268**. The actual orientation of the patient **2130** relative to the proton beam path **268** is optionally any orientation. The actual number of comparative X-ray images is also optionally any number of images, though the preferable number of comparative X-ray images is about 2 to 5 comparative images. The comparative X-ray images are compared to the reference X-ray images and differences are detected. A medical expert or an algorithm determines if the difference between the reference images and the comparative images is significant. Based upon the differences, the medical expert or algorithm determines if: proton treatment should commence, be halted, or adapted in real-time. For example, if significant differences in the X-ray images are observed, then the treatment is preferably halted and the process of collecting a reference 3-D picture of the patient's tumor is reinitiated. In a second example, if the differences in the X-ray images are observed to be small, then the proton irradiation plan commences. In a third example, the algorithm or medical expert can adapt the proton irradiation plan in real-time to adjust for differences in tumor location resulting from changes in position of the tumor **2120** in the patient **2130** or from differences in the patient **2130** placement. In the third example, the adaptive proton therapy increases patient throughput and enhances precision and accuracy of proton irradiation of the tumor **2120** relative to the healthy tissue of the patient **2130**.

Patient Immobilization

Accurate and precise delivery of a proton beam to a tumor of a patient requires: (1) positioning control of the proton beam and (2) positioning control of the patient. As described, supra, the proton beam is controlled using algorithms and magnetic fields to a diameter of about 0.5, 1, or 2 millimeters. This section addresses partial immobilization, restraint, and/or alignment of the patient to insure the tightly controlled proton beam efficiently hits a target tumor and not surrounding healthy tissue as a result of patient movement.

Herein, an x-, y-, and z-axes coordinate system and rotation axis is used to describe the orientation of the patient relative to the proton beam. The z-axis represent travel of the proton beam, such as the depth of the proton beam into the patient. When looking at the patient down the z-axis of travel of the proton beam, the x-axis refers to moving left or right across the patient and the y-axis refers to movement up or down the patient. A first rotation axis is rotation of the patient about the y-axis and is referred to herein as a rotation axis, bottom unit **2112** rotation axis, or y-axis of rotation **2117**. In addition, tilt is rotation about the x-axis, yaw is rotation about the y-axis, and roll is rotation about the z-axis. In this coordinate system, the proton beam path **269** optionally runs in any direction. As an illustrative matter, the proton beam path running through a treatment room is described as running horizontally through the treatment room.

In this section, three examples of positioning systems are provided: (1) a semi-vertical partial immobilization system **3200**; (2) a sitting partial immobilization system **3300**; and (3) a laying position **3400**. Elements described for one immobilization system apply to other immobilization systems with small changes. For example, a headrest, a head support, or head restraint will adjust along one axis for a reclined position, along a second axis for a seated position, and along a third axis for a laying position. However, the headrest itself is similar for each immobilization position.

Vertical Patient Positioning/Immobilization

Referring now to FIG. **32**, the semi-vertical patient positioning system **3200** is preferably used in conjunction with proton therapy of tumors in the torso. The patient positioning and/or immobilization system controls and/or restricts movement of the patient during proton beam therapy. In a first partial immobilization embodiment, the patient is positioned in a semi-vertical position in a proton beam therapy system. As illustrated, the patient is reclining at an angle alpha, a, about 45 degrees off of the y-axis as defined by an axis running from head to foot of the patient. More generally, the patient is optionally completely standing in a vertical position of zero degrees off the of y-axis or is in a semi-vertical position alpha that is reclined about 5, 10, 15, 20, 25, 30, 35, 40, 45, 50, 55, 60, or 65 degrees off of the y-axis toward the z-axis.

Patient positioning constraints **3215** that are used to maintain the patient in a treatment position, include one or more of: a seat support **3220**, a back support **3230**, a head support **3240**, an arm support **3250**, a knee support **3260**, and a foot support **3270**. The constraints are optionally and independently rigid or semi-rigid. Examples of a semi-rigid material include a high or low density foam or a visco-elastic foam. For example the foot support is preferably rigid and the back

support is preferably semi-rigid, such as a high density foam material. One or more of the positioning constraints **3215** are movable and/or under computer control for rapid positioning and/or immobilization of the patient. For example, the seat support **3220** is adjustable along a seat adjustment axis **3222**, which is preferably the y-axis; the back support **3230** is adjustable along a back support axis **3232**, which is preferably dominated by z-axis movement with a y-axis element; the head support **3240** is adjustable along a head support axis **3242**, which is preferably dominated by z-axis movement with a y-axis element; the arm support **3250** is adjustable along an arm support axis **3252**, which is preferably dominated by z-axis movement with a y-axis element; the knee support **3260** is adjustable along a knee support axis **3262**, which is preferably dominated by z-axis movement with a y-axis element; and the foot support **3270** is adjustable along a foot support axis **3272**, which is preferably dominated by y-axis movement with a z-axis element.

If the patient is not facing the incoming proton beam, then the description of movements of support elements along the axes change, but the immobilization elements are the same.

An optional camera **3280** is used with the patient immobilization system. The camera views the patient/subject **2130** creating a video image. The image is provided to one or more operators of the charged particle beam system and allows the operators a safety mechanism for determining if the subject has moved or desires to terminate the proton therapy treatment procedure. Based on the video image, the operators optionally suspend or terminate the proton therapy procedure. For example, if the operator observes via the video image that the subject is moving, then the operator has the option to terminate or suspend the proton therapy procedure.

An optional video display or display monitor **3290** is provided to the patient. The video display optionally presents to the patient any of: operator instructions, system instructions, status of treatment, or entertainment.

Motors for positioning the patient positioning constraints **3215**, the camera **3280**, and/or video display **3290** are preferably mounted above or below the proton transport path **268** or momentary proton scanning path **269**.

Respiration control is optionally performed by using the video display. As the patient breathes, internal and external structures of the body move in both absolute terms and in relative terms. For example, the outside of the chest cavity and internal organs both have absolute moves with a breath. In addition, the relative position of an internal organ relative to another body component, such as an outer region of the body, a bone, support structure, or another organ, moves with each breath. Hence, for more accurate and precise tumor targeting, the proton beam is preferably delivered at a point in time where the position of the internal structure or tumor is well defined, such as at the bottom or top of each breath. The video display is used to help coordinate the proton beam delivery with the patient's respiration cycle. For example, the video display optionally displays to the patient a command, such as a hold breath statement, a breathe statement, a countdown indicating when a breath will next need to be held, or a countdown until breathing may resume.

Sitting Patient Positioning/Immobilization

In a second partial immobilization embodiment, the patient is partially restrained in a seated position **3300**. The sitting restraint system uses support structures similar to the support structures in the semi-vertical positioning system, described supra, with an exception that the seat support is replaced by a chair and the knee support is not required. The seated restraint system generally retains the adjustable support, rotation about the y-axis, camera, video, and breadth control parameters described in the semi-vertical embodiment, described supra.

Referring now to FIG. **33**, a particular example of a sitting patient semi-immobilization system **3300** is provided. The sitting system is preferably used for treatment of head and/or neck tumors. As illustrated, the patient is positioned in a seated position on a chair **3310** for particle therapy. The patient is further immobilized using any of the: the head support **3240**, the back support **3230**, the hand support **3250**, the knee support **3260**, and the foot support **3270**. The supports **3220**, **3230**, **3240**, **3250**, **3260**, **3270** preferably have respective axes of adjustment **3222**, **3232**, **3242**, **3252**, **3262**, **3272** as illustrated. The chair **3310** is either readily removed to allow for use of a different patient constraint system or adapts under computer control to a new patient position, such as the semi-vertical system.

Laying Patient Positioning/Immobilization

In a third partial immobilization embodiment, the patient is partially restrained in a laying position. The laying restraint system **3400** has support structures that are similar to the support structures used in the sitting positioning system **3300** and semi-vertical positioning system **3200**, described supra. In the laying position, optional restraint, support, or partial immobilization elements include one or more of: the head support **3240** and the back support, hip, and shoulder **3230** support. The supports preferably have respective axes of adjustment that are rotated as appropriate for a laying position of the patient. The laying position restraint system generally retains the adjustable supports, rotation about the y-axis, camera, video, and breadth control parameters described in the semi-vertical embodiment, described supra.

If the patient is very sick, such as the patient has trouble standing for a period of about one to three minutes required for treatment, then being in a partially supported system can result in some movement of the patient due to muscle strain. In this and similar situations, treatment of a patient in a laying position on a support table **3420** is preferentially used. The support table has a horizontal platform to support the bulk of the weight of the patient. Preferably, the horizontal platform is detachable from a treatment platform. In a laying positioning system **3400**, the patient is positioned on a platform **3410**, which has a substantially horizontal portion for supporting the weight of the body in a horizontal position. Optional hand grips are used, described infra. In one embodiment, the platform **3410** affixes relative to the table **3420** using a mechanical stop or lock element **3430** and matching key element **3435** and/or the patient **2130** is aligned or positioned relative to a placement element **3460**.

Additionally, upper leg support **3444**, lower leg support **3440**, and/or arm support **3450** elements are optionally added to raise, respectively, an arm or leg out of the proton beam path **269** for treatment of a tumor in the torso or to move an arm or leg into the proton beam path **269** for treatment of a tumor in the arm or leg. This increases proton delivery efficiency, as described supra. The leg supports **3440**, **3444** and arm support **3450** are each optionally adjustable along support axes or arcs **3442**, **3446**, **3452**. One or more leg support elements are optionally adjustable along an arc to position the leg into the proton beam path **269** or to remove the leg from the proton beam path **269**, as described infra. An arm support element is preferably adjustable along at least one arm adjustment axis or along an arc to position the arm into the proton beam path **269** or to remove the arm from the proton beam path **269**, as described infra.

Preferably, the patient is positioned on the platform **3410** in an area or room outside of the proton beam path **268** and is

wheeled or slid into the treatment room or proton beam path area. For example, the patient is wheeled into the treatment room on a gurney where the top of the gurney, which is the platform, detaches and is positioned onto a table. The platform is preferably lifted onto the table or slid onto the table so that the gurney or bed need not be lifted onto the table.

The semi-vertical patient positioning system **3200** and sitting patient positioning system **3300** are preferentially used to treatment of tumors in the head or torso due to efficiency. The semi-vertical patient positioning system **3200**, sitting patient positioning system **3300**, and laying patient positioning system **3400** are all usable for treatment of tumors in the patient's limbs.

Support System Elements

Positioning constraints **3215** include all elements used to position the patient, such as those described in the semi-vertical positioning system **3200**, sitting positioning system **3300**, and laying positioning system **3400**. Preferably, positioning constraints or support system elements are aligned in positions that do not impede or overlap the proton beam path **269**. However, in some instances the positioning constraints are in the proton beam path **269** during at least part of the time of treatment of the patient. For instance, a positioning constraint element may reside in the proton beam path **269** during part of a time period where the patient is rotated about the y-axis during treatment. In cases or time periods that the positioning constraints or support system elements are in the proton beam path, then an upward adjustment of proton beam energy is preferably applied that increases the proton beam energy to offset the positioning constraint element impedance of the proton beam. This time period and energy is a function of rotational orientation of the patient. In one case, the proton beam energy is increased by a separate measure of the positioning constraint element impedance determined during a reference scan of the positioning constraint system element or set of reference scans of the positioning constraint element as a function of rotation about the y-axis.

For clarity, the positioning constraints **3215** or support system elements are herein described relative to the semi-vertical positioning system **3200**; however, the positioning elements and descriptive x-, y-, and z-axes are adjustable to fit any coordinate system, to the sitting positioning system **3300**, or the laying positioning system **3400**.

An example of a head support system is described to support, align, and/or restrict movement of a human head. The head support system preferably has several head support elements including any of: a back of head support, a right of head alignment element, and a left of head alignment element. The back of head support element is preferably curved to fit the head and is optionally adjustable along a head support axis, such as along the z-axis. Further, the head supports, like the other patient positioning constraints, is preferably made of a semi-rigid material, such as a low or high density foam, and has an optional covering, such as a plastic or leather. The right of head alignment element and left of head alignment elements or head alignment elements, are primarily used to semi-constrain movement of the head or to fully immobilize the head. The head alignment elements are preferably padded and flat, but optionally have a radius of curvature to fit the side of the head. The right and left head alignment elements are preferably respectively movable along translation axes to make contact with the sides of the head. Restricted movement of the head during proton therapy is important when targeting and treating tumors in the head or neck. The head alignment elements and the back of head support element combine to restrict tilt, rotation or yaw, roll and/or position of the head in the x-, y-, z-axes coordinate system.

Referring now to FIG. **35** another example of a head support system **3500** is described for positioning and/or restricting movement of a human head **2102** during proton therapy of a solid tumor in the head or neck. In this system, the head is restrained using 1, 2, 3, 4, or more straps or belts, which are preferably connected or replaceably connected to a back of head support element **3510**. In the example illustrated, a first strap **3520** pulls or positions the forehead to the head support element **3510**, such as by running predominantly along the z-axis. Preferably a second strap **3530** works in conjunction with the first strap **3520** to prevent the head from undergoing tilt, yaw, roll or moving in terms of translational movement on the x-, y-, and z-axes coordinate system. The second strap **3530** is preferably attached or replaceable attached to the first strap **3520** at or about: (1) a forehead position **3532**; (2) at a position on one or both sides of the head **3534**; and/or (3) a position at or about the support element **3510**. A third strap **3540** preferably orientates the chin of the subject relative to the support element **3510** by running dominantly along the z-axis. A fourth strap **3550** preferably runs along a predominantly y- and z-axes to hold the chin relative to the head support element **3510** and/or proton beam path. The third **3540** strap preferably is attached to or is replaceably attached to the fourth strap **3550** during use at or about the patient's chin position **3542**. The second strap **3530** optionally connects **3536** to the fourth strap **3550** at or about the support element **3510**. The four straps **3520**, **3530**, **3540**, **3550** are illustrative in pathway and interconnection. Any of the straps optionally hold the head along different paths around the head and connect to each other in separate fashion. Naturally, a given strap preferably runs around the head and not just on one side of the head. Any of the straps **3520**, **3530**, **3540**, and **3550** are optionally used independently or in combinations and permutations with the other straps. The straps are optionally indirectly connected to each other via a support element, such as the head support element **3510**. The straps are optionally attached to the head support element **3510** using hook and loop technology, a buckle, or fastener. Generally, the straps combine to control position, front-to-back movement of the head, side-to-side movement of the head, tilt, yaw, roll, and/or translational position of the head.

The straps are preferably of known impedence to proton transmission allowing a calculation of peak energy release along the z-axis to be calculated. For example, adjustment to the Bragg peak energy is made based on the slowing tendency of the straps to proton transport.

Referring now to FIG. **36**, still another example of a head support system **3240** is described. The head support **3240** is preferably curved to fit a standard or child sized head. The head support **3240** is optionally adjustable along a head support axis **3242**. Further, the head supports, like the other patient positioning constraints, is preferably made of a semi-rigid material, such as a low or high density foam, and has an optional covering, such as a plastic or leather.

Elements of the above described head support, head positioning, and head immobilization systems are optionally used separately or in combination.

Still referring to FIG. **36**, an example of the arm support **3250** is further described. The arm support preferably has a left hand grip **3610** and a right hand grip **3620** used for aligning the upper body of the patient **2130** through the action of the patient **2130** gripping the left and right hand grips **3610**, **3620** with the patient's hands **2134**. The left and right hand grips **3610**, **3620** are preferably connected to the arm support **3250** that supports the mass of the patient's arms. The left and right hand grips **3610**, **3620** are preferably constructed using a semi-rigid material. The left and right hand grips **3610**, **3620**

are optionally molded to the patient's hands to aid in alignment. The left and right hand grips optionally have electrodes, as described supra.

Patient Respiration Monitoring

Preferably, the patient's breathing pattern is monitored. When a subject or patient **2130** is breathing many portions of the body move with each breath. For example, when a subject breathes the lungs move as do relative positions of organs within the body, such as the stomach, kidneys, liver, chest muscles, skin, heart, and lungs. Generally, most or all parts of the torso move with each breath. Indeed, the inventors have recognized that in addition to motion of the torso with each breath, various motion also exists in the head and limbs with each breath. Motion is to be considered in delivery of a proton dose to the body as the protons are preferentially delivered to the tumor and not to surrounding tissue. Motion thus results in an ambiguity in where the tumor resides relative to the beam path. To partially overcome this concern, protons are preferentially delivered at the same point in each of a series of respiration cycles.

Initially a rhythmic pattern of breathing of a subject is determined. The cycle is observed or measured. For example, an X-ray beam operator or proton beam operator can observe when a subject is breathing or is between breaths and can time the delivery of the protons to a given period of each breath. Alternatively, the subject is told to inhale, exhale, and/or hold their breath and the protons are delivered during the commanded time period.

Preferably, one or more sensors are used to determine the respiration cycle of the individual. Two examples of a respiration monitoring system are provided: (1) a thermal monitoring system and (2) a force monitoring system.

Referring again to FIG. **35**, a first example of the thermal respiration monitoring system is provided. In the thermal respiration monitoring system, a sensor is placed by the nose and/or mouth of the patient. As the jaw of the patient is optionally constrained, as described supra, the thermal respiration monitoring system is preferably placed by the patient's nose exhalation path. To avoid steric interference of the thermal sensor system components with proton therapy, the thermal respiration monitoring system is preferably used when treating a tumor not located in the head or neck, such as a when treating a tumor in the torso or limbs. In the thermal monitoring system, a first thermal resistor **3570** is used to monitor the patient's respiration cycle and/or location in the patient's respiration cycle. Preferably, the first thermal resistor **3570** is placed by the patient's nose, such that the patient exhaling through their nose onto the first thermal resistor **3570** warms the first thermal resistor **3570** indicating an exhale. Preferably, a second thermal resistor **3560** operates as an environmental temperature sensor. The second thermal resistor **3560** is preferably placed out of the exhalation path of the patient but in the same local room environment as the first thermal resistor **3570**. Generated signal, such as current from the thermal resistors **3570**, **3560**, is preferably converted to voltage and communicated with the main controller **110** or a sub-controller of the main controller. Preferably, the second thermal resistor **3560** is used to adjust for the environmental temperature fluctuation that is part of a signal of the first thermal resistor **3570**, such as by calculating a difference between the values of the thermal resistors **3570**, **3560** to yield a more accurate reading of the patient's respiration cycle.

Referring again to FIG. **33**, a second example of a monitoring system is provided. In an example of a force respiration monitoring system, a sensor is placed by the torso. To avoid steric interference of the force sensor system components with proton therapy, the force respiration monitoring system is preferably used when treating a tumor located in the head, neck, or limbs. In the force monitoring system, a belt or strap **3350** is placed around an area of the patient's torso that expands and contracts with each respiration cycle of the patient. The belt **3350** is preferably tight about the patient's chest and is flexible. A force meter **3352** is attached to the belt and senses the patients breathing pattern. The forces applied to the force meter **3352** correlate with periods of the respiration cycle. The signals from the force meter **3352** are preferably communicated with the main controller **110** or a sub-controller of the main controller.

Respiration Control

Referring now to FIG. **37**, a patient is positioned **3710** and once the rhythmic pattern of the subject's breathing or respiration cycle is determined **3720**, a signal is optionally delivered to the patient, such as via the display monitor **3290**, to more precisely control the breathing frequency **3730**. For example, the display screen **3290** is placed in front of the patient and a message or signal is transmitted to the display screen **3290** directing the subject when to hold their breath and when to breathe. Typically, a respiration control module uses input from one or more of the breathing sensors. For example, the input is used to determine when the next breath exhale is to complete. At the bottom of the breath, the control module displays a hold breath signal to the subject, such as on a monitor, via an oral signal, digitized and automatically generated voice command, or via a visual control signal. Preferably, a display monitor **3290** is positioned in front of the subject and the display monitor displays breathing commands to the subject. Typically, the subject is directed to hold their breath for a short period of time, such as about ½, 1, 2, 3, 5, or 10 seconds. The period of time the breath is held is preferably synchronized to the delivery time of the proton beam to the tumor, which is about ½, 1, 2, or 3 seconds. While delivery of the protons at the bottom of the breath is preferred, protons are optionally delivered at any point in the respiration cycle, such as upon full inhalation. Delivery at the top of the breath or when the patient is directed to inhale deeply and hold their breath by the respiration control module is optionally performed as at the top of the breath the chest cavity is largest and for some tumors the distance between the tumor and surrounding tissue is maximized or the surrounding tissue is rarefied as a result of the increased volume. Hence, protons hitting surrounding tissue is minimized. Optionally, the display screen tells the subject when they are about to be asked to hold their breath, such as with a 3, 2, 1, second countdown so that the subject is aware of the task they are about to be asked to perform.

X-Ray Synchronization with Patient Respiration

In one embodiment, X-ray images are collected in synchronization with patient respiration. The synchronization enhances X-ray image clarity by removing position ambiguity due to the relative movement of body constituents during a patient respiration cycle.

In a second embodiment, an X-ray system is orientated to provide X-ray images of a patient in the same orientation as viewed by a proton therapy beam, is synchronized with patient respiration, is operable on a patient positioned for proton therapy, and does not interfere with a proton beam treatment path. Preferably, the synchronized system is used in conjunction with a negative ion beam source, synchrotron, and/or targeting method and apparatus to provide an X-ray timed with patient respiration. Preferably, X-ray images are collected immediately prior to and/or concurrently with particle beam therapy irradiation to ensure targeted and controlled delivery of energy relative to a patient position result-

ing in efficient, precise, and/or accurate in-vivo treatment of a solid cancerous tumor with minimization of damage to surrounding healthy tissue.

An X-ray delivery control algorithm is used to synchronize delivery of the X-rays to the patient **2130** within a given period of each breath, such as at the top or bottom of a breath, and/or when the subject is holding their breath. For clarity of combined X-ray images, the patient is preferably both accurately positioned and precisely aligned relative to the X-ray beam path **2970**. The X-ray delivery control algorithm is preferably integrated with the respiration control module. Thus, the X-ray delivery control algorithm knows when the subject is breathing, where in the respiration cycle the subject is, and/or when the subject is holding their breath. In this manner, the X-ray delivery control algorithm delivers X-rays at a selected period of the respiration cycle. Accuracy and precision of patient alignment allow for (1) more accurate and precise location of the tumor **2120** relative to other body constituents and (2) more accurate and precise combination of X-rays in generation of a 3-dimensional X-ray image of the patient **2130** and tumor **2120**.

Referring again to FIG. **37**, an example of generating an X-ray image of the patient **2130** and tumor **2120** using the X-ray generation device **2800** or 3-dimensional X-ray generation device **2800** as a known function of time of the patient's respiration cycle is provided. In one embodiment, as a first step the main controller **110** instructs, monitors, and/or is informed of patient positioning **3710**. In a first example of patient positioning **3710**, the automated patient positioning system, described supra, under main controller **110** control, is used to align the patient **2130** relative to the X-ray beam path **2970**. In a second example of patient positioning, the main controller **110** is told via sensors or human input that the patient **2130** is aligned. In a second step, patient respiration is then monitored **3720**, as described infra. As a first example of breathing monitoring, an X-ray is collected **3740** at a known point in the patient respiration cycle. In a second example of breathing monitoring, the patient's respiration cycle is first controlled in a third step of controlling patient respiration **3730** and then as a fourth step an X-ray is collected **3740** at a controlled point in the patient respiration cycle. Preferably, the cycle of patient positioning **3710**, patient respiration monitoring **3720**, patient respiration control **3730**, and collecting an X-ray **3740** is repeated with different patient positions. For example, the patient **2130** is rotated about an axis **2117** and X-rays are collected as a function of the rotation. In a fifth step, a 3-dimensional X-ray image **3745** is generated of the patient **2130**, tumor **2120**, and body constituents about the tumor using the collected X-ray images, such as with the 3-dimensional X-ray generation device **2800**, described supra. The patient respiration monitoring and control steps are further described, infra.

Proton Beam Therapy Synchronization with Respiration

In one embodiment, charged particle therapy and preferably multi-field proton therapy is coordinated and synchronized with patient respiration via use of the respiration feedback sensors, described supra, used to monitor and/or control patient respiration. Preferably, the charged particle therapy is performed on a patient in a partially immobilized and repositionable position and the proton delivery to the tumor **2120** is timed to patient respiration via control of charged particle beam injection, acceleration, extraction, and/or targeting methods and apparatus. The synchronization enhances proton delivery accuracy by removing position ambiguity due to the relative movement of body constituents during a patient respiration cycle.

In a second embodiment, the X-ray system, described supra, is used to provide X-ray images of a patient in the same orientation as viewed by a proton therapy beam and both the X-ray system and the proton therapy beam are synchronized with patient respiration. Preferably, the synchronized system is used in conjunction with the negative ion beam source, synchrotron, and/or targeting method and apparatus to provide an X-ray timed with patient respiration where the X-ray is collected immediately prior to and/or concurrently with particle beam therapy irradiation to ensure targeted and controlled delivery of energy relative to a patient position resulting in efficient, precise, and/or accurate treatment of a solid cancerous tumor with minimization of damage to surrounding healthy tissue in a patient using the proton beam position verification system.

A proton delivery control algorithm is used to synchronize delivery of the protons to the tumor within a given period of each breath, such as at the top of a breath, at the bottom of a breath, and/or when the subject is holding their breath. The proton delivery control algorithm is preferably integrated with the respiration control module. Thus, the proton delivery control algorithm knows when the subject is breathing, where in the respiration cycle the subject is, and/or when the subject is holding their breath. The proton delivery control algorithm controls when protons are injected and/or inflected into the synchrotron, when an RF signal is applied to induce an oscillation, as described supra, and when a DC voltage is applied to extract protons from the synchrotron, as described supra. Typically, the proton delivery control algorithm initiates proton inflection and subsequent RF induced oscillation before the subject is directed to hold their breath or before the identified period of the respiration cycle selected for a proton delivery time. In this manner, the proton delivery control algorithm delivers protons at a selected period of the respiration cycle by simultaneously or nearly simultaneously delivering the high DC voltage to the second pair of plates, described supra, which results in extraction of the protons from the synchrotron and subsequent delivery to the subject at the selected time point. Since the period of acceleration of protons in the synchrotron is constant or known for a desired energy level of the proton beam, the proton delivery control algorithm is used to set an AC RF signal that matches the respiration cycle or directed respiration cycle of the subject.

The above described charged particle therapy elements are combined in combinations and/or permutations in developing and implementing a tumor treatment plan, described infra.

Developing and Implementing a Tumor Irradiation Plan

A series of steps are performed to design and execute a radiation treatment plan for treating a tumor **2120** in a patient **2130**. The steps include one or more of:

positioning and immobilizing the patient;
recording the patient position;
monitoring patient respiration;
controlling patient respiration;
collecting multi-field images of the patient to determine tumor location relative to body constituents;
developing a radiation treatment plan;
repositioning the patient;
verifying tumor location; and
irradiating the tumor.

In this section, an overview of developing the irradiation plan and subsequent implementation of the irradiation plan is initially presented, the individual steps are further described, and a more detailed example of the process is then described.

Referring now to FIG. **38**, an overview of a system for development of an irradiation plan and subsequent implementation of the irradiation plan **3800** is provided. Preferably,

all elements of the positioning, respiration monitoring, imaging, and tumor irradiation system **3800** are under main controller **110** control.

Initially, the tumor containing volume of the patient **2130** is positioned and immobilized **3710** in a controlled and reproducible position. The process of positioning and immobilizing **3710** the patient **2310** is preferably iterated **3812** until the position is accepted. The position is preferably digitally recorded **3815** and is later used in a step of computer controlled repositioning of the patient **3817** in the minutes or seconds prior to implementation of the irradiation element **3870** of the tumor treatment plan. The process of positioning the patient in a reproducible fashion and reproducibly aligning the patient **2310** to the controlled position is further described, infra.

Subsequent to patient positioning **3710**, the steps of monitoring **3720** and preferably controlling **3730** the respiration cycle of the patient **2130** are preferably performed to yield more precise positioning of the tumor **2120** relative to other body constituents, as described supra. Multi-field images of the tumor are then collected **3840** in the controlled, immobilized, and reproducible position. For example, multi-field X-ray images of the tumor **2120** are collected using the X-ray source proximate the proton beam path, as described supra. The multi-field images are optionally from three or more positions and/or are collected while the patient is rotated, as described supra.

At this point the patient **2130** is either maintained in the treatment position or is allowed to move from the controlled treatment position while an oncologist processes the multi-field images **3845** and generates a tumor treatment plan **3850** using the multi-field images. Optionally, the tumor irradiation plan is implemented **3870** at this point in time.

Typically, in a subsequent treatment center visit, the patient **2130** is repositioned **3817**. Preferably, the patient's respiration cycle is again monitored **3722** and/or controlled **3732**, such as via use of the thermal monitoring respiration sensors, force monitoring respiration sensor, and/or via commands sent to the display monitor **3290**, described supra. Once repositioned, verification images are collected **3860**, such as X-ray location verification images from 1, 2, or 3 directions. For example, verification images are collected with the patient facing the proton beam and at rotation angles of 90, 180, and 270 degrees from this position. At this point, comparing the verification images to the original multi-field images used in generating the treatment plan, the algorithm or preferably the oncologist determines if the tumor **2120** is sufficiently repositioned **3865** relative to other body parts to allow for initiation of tumor irradiation using the charged particle beam. Essentially, the step of accepting the final position of the patient **3865** is a safety feature used to verify that that the tumor **2120** in the patient **2130** has not shifted or grown beyond set specifications. At this point the charged particle beam therapy commences **3870**. Preferably the patient's respiration is monitored **3724** and/or controlled **3734**, as described supra, prior to commencement of the charged particle beam treatment **3870**.

Optionally, simultaneous X-ray imaging **3890** of the tumor **2120** is performed during the multi-field proton beam irradiation procedure and the main controller **110** uses the X-ray images to adapt the radiation treatment plan in real-time to account for small variations in movement of the tumor **2120** within the patient **2130**.

Herein the step of monitoring **3720**, **3722**, **3724** and controlling **3730**, **3732**, **3734** the patient's respiration is optional, but preferred. The steps of monitoring and controlling the patient's respiration are performed before and/or during the multi-filed imaging **3840**, position verification **3860**, and/or tumor irradiation **3870** steps.

The patient positioning **3710** and patient repositioning **3817** steps are further described, infra.

Computer Controlled Patient Repositioning

One or more of the patient positioning unit components and/or one of more of the patient positioning constraints are preferably under computer control. For example, the computer records or controls the position of the patient positioning elements **3215**, such as via recording a series of motor positions connected to drives that move the patient positioning elements **3215**. For example, the patient is initially positioned **3710** and constrained by the patient positioning constraints **3215**. The position of each of the patient positioning constraints is recorded and saved by the main controller **110**, by a sub-controller of the main controller **110**, or by a separate computer controller. Then, imaging systems are used to locate the tumor **2120** in the patient **2130** while the patient is in the controlled position of final treatment. Preferably, when the patient is in the controlled position, multi-field imaging is performed, as described herein. The imaging system **170** includes one or more of: MRI's, X-rays, CT's, proton beam tomography, and the like. Time optionally passes at this point while images from the imaging system **170** are analyzed and a proton therapy treatment plan is devised. The patient optionally exits the constraint system during this time period, which may be minutes, hours, or days. Upon, and preferably after, return of the patient and initial patient placement into the patient positioning unit, the computer returns the patient positioning constraints to the recorded positions. This system allows for rapid repositioning of the patient to the position used during imaging and development of the multi-field charged particle irradiation treatment plan, which minimizes setup time of patient positioning and maximizes time that the charged particle beam system **100** is used for cancer treatment.

Reproducing Patient Positioning and Immobilization

In one embodiment, using a patient positioning and immobilization system **3800**, a region of the patient **2130** about the tumor **2120** is reproducibly positioned and immobilized, such as with the motorized patient translation and rotation positioning system **2110** and/or with the patient positioning constraints **3215**. For example, one of the above described positioning systems, such as (1) the semi-vertical partial immobilization system **3200**; (2) the sitting partial immobilization system **3300**; or (3) the laying position system **3400** is used in combination with the patient translation and rotation system **2110** to position the tumor **2120** of the patient **2130** relative to the proton beam path **268**. Preferably, the position and immobilization system **3800** controls position of the tumor **2120** relative to the proton beam path **268**, immobilizes position of the tumor **2120**, and facilitates repositioning the tumor **2120** relative to the proton beam path **268** after the patient **2130** has moved away from the proton beam path **268**, such as during development of the irradiation treatment plan **3845**.

Preferably, the tumor **2120** of the patient **2130** is positioned in terms of 3-D location and in terms of orientation attitude. Herein, 3-D location is defined in terms of the x-, y-, and z-axes and orientation attitude is the state of pitch, yaw, and roll. Roll is rotation of a plane about the z-axis, pitch is rotation of a plane about the x-axis, and yaw is the rotation of a plane about the y-axis. Tilt is used to describe both roll and pitch. Preferably, the positioning and immobilization system **3800** controls the tumor **2120** location relative to the proton beam path **268** in terms of at least three of and preferably in

terms of four, five, or six of: pitch, yaw, roll, x-axis location, y-axis location, and z-axis location.

Chair

The patient positioning and immobilization system **3800** is further described using a chair positioning example. For clarity, a case of positioning and immobilizing a tumor in a shoulder is described using chair positioning. Using the semi-vertical immobilization system **3200**, the patient is generally positioned using the seat support **3220**, knee support **3260**, and/or foot support **3270**. To further position the shoulder, a motor in the back support **3230** pushes against the torso of the patient. Additional arm support **3250** motors align the arm, such as by pushing with a first force in one direction against the elbow of the patient and the wrist of the patient is positioned using a second force in a counter direction. This restricts movement of the arm, which helps to position the shoulder. Optionally, the head support is positioned to further restrict movement of the shoulder by applying tension to the neck. Combined, the patient positioning constraints **3215** control position of the tumor **2120** of the patient **2130** in at least three dimensions and preferably control position of the tumor **2120** in terms of all of yaw, roll, and pitch movement as well as in terms of x-, y-, and z-axis position. For instance, the patient positioning constraints position the tumor **2120** and restricts movement of the tumor, such as by preventing patient slumping. Optionally, sensors in one or more of the patient positioning constraints **3215** record an applied force. In one case, the seat support senses weight and applies a force to support a fraction of the patient's weight, such as about 50, 60, 70, or 80 percent of the patient's weight. In a second case, a force applied to the neck, arm, and/or leg is recorded.

Generally, the patient positioning and immobilization system **3800** removes movement degrees of freedom from the patient **2130** to accurately and precisely position and control the position of the tumor **2120** relative to the X-ray beam path **2970**, proton beam path **268**, and/or an imaging beam path. Further, once the degrees of freedom are removed, the motor positions for each of the patient positioning constraints are recorded and communicated digitally to the main controller **110**. Once the patient moves from the immobilization system **3800**, such as when the irradiation treatment plan is generated **3850**, the patient **2130** must be accurately repositioned before the irradiation plan is implemented. To accomplish this, the patient **2130** sits generally in the positioning device, such as the chair, and the main controller sends the motor position signals and optionally the applied forces back to motors controlling each of the patient positioning constraints **3215** and each of the patient positioning constraints **3215** are automatically moved back to their respective recorded positions. Hence, repositioning and re-immobilizing the patient **2130** is accomplished from a time of sitting to fully controlled position in less than about 10, 30, 60, or 120 seconds.

Using the computer controlled and automated patient positioning system, the patient is re-positioned in the positioning and immobilization system **3800** using the recalled patient positioning constraint **3215** motor positions; the patient **2130** is translated and rotated using the patient translation and rotation system **2120** relative to the proton beam **268**; and the proton beam **268** is scanned to its momentary beam position **269** by the main controller **110**, which follows the generated irradiation treatment plan **3850**.

Although the invention has been described herein with reference to certain preferred embodiments, one skilled in the art will readily appreciate that other applications may be substituted for those set forth herein without departing from the spirit and scope of the present invention. Accordingly, the invention should only be limited by the Claims included below.

The invention claimed is:

1. An apparatus for irradiating a tumor of a patient with charged particles, comprising:

a charged particle therapy system, comprising:

a synchrotron, said synchrotron comprising:

a radio-frequency cavity system configured to induce and amplify betatron oscillation of the charged particles;

an extraction foil, said extraction foil comprising a thickness of between ten and one hundred fifty micrometers, said extraction foil consisting essentially of atoms comprising six or fewer protons per atom, said extraction foil configured to emit electrons when struck by the charged particles undergoing betatron oscillation;

an intensity controller configured to: (1) receive a signal related to the emitted electrons and (2) instruct said radio-frequency cavity system to enhance the betatron oscillation when a pathlength through healthy tissue to the tumor decreases and to decrease the betatron oscillation when the pathlength through the healthy tissue to the tumor increases;

a charged particle beam path; and

a rotatable platform,

wherein said charged particle beam path runs through said synchrotron and above a portion of said rotatable platform,

said rotatable platform configured to rotate at least ninety degrees during an irradiation period,

wherein, during use in said irradiation period, said rotatable platform rotates to at least five irradiation positions.

2. The apparatus of claim **1**, said rotatable platform configured to hold the patient during said irradiation period, wherein the charged particle beam path circumferentially surrounds the charged particles, and wherein, during use, the charged particles irradiate the tumor during each of said at least five irradiation positions.

3. The apparatus of claim **1**, wherein, during use, said rotatable platform rotates through about three hundred sixty degrees during said irradiation period.

4. The apparatus of claim **3**, said charged particle therapy system further comprising:

an irradiation control module, wherein the tumor comprises a distal region, said distal region furthest from point of entry of the charged particles into the patient, said irradiation control module configured to terminate said charged particle beam path in said distal region of the tumor for each of said at least five irradiation positions.

5. The apparatus of claim **4**, wherein said irradiation control module controls both rotation of said rotatable platform and energy of the charged particles to irradiate, with Bragg peak energy of the charged particles, a changing distal position of the tumor as a function of position of said rotatable platform.

6. The apparatus of claim **4**, wherein said irradiation control module controls energy of the charged particles to maximize charged particle delivery efficiency of charged particle delivery of the tumor, wherein said charged particle delivery efficiency comprises a measure of charged particle energy delivered to the tumor relative to charged particle energy delivered to healthy tissue.

7. The apparatus of claim **1**, said charged particle therapy system further comprising:

a control module, said control module configured to distribute distal energy of the charged particles about an outer perimeter of the tumor, wherein ingress energy of the charged particles comprises circumferential distribution about the tumor.

8. The apparatus of claim **1**, further comprising a control algorithm, said control algorithm configured to control both energy and intensity of the charged particles during an extraction phase of the charged particles from said synchrotron.

9. The apparatus of claim **1**, said charged particle therapy system configured to increase intensity of the charged particles when charged particle delivery efficiency increases and decrease said intensity when said charged particle delivery efficiency decreases, wherein said charged particle delivery efficiency comprises a measure of relative energy delivered to the tumor versus surrounding healthy tissue.

10. The apparatus of claim **9**,

said extraction foil proximate said charged particle beam path in said synchrotron, wherein said thickness of said extraction foil comprises a width of forty to sixty micrometers.

11. The apparatus of claim **1**, wherein a first intensity of the charged particles is used when energy levels of the charged particles reach a distal region of the tumor during each of said at least five irradiation positions, wherein a second intensity of the charged particles is used when energy levels of the charged particles reach an ingress region of the tumor during said each of said at least five irradiation positions, wherein said first intensity is greater than said second intensity.

12. The apparatus of claim **1**, wherein intensity of the charged particles and energy of the charged particles correlate with a correlation factor of at least one-half.

13. The apparatus of claim **1**, said charged particle therapy system further comprising:

a control module, said control module configured to increase intensity of the charged particles as energy of the charged particles increases for at least three of said at least five irradiation positions.

14. The apparatus of claim **1**, wherein, during use, said rotatable platform rotates through about three hundred sixty degrees during said irradiation period, wherein irradiation of the tumor occurs with the charged particles in at least thirty rotation positions of said rotatable platform during said irradiation period.

15. The apparatus of claim **1**, wherein said charged particle therapy system further comprises:

an active scanning system configured to scan the charged particles along at least three axes, said active scanning system comprising a focal spot of the charged particles of less than three millimeters diameter, wherein said three axes comprise: a horizontal axis, a vertical axis, and an applied energy axis.

16. The apparatus of claim **15**, wherein, during use, said rotatable platform rotates to a new position of said at least five irradiation positions between movement of said focal spot by said active scanning system.

17. A method for irradiating a tumor of a patient with charged particles, comprising the steps of:

providing a charged particle therapy system, comprising:

a synchrotron, said synchrotron comprising:

a radio-frequency cavity system configured to induce and amplify betatron oscillation of the charged particles,

an extraction foil, said extraction foil comprising a thickness of between ten and one hundred fifty micrometers, said extraction foil consisting essentially of atoms comprising six or fewer protons per atom;

said extraction foil emitting electrons when struck by the charged particles undergoing betatron oscillation;

receiving to an intensity controller a signal related to the emitted electrons;

instructing said radio-frequency cavity system to increase the betatron oscillation when a pathlength through healthy tissue to the tumor decreases and to decrease the betatron oscillation when the pathlength through the healthy tissue to the tumor increases;

rotating a rotatable platform at least ninety degrees during an irradiation period; and

rotating said rotatable platform to at least five irradiation positions during the irradiation period,

wherein a charged particle beam path runs through said synchrotron and above a portion of said rotatable platform.

* * * * *